



Curriculum 1. Civil and Environmental Engineering

Stefano Mallucci

Hydro-climatic shifts in the Alpine region under a changing climate: trends, drivers detection and scale issues





Except where otherwise noted, contents on this book are licensed under a Creative
Common Attribution - Non Commercial - No Derivatives
4.0 International License

University of Trento
Doctoral School in Civil, Environmental and Mechanical Engineering
<http://web.unitn.it/en/dricam>
Via Mesiano 77, I-38123 Trento
Tel. +39 0461 282670 / 2611 - dicamphd@unitn.it

UNIVERSITY OF TRENTO - Italy

Department of Civil, Environmental
and Mechanical Engineering



Doctoral School in Civil, Environmental and Mechanical Engineering
Doctoral Thesis - April 2018

STEFANO MALLUCCI

**Hydro-climatic shifts in the Alpine region
under a changing climate: trends, drivers
detection and scale issues**

Supervisors:

Alberto BELLIN (University of Trento, Italy)

Bruno MAJONE (University of Trento, Italy)

*Our problems are man-made,
therefore they may be solved by man.*

JOHN F. KENNEDY

ABSTRACT

The impact of changing climate on the hydrological cycle in Alpine regions has attracted in the last decades a wealth of attention by the scientific community and decision makers. Indeed, the implications of changes in the intensity and in the temporal and spatial patterns of precipitation, temperature and other climatic forcing have been widely observed accompanied with an increased frequency of drought and flood events, and a general degradation of water quality and health of aquatic ecosystems. Accordingly, in the present thesis, the effect of changes in hydro-climatic variables on the hydrological cycle is investigated over a range of temporal and spatial scales. In particular, the research moves along two main directions: 1) changes in historical time series of streamflow, precipitation and temperature, recorded in the Adige River Basin (i.e., Northeastern Italy), are analyzed with a water balance approach and compared to those of other large European river basins (i.e., Ebro and Sava) in order to quantify alterations of the main hydrological fluxes due to climate change and water uses and to disentangle their reciprocal effects; 2) a framework for evaluating the hydrological coherence of available gridded meteorological datasets, including one developed in the first part of the thesis, is introduced and tested. Regarding the first line of research, hydro-climatic and water quality variables of some important European river basins have been analyzed in order to quantify the main alterations of streamflow and to understand the most important factors controlling them. Particular attention is drawn to the Adige River Basin (an Alpine catchment located in the North-East of Italy), for which in depth studies, data measures and analyses have been performed. At this purpose,

advanced techniques, besides novel approaches, have been applied. In particular, statistical methods (i.e., Mann-Kendall trend tests, Sen's slope estimates, multivariate data analyses and Kriging algorithms) have been used to assess the water budgets and the variations in time and space of the aforementioned variables. Disentangling climatic and human impacts on the hydrological fluxes is a difficult task and it has not been fully explored yet, since concurring drivers of hydrological alterations (e.g., climate and land use changes, hydropower and agricultural developments and increasing population) are intimately intertwined one to each other and combined in a complex nonlinear manner. At this purpose, spatial and temporal patterns of change in the hydrological cycle of the Adige River Basin have been identified by comparing annual and seasonal water budgets performed in four representative sub-basins (sized from 207 to 9,852 km^2) characterized by different climatic and water uses conditions. A significant downward trend of streamflow is found in the lower part of the Adige since the '70s, which can be attributed to the intense development of irrigated agriculture in the drainage area of the Noce River (one of the main tributaries of the Adige River). Conversely, headwater catchments showed a significant positive trend in streamflow due to a shift in the seasonal distribution of precipitation. These results suggest that climate change is the main driver only in headwater basins, while water uses overcome its effect along the main stream and the lower end of the tributaries. Therefore, a comparative analysis of recent trends in hydro-climatic parameters in three climatologically different European watersheds (i.e., the Adige, Ebro and Sava River Basins) has been performed. The main results suggest that the highest risk of increasing water scarcity refers to the Ebro, whereas the Adige shows better resilience to a changing climate. In the second part, this thesis deals with the uncertainty associated with climate datasets, that typically represents the largest part of the total uncertainty in hydrological modeling and, more in general, in climate change impact studies. In particular, this thesis describes a new framework for assessing the coherence of gridded meteorological datasets with streamflow observations (i.e.,

HyCoT - Hydrological Coherence Test). Application to the Adige catchment reveals that using inverse hydrological modeling allows testing the accuracy of gridded temperature and precipitation datasets and it may represent a tool for excluding those that are inconsistent with the hydrological response.

DEDICATION AND ACKNOWLEDGEMENTS

This thesis is the result of three fruitful working years in the research group of Professor Alberto Bellin, hence I want to firstly thank him for the opportunity he gave me. Equally, I acknowledge the fundamental help of Bruno Majone, with which I worked side-by-side during all my PhD. Moreover, I want to hug all my office mates, far and near, for the friendship and the reciprocal support. Naturally, I have to thank my family (i.e., my parents, my brothers, Giorgio and Stella and Renato) for the warmth and the affection demonstrated, though hundreds of kilometers divide us. A special thanks goes to Ulisse, loyal friend, always patient, always good. He become a fully-fledged part of me. Finally, I owe all that I am to Elena. Her love is the engine of my life.

TABLE OF CONTENTS

	Page
List of Tables	xiii
List of Figures	xv
1 Introduction	1
1.1 Hydrological changes: detection and attribution	1
1.2 On the use of hydrological modeling for testing the spatio-temporal coherence of high-resolution gridded precipitation and temperature datasets in the Alpine region	9
2 Study sites, data and methods	15
2.1 Study sites	15
2.1.1 Adige River Basin	15
2.1.2 Ebro River Basin	21
2.1.3 Sava River Basin	22
2.2 Data	23
2.2.1 Meteorological data	23
2.2.2 Streamflow data	26
2.3 Methods	29
2.3.1 Attribution of hydrological changes in the Adige River Basin	29
2.3.2 Auxiliary statistical methods	36
2.3.3 Comparison of hydrological trends in Europe	36

2.3.4	Hydrological Coherence Test (HyCoT) . . .	37
3	Results	41
3.1	Hydrological changes: detection and attribution	41
3.1.1	Detection and attribution of hydrological changes in a large Alpine river basin . . .	41
3.1.2	Hydroclimatic and water quality trends across three European river basins	49
3.2	On the use of hydrological modeling for testing the spatio-temporal coherence of high-resolution gridded precipitation and temperature datasets in the Alpine region	58
3.2.1	Uncertainty of climate datasets	58
3.2.2	Testing the hydrological coherence of the datasets	62
3.2.3	Analysis of a simple correction scheme applied to precipitation forcing	65
4	Discussion	69
4.1	Hydrological changes: detection and attribution	69
4.1.1	Detection and attribution of hydrological changes in a large Alpine river basin . . .	69
4.1.2	Hydroclimatic and water quality trends across three European river basins	80
4.2	On the use of hydrological modeling for testing the spatio-temporal coherence of high-resolution gridded precipitation and temperature datasets in the Alpine region	86
5	Conclusions	93
5.1	Hydrological changes: detection and attribution	94

5.2 On the use of hydrological modeling for testing the spatio-temporal coherence of high-resolution gridded precipitation and temperature datasets in the Alpine region	98
Bibliography	101

LIST OF TABLES

TABLE	Page
5.1 <i>Summary of the attribution exercise.</i>	95

LIST OF FIGURES

FIGURE	Page
1.1 <i>Time series of the monthly (black) and annual (red) mean temperatures of the Adige River Basin in the period 1924-2013.</i>	6
2.1 <i>Overview of location of study basins and relief in the Ebro, Sava, and Adige River Basins.</i>	23
2.2 <i>Location of the four selected sub-catchments within the Adige River Basin. The inset in the lower-left panel shows the location of the Adige River in the Italian territory.</i>	28
2.3 <i>On the left it is schematized the surface flow generation module, on the right it is represented the HYPERstream routing scheme applied at each 5-km cell of the computational grid. The conceptual scheme of the hydrological modeling framework is provided by the coupling of the two modules.</i>	38
3.1 <i>Maps of average annual precipitation (a), mean temperature (b) and climatic evapotranspiration AET_{clim} (c) over the Adige River Basin. Averages refer to the period 1956-2013.</i>	43

3.2 *Time series of total annual streamflow volume (a), annual precipitation (b), annual mean temperature (c) and annual climatic evapotranspiration AET_{clim} (d) referred to the four selected sub-catchments. All the annual cumulate fluxes are expressed in mm. . .* 44

3.3 *Trend analysis of the selected hydro-climatic variables in the Adige river basin at Trento (a), Bronzolo (b), Mantana, on the Gadera tributary, (c) and Soraga, on the Avisio tributary (d). Trends in annual precipitation (P), annual streamflow volume (Q) and climate-driven evapotranspiration (AET_{clim}) are calculated, in addition to trends in standard deviation of Q, with Mann-Kendall test on 30 years moving time windows for the 4 analyzed basins at annual and seasonal scales. The values of trend is associated to the starting year of the respective time windows. .* 48

3.4 *Mann-Kendall trend analysis of annual mean temperature (left-panels) and total precipitation (right-panels) in the Adige (a, b), Ebro (c, d) and Sava (e, f) river basins (1971-2010). Colours show Sen's slope estimator ($^{\circ}\text{C year}^{-1}$ for temperature and mm year^{-1} for precipitation, respectively) for each grid cell. Significant trends ($\alpha = 0.1$) are shown as hatched areas.* 52

- 3.5 *Trends in annual mean streamflow (dots and triangles in both panels) and trends in (left-side panels) annual mean sub-basin temperature and (right-side panels) annual sub-basin precipitation totals in the Adige (a, b), Ebro (c, d) and Sava (e, f) river basins according to Mann-Kendall trend analysis (between 1971 and 2010; significance level of $\alpha = 0.1$). Significant trends in streamflow are presented as triangles (upward-pointing for upward trend and downward-pointing for downward trend) and non-significant streamflow as dots, respectively. Significant trends in sub-basin climate are shown as hatched areas. 57*
- 3.6 *Maps of mean annual precipitation totals (1989-2008 average) according to the five different climate datasets. 60*
- 3.7 *Annual cycle of monthly mean precipitation totals (1989-2008 average), averaged over the entire study area, according to the five different climate datasets (color bars). The associated evolution of cumulated precipitation totals is also shown (color lines). 61*
- 3.8 *Maps of mean annual temperature (1989-2008 average) according to the three climate datasets providing temperature data. 62*
- 3.9 *Monthly mean temperature (1989-2008 average), averaged over the entire study area, according to the three climate datasets providing temperature data. . 62*

- 3.10 (A) Map of the NSE values calculated at the gauging stations of the Adige river basin. (B): as in (A) but for PBIAS values. Positive PBIAS values indicate underestimates of observations by the model, while negative values indicate overestimates. Simulated streamflow are obtained through HYPERstream with model's parameters selected such as to maximize the average NS at the gauging stations of Trento and Bronzolo, separately for each dataset. 65
- 3.11 Comparison of NSE indexes associated with the four LS scenarios (MESAN₁ to MESAN₄), together with the values obtained during the optimization of the hydrological model using APGD (black) and MESAN (in green scale) as input meteorological forcing. . . . 68
- 4.1 Trend analysis of the selected hydro-climatic variables in the Adige River Basin at Trento in the summer season. Trends in precipitation (P), streamflow volume (Q) and climatic evapotranspiration (AET_{clim}) are showed, in addition to trends in standard deviation of Q, computed by the Mann Kendall test with a 30 years moving time windows. The resulting trends are plotted versus the starting year of the time windows. Filled symbols indicate statistically significant trends with 5% level of confidence, while open symbols indicate statistically non-significant trends. 71

- 4.2 *Difference of Adige streamflow between Trento and Bronzolo in the period 1956 - 2013, aggregated at annual scale. Observed aggregated time series are shown as black lines, whereas the simulated values are reported as red lines. A significant break point is detected in the year 1990, only in the observed streamflows, by means of Pettitt's test (the black dashed line traces the local means in the two periods before and after 1990). 74*
- 4.3 *Trend analysis of the selected hydro-climatic variables in the Gadera at Mantana and Avisio at Soraga in the winter season. Trends in precipitation (P), streamflow volume (Q) and climatic evapotranspiration (AET_{clim}) are showed, in addition to trends in standard deviation of Q, computed by the Mann Kendall test with a 30 years moving time windows. The resulting trends are plotted versus the starting year of the time windows. Filled symbols indicate statistically significant trends with 5% level of confidence, while open symbols indicate statistically non-significant trends. 76*
- 4.4 *Average annual number of freezing days as a function of the percentage area of the basin with mean daily temperature below 0 °C in the Adige river basin closed at Trento. Colored continuous lines indicate different decades. The hypsographic curve of the basin, that provides the percentages of catchment area above a given elevations, is also shows with a black dashed line (elevations are provided on the secondary ordinate axis on the right). 78*

INTRODUCTION

1.1 Hydrological changes: detection and attribution

A variety of anthropogenic stressors such as industry, agriculture, water abstraction or pollution affects negatively water resources worldwide. The sustainable management of these impacting actions is one of the major societal challenges to address in the near future [8, 37, 94, 107, 124, 167].

Changing climate is an additional stressor that can enhance the effects of these anthropogenic influences. In particular, higher temperatures lead to increased evapotranspiration and thus, if not counterbalanced by increased precipitation, to declining streamflow [103, 108, 129].

The relevant role of climate change on the observed alterations of the water cycle in snow-dominated regions is widely recognized, particularly in the European Alps [see e.g., 10, 15, 42, 57, 63, 65, 112, 128]. A number of contributions suggest that recent changes in the precipitation patterns and

the contemporaneous rise of temperatures have led to rapid glaciers melting and intensification of evaporation with a consequent alteration of the typical Alpine hydrological regime [see e.g., 20, 96]. Furthermore, other pressure factors such as land use changes, hydropower and agricultural developments, increasing population and other anthropogenic stress factors are shown to drive important streamflow alterations in some Alpine catchments [see e.g., 37, 150, 181, 182] and their influence should be carefully quantified and separated from the climatic one.

Comparing the observed alterations of the hydro-climatic characteristics in the Alpine region to those of other large European river basins is an interesting task, since most of the European region suffered increases in mean and extreme temperature [see e.g., 2, 54, 64, 175] and seasonal decreases in precipitation [see e.g., 144, 155, 164] over the past decades. At the same time, intensification of agriculture and hydropower generation, especially in the Mediterranean region, have required increasing amount of water and altered the hydrological regime of human-influenced basins [104, 106, 181]. Hence, the Mediterranean region is particularly exposed to both changing climate and additional anthropogenic pressures, and the combined effect of these pressures is likely to result in increased water scarcity, declining crop yields, less biodiversity and, ultimately, higher risks to human health [see e.g., 61, report by the European Environment Agency]. It is crucial to identify recent trends, their drivers and impacts in order to adapt the management of water resources and land use in river basins.

The first part of my PhD was useful to gather data of the Adige River Basin (northeast of Italy) and to investigate the hydrological and chemical stressors in this important Alpine

region. The outcomes of this preliminary study have been published in the paper by Chiogna et al. [37] in Science of the Total Environment.

Detection and attribution of hydrological changes in a large

Alpine river basin Disentangling climatic and human impacts on hydrological fluxes is a difficult task since they combine in a complex nonlinear manner. Recent studies attempted to use satellite products to perform such partitioning [e.g., 52, 105], though the analysis is limited by the relatively short time span in which such products are available. Other studies addressed this issue through water balance, often coupled with modeling, which accuracy depends on the availability and quality of hydro-climatic and land use data [see e.g., 1, 49, 86, 104, 142, 161, 180]. Currently, most of the literature focuses on the attribution of flood changes [see e.g., 117], whereas other components of hydrological alterations are treated to a lesser extent [150] despite a systematic spatially distributed hydrological monitoring is active since the beginning of the past century in the Alpine region. Indeed, several studies analyzed trends in streamflow [see e.g., 9, 20, 30, 36], precipitation [see e.g., 27] or temperature [see e.g., 169] separately, without assessing their interplay in connection with changes of the water budget. The need of assessing the multiple and concurring causes of streamflow alterations observed in the Alpine region, especially after 1961 when these changes became more evident, was highlighted by Birsan et al. [20]. A similar conclusion was drawn by Kormann et al. [96] who specified that an integrated approach would be desirable, since available studies in Alpine catchments usually analyze the trends of a single driver of change. Furthermore, Bocchiola [22] highlighted the importance of making additional

effort to better understand the hydrological balance of Alpine catchments to unravel small-scale meteo-hydrological mechanisms undergoing the observed patterns and to further separate the effect of anthropic driven regulations when present. Many studies have investigated the hydrological interactions between melting water, streamflow and groundwater, in the attempt to quantify the main contributions to runoff [see e.g., 31, 33, 101, 125]. Other hydrological studies investigated spatial and temporal variability of runoff water sources [38, 132, 133, 163]. Others, analyzed the streamflow generation process in karst systems [110, 111]. This background shows that local studies are available for the hydrological characterization, however, a comprehensive framework to integrate the different sources of available information, to draw conclusions about hydrological alterations at larger scale and to assess the uncertainty of hydrological models and to improve their predictive capability, is still lacking at the river basin scale. Most of the papers in literature approach trend attribution of flood magnitude and frequency [see e.g., 79] in a qualitative way without systematically proving the existence of the relationships between the changes in the assumed driver and the changes in hydrological behavior. Recently, a rigorous framework for trend attribution has been proposed by Merz et al. [117]. The framework is based on three main steps: 1) evidence of consistency, 2) evidence of inconsistency and 3) provision of a confidence level, and it proposes that any attribution study should consider all the possible drivers which may have affected the observed changes and should try to disentangle their individual effects. Steps 1 and 2 can be performed with inferential statistics techniques, among which is worth citing the optimal fingerprinting [see e.g., 4, 75]. This technique, often used in the contest of climate change

detection and attribution, is based on a multivariate regression approach in which the analyzed time series are represented as a linear combination of signal patterns (i.e., fingerprints). Whatever the inferential technique is used, the knowledge of the time series of all the possible drivers is needed, which requires in general huge efforts in monitoring changes in catchments beyond typical hydrological variables. [73]. Focusing the attention to the Alpine region, most of the studies indicate the increasing temperature as the principal cause of both higher winter streamflow, providing a shift from solid (i.e., snowfall) to liquid (i.e., rainfall) precipitation, and decreasing summer streamflow, as a consequence of increased evapotranspiration [see e.g., 10, 20, 22, 151]. Here we challenge the general validity of such assumptions by employing a multi-method approach in which inferential statistics techniques, change point detection methods and distributed hydrological modeling are used for a rigorous identification of the drivers of hydrological changes in a large Alpine catchment, i.e. the Adige River Basin (northeastern Italy). From a preliminary data analysis (Figure 1.1), it is worth noting that there are not evidently increasing temperature trends in the Adige catchment in the last 90 years. The time series of the mean monthly and annual temperatures, obtained by averaging daily data from all the stations within the catchment, cover the period 1924-2013.

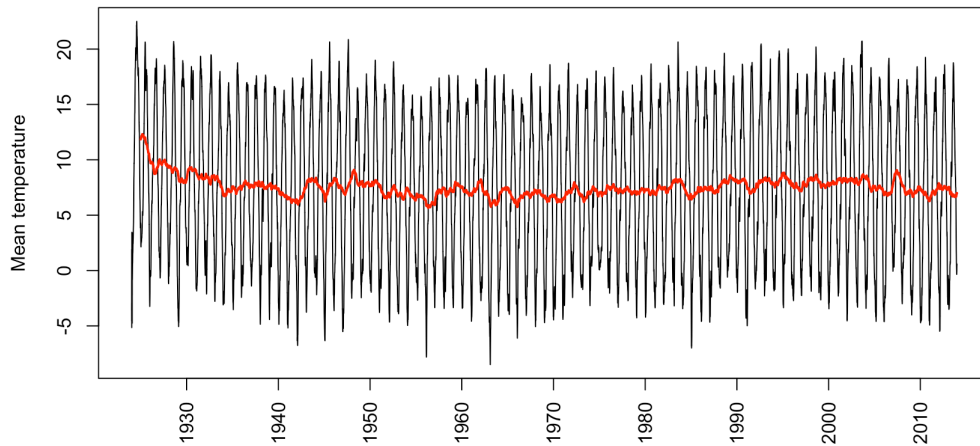


Figure 1.1: Time series of the monthly (black) and annual (red) mean temperatures of the Adige River Basin in the period 1924-2013.

The Adige catchment has been selected as a case-study in the FP7 project GLOBAQUA [124], because representative of the following stressors affecting Alpine river basins: i) hydropeaking and thermopeaking caused by hydropower production [181, 182]; ii) emerging and regulated pollutants released by waste water treatment plants depending on the touristic fluxes, which lead to variations in the local population of more than 600% in some touristic areas of the Adige catchment; iii) climate change which is expected to impact the hydrological cycle by reducing winter snowfall with the consequent reduction of late spring and summer runoff [32]; iv) pollutants transported by atmospheric circulations and stored in retreating glaciers which are released at low concentrations as an effect of increasing temperatures as observed in the Italian Alps [165] and in other Alpine regions [23].

In particular, we analyzed changes of hydrological time series in the southeastern part of the Alpine region by considering nested catchments of size ranging from 207 km^2 to $9,852 \text{ km}^2$ within the Adige River Basin. Traditional trend analysis [see e.g., 78, 88, 114] was performed for the hydro-meteorological variables aggregated at the sub-catchment scale, with the

comparison among observed changes which permitted to detect spatial patterns of change and to identify the associated local drivers' effects. In addition, since the temporal patterns of precipitation and temperature are important determinants of the water budget [150], seasonal analysis was also performed in order to detect intra-annual variations of the hydrological fluxes, and hence to attribute them to season-specific drivers. Great effort was made in the attempt to explore variability at the finer spatial and temporal resolution that the data allow, using for the present work daily data at a 1 km^2 grid resolution. Notice that previous studies worked at most at monthly scale and about 40 km^2 grid resolution. Aimed at quantifying the reliability of the results, we implemented an uncertainty analysis of the interpolated precipitation. To this purpose, we performed the spatial inference of meteorological variables by means of kriging algorithm, which allowed to compute the conditional variance in each location and hence to measure the uncertainty associated with the estimate. Indeed, in Alpine regions, the major source of uncertainty is the smoothing, and in some cases the bias, introduced in the precipitation field by the techniques used to transfer the available data on the computational grid [98, 171]. Furthermore, correlation and multi-regressive analyses have been performed to identify linear relationships between changes in streamflow and possible concurrent drivers [see e.g., 73, 83]. Finally, we applied distributed hydrological modeling with a natural scenario (i.e., excluding the presence of human infrastructures) in order to explicitly identify the climatic effects on streamflow. We compared these simulated fluxes with the observed streamflow by means of a change point detection method (i.e., the Pettitt's test) which recognizes statistically significant discontinuities in the time series and, coupled with hydrological modeling, allows

to identify the moment in time in which anthropogenic effects have altered the natural behavior of the hydrological fluxes. This branch of research led to a contribution submitted to Water Resources Research [113].

Hydroclimatic trends across three European river basins

Whereas numerous studies have analyzed climate trends in Europe, only few consider trends in climate and streamflow [104] of the river basins in this region. For example, several studies have focussed on trends in water quality parameters in the Iberian Ebro River Basin without explicitly considering the influence of long-term streamflow patterns on those trends [3, 25, 100]. Similarly, while local studies of specific stressors have been conducted, there is a lack of integrative studies at basin scale for the Adige catchment in North Italy [37]. In addition, data limitations in major river basins often restrict analyses of streamflow trends to a relatively short time period or a few gauging stations along the main river course [21, 104, 168]. Hence, there is a lack of research on the linkages between long-term trends in climate and streamflow in European river basins. Moreover, there has been little discussion about differences in these trends across Europe. Studies that do compare trend patterns in different European regions are mostly limited to temperature and precipitation analyses [87, 135]. This study, in contrast, seeks to provide an integrated analysis of recent trends in climate and streamflow, applied in three contrasting European catchments. The river basins in this study cover different climatic conditions (i.e., alpine, continental and semi-arid) and diverge in their climate predictions from General Circulation Models [61]. Due to the variety in the study basins, this work can thus be considered as a benchmark for future investigations of hydro-meteorological

trends in European catchments. Moreover, the trend analyses in this study have been harmonized between the different river basins to facilitate comparability among the study basins. Hence, the research goal is (i) to analyze hydroclimatic trends and associated stressors in each river basin, (ii) to identify links and feedbacks between hydroclimatic trends in each basin, and (iii) to compare the study basins with respect to their vulnerability to the identified drivers of change. The comparison between the study basins might be particularly beneficial due to the presence of different spatial patterns of changing climate, which indicates that resilience to changes is not uniformly distributed among the three catchments and depends on local conditions [see e.g., 24]. This research activity resulted in two scientific contributions (i.e., by Lutz et al. [108] and Diamantini et al. [51]) to Science of the Total Environment.

1.2 On the use of hydrological modeling for testing the spatio-temporal coherence of high-resolution gridded precipitation and temperature datasets in the Alpine region

Accuracy of precipitation and temperature data is a crucial requirement for reliable climate impact studies and other analyses such as trends both in present and past hydro-climatic variables and hydrological modeling of future alterations. Indeed, gridded datasets of these climatic forcing [see e.g., 74, 119, for precipitation and temperature respectively] are increasingly used for evaluating, statistical downscaling and bias correction of climate models outputs, as well as direct input of hydrological models. Nevertheless, gridded climate datasets are typically affected by uncertainties and, unfortunately, the error associated with the climate

datasets is generally unknown, since the nature of the sources of uncertainty and the interactions between them are difficult to quantify. In particular, data can be obtained from the interpolation of in-situ measurements, satellite remote sensing or atmospheric reanalysis. The low spatial density of in-situ observations represents a severe limitation for the definition of the effective resolution, and thus for the accuracy, of datasets obtained by interpolation [76]. This is particularly true for precipitation data in complex-terrain regions [84]. In fact, local conditions may add significant inaccuracies in derived gridded products, especially in mountainous areas where the weather stations are typically sparser than in lowlands and valley floors, and their observations are affected by larger errors and longer breakdown periods, due to harsh operational conditions [60]. Hence, precipitation and temperature fields are under sampled at high elevations, thereby leading to over-smoothing effects in the interpolated fields, which may negatively impact accuracy in the distribution of climate variables, particularly of extremes [81]. The interpolation method is an additional source of error, even when sophisticated geostatistical spatial analysis techniques are adopted and auxiliary predictors, like terrain elevation and morphology, are included [14, 46]. For what concerns gridded climate data derived by remote sensing techniques, their accuracy is closely linked to their spatio-temporal resolution (i.e., pixel size and acquisition frequency of satellite images), as well as to the inherent accuracy of the retrieval algorithms applied [39]. For example, satellite rainfall estimates, either based on empirical calibration or physical modeling, are known to be prone to systematic biases, insensitivity to light precipitation, and failure over snow and ice surfaces [90]. Atmospheric re-analyses may also suffer from significant accuracy limitations, mainly due to their

typically low spatial resolution and to the poor representation of sub-grid processes (e.g., convection and associated precipitation) by the selected model parameterization [91, 141], both issues being especially relevant for complex terrain [97]. A comprehensive review of studies investigating the uncertainty of gridded precipitation datasets at European scale can be found in Prein and Gobiet [140], where the authors estimated precipitation uncertainties over Europe by comparing multiple observational and re-analyses products. Differences between datasets (i.e., uncertainties) were found to be of the same order of magnitude of the precipitation biases derived from an ensemble of 8 state-of-the-art Regional Climate Models (RCMs). Differently from the common practice of neglecting this source of uncertainty by selecting a priori a single dataset as observational reference, Prein and Gobiet [140] recommended to consider the full ensemble of precipitation datasets in the RCM evaluation process [see also 41, 158]. Uncertainty in the spatial distribution of meteorological variables propagates through the modeling chain adding uncertainty to the controlling variables in impact studies (the "uncertainty cascade" concept introduced by Wilby and Dessai [173]). In this respect, Weiland et al. [170] observed that the major source of uncertainty is the meteorological forcing, with hydrological parametric uncertainty playing a minor role [see also 67, 123]. At the global scale, the need for accurate precipitation inputs in order to obtain reliable water balance calculations was highlighted by Fekete et al. [56]. Nevertheless, many climate studies based their evaluations on a single observational climatic dataset, without considering the effects of uncertainty associated with that particular choice on the hydrological response [e.g., 176]. On the other hand, with the increasing availability of computational resources, one may be

tempted to fully propagate the observational uncertainty, as well as all other sources of uncertainty, along the modeling chain, with the immediate consequence of generating a large ensemble of plausible projections. These projections may artificially inflate uncertainty by including datasets that perform poorly. The need for reducing uncertainty to generate a plausible range of hydrologic storylines in climate change impact assessments has recently been highlighted in the review by Clark et al. [40]. Furthermore, we argue that the selection of observational gridded datasets should not be "democratic" (using the definition introduced by Knutti [93]), and it should be reasonable to accept that not all the datasets are equally performing.

Here we propose an efficient methodology to rank gridded meteorological datasets according to their coherence with observed streamflow data and possibly reject them when their coherence is judged too low. Coherence is evaluated by benchmarking streamflow, computed with a hydrological model fed by the selected dataset and applied in an inverse modeling framework, against measured streamflow. The rationale behind the proposed approach is to use a physically-based hydrological model as a tool to test the coherence of the meteorological dataset with hydrological observations, namely streamflow. We call this procedure Hydrological Coherence Test (HyCoT). The advantage of such approach is that it condenses in simple and easy to grasp metrics the complex benchmarking process of observational meteorological datasets that would otherwise require a detailed evaluation of the spatio-temporal differences with respect to reference meteorological data. HyCoT conforms with the Bayesian update rules, in the sense that the selection of the datasets showing enough coherence can be interpreted as the choice of both an informed prior

distribution and the likelihood used to obtain the a-posteriori distribution, being proportional to the efficiency index of each dataset [e.g., 19, 112, 147]. We focus on prediction of streamflow at the basin scale, hence the selection of the hydrological model, its level of complexity and the metric to be employed for the comparisons is goal-oriented. Other objectives (e.g., the prediction of streamflow, water content, groundwater flow or any other hydrological quantity of interest) would have required other approaches or setting [e.g., 58, 70]. Hence, this work may represent a methodological framework easily extendible to other hydrological conceptual models, hydrological quantities and efficiency metrics. Accordingly, the present contribution is built over three main steps: i) to present the uncertainty of an ensemble of observational gridded datasets of precipitation and temperature available in the Alpine region, evaluated by comparing them in terms of spatio-temporal distributions; ii) to perform an integrated assessment of the datasets coherence by employing the HyCoT framework in which simulated and observed streamflow time series are compared; iii) to investigate possible corrections of the relatively poor behavior of some datasets by means of a simple rescaling of rainfall totals. To this end, the upper portion of the Adige River Basin is selected as study area, and five climate datasets are included in the analysis, chosen among those characterized by the highest available spatial resolution (from about 22 to 1 km grid spacing). This work led to the paper by Laiti et al. [98], published in *Water Resources Research*.

STUDY SITES, DATA AND METHODS

2.1 Study sites

In this section, a description of the analyzed river basins is presented (i.e., the Adige, Ebro and Sava river basins). Particular attention is drawn to the Adige River Basin, since it has been selected as the reference site for most of the work of this thesis.

2.1.1 Adige River Basin

The Adige is the third largest Italian river (after Po and Tiber) with a contributing area of $12,100 \text{ km}^2$ and the second longest (after Po) with a total length of the main stem of 410 km . It starts its course from a spring close to the Resia lake at the elevation of 1586 m a.s.l. and it ends in the Adriatic sea at Porto Fossone between Brenta estuary and Po river delta [127]. The average water discharge registered at Boara Pisani gauging station ($11^\circ 46' 57.18'' \text{E}$, $45^\circ 06' 27.7'' \text{N}$) is about $202 \text{ m}^3 \text{s}^{-1}$ [7], with peaks usually registered in the period from June to September [138], showing the typical behavior of Alpine

catchments. The Adige river flows through the territories of the Province of Bolzano (62% of the overall river basin surface), the Province of Trento (29%) and the Veneto region (9%). From the source to Merano the Adige flows east through the Venosta valley (with a drainage area of $1,680 \text{ km}^2$). Then, it turns south where it receives the contribution of the Isarco river at Bolzano, and the contributions of both the Noce and Avisio rivers just upstream of Trento, where the drainage area of the Adige river rises, thanks to these contributions, to $9,852 \text{ km}^2$. Finally, it reaches Verona and then it turns east again and flows through the Padana plain without receiving other significant contributions since, from the town of Albaredo and for about 110 km to the Adriatic sea, the river is mainly suspended through argins. For this reason, hydrological analyses have been conducted in the northern part of the catchment (i.e., closed at the gauging station of Vó Destro; $10^\circ 57' 27.2'' \text{ E}$, $45^\circ 44' 06.7'' \text{ N}$). The main tributaries of the Adige river are the following: Passirio, Isarco, Noce, Avisio and Fersina. The river basin encompasses 550 lakes, most of which have a surface smaller than 1 ha and of glacial origin. The biggest natural lake is Caldaro (140 ha), followed by Anterselva, Braies and Carezza in the Province of Bolzano, Lake Tovel and Terlago in the Province of Trento. Glaciers are carefully monitored within the catchment, since they strongly influence the annual flow regime and due to the increasing concern related to the observed acceleration in melting caused by rising air temperatures [7]. Analysis of land cover changes as retrieved by CORINE (<http://www.eea.europa.eu/publications/COR0-landcover>) products in 1990 and 2012 showed that glaciers have reduced their surface extent with a negative trend of about $2.3 \text{ km}^2 \text{ year}^{-1}$. According to the last report from the basin authority [7], glaciers cover an area of 212 km^2 , corresponding to 1.9% of

the catchment's area at Verona. Climate in the Adige River Basin is characterized by dry winters, snow and glacier-melt in spring, whereas it is humid during summer and autumn. Annual average precipitation values range between 500 *mm* in Val Venosta and 1,600*mm* in the southern part of the basin. Streamflow shows a typical Alpine regime with two peaks, one in spring due to snowmelt and the other in autumn due to cyclonic storms, which are the main cause of flooding events. In winter, when the precipitations within the catchment are chiefly solid, streamflow is minimum. Summers are typically wet and dominated by short and intense convective storms. The Adige river provides water to 34 large hydropower plants (average nominal capacity larger than 3 *MW*) with a total effective power of 650 *MW* [7]. Water management for hydropower production is performed with 28 reservoirs, 15 in the Province of Bolzano and 13 in the Province of Trento, with an operational total storage of $561 \times 10^6 \text{ m}^3$. The two largest reservoirs are Resia and Santa Giustina, with a storage of $116 \times 10^6 \text{ m}^3$ and $172 \times 10^6 \text{ m}^3$, respectively; 11 reservoirs have a storage between 10×10^6 and $50 \times 10^6 \text{ m}^3$; 11 between 1×10^6 and $10 \times 10^6 \text{ m}^3$, whereas the remaining 4 have storage smaller than $1 \times 10^6 \text{ m}^3$ [7]. In addition to the aforementioned large hydropower plants, about 1,050 small hydropower plants are distributed within the river basin [127, 130]. We notice that aggregated values relative to hydropower production are reported differently depending on the information provided by the two managing authorities [127, 130]. In the Province of Bolzano, the mean annual hydropower production amounts to 6940 *GWh*, while total average nominal licensed water discharge for hydropower production in the Province of Trento is about $404 \text{ m}^3 \text{ s}^{-1}$. Besides the presence of hydropower the basin is intensively exploited with a large number of small

withdrawals associated to a variety of water uses: agricultural, civil and industrial. Average nominal licensed water discharge is lower than 0.5 l s^{-1} for 70% of the derivations, percentage that increases to 90% for a threshold of 1 l s^{-1} . In the Province of Bolzano the second highest water demand, after hydropower, is for irrigation, followed by industrial and other uses, and finally for drinking water supply [127]. Similarly, in the Province of Trento, the largest licensed average annual volume is for hydropower, followed by irrigation, domestic and livestock, and industrial uses [130]. Moreover, 153 water withdrawals from the Adige main stream, its tributaries and channels connected to the river network in the portion of the basin within the Veneto region. In this case the main water uses are for agriculture, with the rest being distributed between civil (i.e., drinking), industrial and other uses. The main streamflow alterations at daily time-scale in the Adige catchment are due to hydropower exploitation, occurring mainly in the northern part of the catchment. Indeed, the large elevation range and the humid climate make the river basin suitable for hydroelectric production. There are 34 major power plants, leading to a significant streamflow alteration in the basin, particularly at intermediate and low flow regimes [181]. As a consequence substantial alterations in stream velocity, turbidity and water temperature [182], and stress to the benthic invertebrates communities [28] have been observed. Droughts are more frequent in the southern part of the river basin (particularly in summer), and increase the risk of salt water intrusion [7]. Such drought events often generate conflicts between stakeholders of the hydropower and agriculture sectors. Imposed water releases from hydropower plants are sometimes unable to counterbalance the droughts, allowing saltwater intrusion to propagate upstream the river

mouth [7] and making streamflow too low to guarantee both agricultural water uses and ecological functionality of the river. In a review paper [37] it is stressed the need for finding suitable water management solutions to alleviate the effects of hydropower exploitation on the ecosystem. Nevertheless, the variety of water uses in the Adige causes increasingly conflicts in spring and summer between irrigation water demand, hydropower, recreational activities and drinking water needs. Competition is likely to increase in the future as a consequence of the observed negative trends in streamflow time series, which showed a reduction of water availability in the last decades. According to current projections, climate change may impact significantly the hydrology of Alpine catchments and its ecosystem [see e.g., 16, 17, 166]. In a recent contribution, Majone et al. [112] highlighted that, in the next decades, warming will lead to changes in the seasonality of streamflow for the Noce catchment as a consequence of less winter precipitation falling as snow and melting of winter snow occurring earlier in spring. Furthermore, a moderate reduction of snow and ice storage is projected for 2020-2050 in the entire Alpine region, with a more drastic change in the second half of the century [55]. The reduction of snowfall accumulation due to the increase of winter temperature will likely reduce streamflow in late spring and summer, while an increase is expected in winter as snowfall elevation is projected to increase. These result are confirmed by a recent analysis conducted by Meteotrentino [118], which estimated for the glaciers of the Province of Trento a reduction of surface by almost 40% in the last 50 years. Changes in the evapotranspiration regime will also affect lower elevation streams due to the combination of increasing temperatures and longer vegetative season, thus leading to higher water demands [48] and likely exacerbation

of conflicts among different and often-competing water uses. Projected impacts on streamflow and water resources availability are expected to significantly affect the hydropower sector. Therefore, actual water management strategies will need to adapt to the changing climatic conditions. Recent studies conducted in the Noce tributary [112] evidenced that changes in water availability are reflected in hydropower potential of the catchment, with larger changes projected for the hydropower plants located at the highest altitudes. Another interesting result is that the introduction of prescriptions for Minimum Ecological Flow may reduce hydropower potential by 8-9% with respect to the situation in which only the effect of climate change is considered. As highlighted in a recent commentary by François et al. [59], integration of hydropower with other renewable energies, and the need of a shared and not conflicting use of water resources with other important water uses (like e.g., agriculture, recreational activities, ecological functionality preservation), pose new challenges to the hydrological community. Available studies conducted in the Adige river basin cover however limited areal extensions and they analyze only individual aspects of the land use-climate change-energy nexus Majone et al. [112]. An integrated environmental assessment of the linkages between these compartments, including effects relevant at different temporal scales, and their impacts on socio-economic sectors is therefore needed. It is worth noting that hydropower production can yield to hydrological alterations chiefly at sub-annual scale, due to the fact that water volumes accumulated by the reservoirs are typically released within the time-span of 1 year. Hence, agricultural activities could have a grater impact on hydrological stresses at larger scales. The Adige catchment a rich large-size catchment, in terms of data

availability. Furthermore, it shows a significant variability in terms of land use, water use and hydrological driving forces. Water management is also differentiated throughout the catchment and different climatic conditions (from Alpine to subcontinental) lead to a considerably high invertebrate biodiversity. This allows using this basin as a benchmark for testing and validating models of ecosystem functioning, pollutants cycling, including their penetration in the food chain, as well as the effects of new water policies and water management strategies on the ecosystem. In addition, the stressors relevant for the Adige catchment are common to most Alpine catchments. The impact of hydropower production on the hydrological cycle is a common issue throughout the Alps [181]. Therefore, the presented data can be used for further comparative studies between Alpine catchments.

2.1.2 Ebro River Basin

The Ebro River Basin is located in the North of Spain with small parts in France and Andorra. It extends from the Pyrenees and the Cantabrian Range in the North (maximum altitude of more than 3,000 *m*) to the Iberian Range in the South (up to more than 2,000 *m*) and the Coastal Range (up to 1,200 *m a.s.l.*) in the East [106]. The Ebro River has a length of 910 *km* and discharges into the Mediterranean Sea with a mean discharge of 425 $m^3 s^{-1}$. With a catchment area of 85,362 km^2 , the Ebro is the largest river basin of Spain. Annual mean temperature between 1920 and 2000 was 11.4°C (with temperature extremes of below -20°C in winter and up to 40°C in summer), and mean annual precipitation in the same period was 620 $mm year^{-1}$ (with extremes of 3,000 $mm year^{-1}$ in the Pyrenees and less than 100 $mm year^{-1}$ in the Ebro river valley [146]). The climate is mostly of continental Mediterranean type

and ranges from semi-arid in the center of the river valley to oceanic in the Pyrenees and Iberian Mountains [146]. The main land use types are agriculture (47.1 %), natural grassland (25.5%), and forest (22.3%; [146]). The main river course and tributaries of the Ebro are profoundly regulated by a total of 187 reservoirs having a capacity of 57 % of the average annual discharge [11]. The main function of the reservoirs is to provide water for hydropower use and irrigation of agricultural land.

2.1.3 Sava River Basin

The Sava River is a transboundary river and flows through 6 countries (i.e., Slovenia, Croatia, Bosnia and Herzegovina, Serbia, Montenegro, and a minor part in Albania). It is formed by two headwaters (i.e., the Sava Dolinka and the Sava) and has a length of 945 *km* excluding the headwaters [85]. The Sava River drains into the Danube in Belgrade (Serbia) with a discharge of about 1,700 $m^3 s^{-1}$ [95]. Having a catchment area of 97,713 km^2 , the Sava River Basin is the second largest tributary basin of the Danube after the Tisza River Basin. Altitudes in the Sava River Basin range from 71 *m* above sea level at the catchment outlet to more than 2,860 *m* in the Slovenian alpine headwaters [85]. Annual mean temperatures range from 6°C in the mountain regions to 13°C close to the river mouth [168]. Mean annual precipitation is 1100 mm, ranging from 2000 to 3000 mm in the Alpine region to 660 mm close the river mouth. Climatic conditions along the Sava River change from alpine to pannonian to continental. The main land cover types are forest and semi-natural areas (55 %) and agriculture (42%; [43]). Forest is the main land cover in the upstream part in Slovenia and South of the main river course. Since the end of the 19th January, 19 large dams have been constructed along the Sava River with the main purpose of hydropower generation [104].

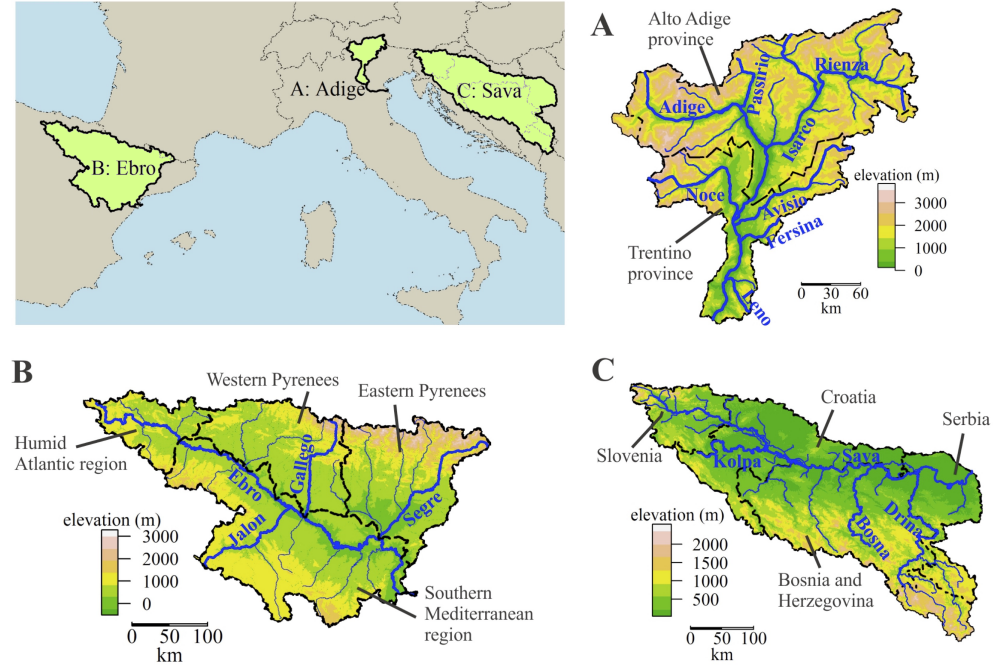


Figure 2.1: Overview of location of study basins and relief in the Ebro, Sava, and Adige River Basins.

2.2 Data

2.2.1 Meteorological data

The rationale in the selection of meteorological data was to use the highest spatial resolution available in each river basin (1 *km* for the Adige River Basin, around 10 *km* in longitude and 14 *km* in latitude for the Ebro River Basin, and around 20 *km* in longitude and 27.5 *km* in latitude for the Sava River Basin). In fact, the attempt to reach a common spatial resolution for all case studies would require a much coarser resolution of the Adige dataset than possible based on the local data, which would not correctly represent the hydro-meteorological phenomena at local scale. The selections of the time windows to analyze were different according to the various objectives of this research.

Adige River Basin On the basis of meteorological station data provided by the Austrian Zentralanstalt für Meteorologie und Geodynamik [www.zamg.ac.at] and the meteorological offices of the Autonomous Provinces of Trento [www.meteotrentino.it] and Bolzano [www.provincia.bz.it/meteo], a regional precipitation and temperature dataset (hereafter named ADIGE) has been independently developed for the Adige river basin. The dataset results from 244 time series of precipitation and 350 of temperature recorded since 1920. The data were interpolated over a 1-km grid at a daily time step by means of the kriging with external drift (KED) algorithm [66]. A detailed description of the methodology applied to obtain this dataset of precipitation and temperature is presented in Section 2.3.1. Other Four gridded climate datasets were selected and added to the analysis. They are characterized by relatively high nominal spatial resolutions (grid spacing $< 25\text{ km}$) and a daily temporal aggregation. Almost all datasets have been extensively described in the literature. In particular three of them have been included in the assessment of precipitation data over the Alpine region by Isotta et al. [84]. Based on data availability, the 1989-2008 period was identified as common time frame for the analysis. Notice that temperature data are not available for MSWEP and APGD datasets.

E-OBS [76] is a pan-European gridded dataset of daily mean, minimum and maximum temperature and total precipitation, available starting from 1950. Interpolation to a 0.25° (about 22 km) latitude-longitude regular grid was performed using observational gauge data from the ECA&D dataset [92]. The product was originally developed under the ENSEMBLES EU-FP6 project [www.ensembles-eu.org] and continuously updated under the EURO4M project [www.euro4m.eu] (here v. 13.0 is used). Since its publication, E-OBS represents the

state-of-the-art reference dataset and has been widely used for regional climate model evaluation and climate monitoring over Europe [see e.g., 154].

The recently released Multi-Source Weighted-Ensemble Precipitation (MSWEP) dataset [13] is a global precipitation dataset specifically designed for hydrological modeling, covering the 1979-2015 period on the same grid of E-OBS. Gridded precipitation is obtained as a weighted combination of data from seven datasets: two from interpolated gauge observations, three based on satellite remote sensing and two reanalysis products from numerical weather prediction models. The database includes an a-posteriori correction for gauge under-catch and orographic effects.

The MESoscale ANalysis system (MESAN; [99]) was developed by the Swedish Meteorological and Hydrological Institute. ERA-Interim global reanalyses [47] are first dynamically downscaled to a 0.22° grid to obtain HIRLAM regional reanalyses [45], that are further downscaled to a 0.05° (about 5 km) grid and then used as first-guess field for the assimilation of surface station measurements from the ECA&D dataset to finally produce the gridded product. For the present work, daily values of temperature (mean, minimum and maximum) and precipitation, available for the years 1989-2010, have been considered.

The Alpine Precipitation Grid Dataset (APGD; [84]) estimates the distribution of daily precipitation over the Greater Alpine Region for the period 1971-2008, on the basis of measurements from more than 8500 rain gauges. The unprecedentedly high density of input observations contributes to its very high effective spatial resolution, estimated by the authors in approximately 10-20 km [84]. APGD data (RapdD 1.2 version) are provided on a grid with a nominal resolution of 5 km.

Ebro River Basin For the Ebro River Basin, temperature and precipitation data were taken from version v4 of the Spain02 dataset (freely available at http://meteo.unican.es/thredds/catalog/Spain_CORDEX_grids-/catalog.html). This dataset provides grids of daily precipitation and average temperature at 0.11°-resolution in rotated coordinates (according to Euro-CORDEX) for Spain and the Balearic Islands between 1971 and 2007. The data were derived from a quality-controlled subset of point measurements of the Spanish Meteorological Agency (AEMET). We opted for this dataset because of its finer spatial resolution compared to the E-OBS gridded dataset available for entire Europe [76]. For this study, the temperature and precipitation grids were first mapped on a 0.125° regular grid and then cropped to the Ebro River Basin area.

Sava River Basin For the Sava River Basin, temperature and precipitation data were extracted from version 12.0 of the E-OBS gridded dataset ([76]; freely available at <http://www.ecad.eu/download/ensembles/download.php>). This quality-controlled dataset comprises daily grids of mean temperature and precipitation from 1950 to June 2015 at different resolutions for entire Europe. In this analysis, the grids with the finest resolution (0.25° regular grid) were used and cropped to the area of the Sava River Basin.

2.2.2 Streamflow data

Adige River Basin Streamflow data in the Adige River Basin, continuously registered at 58 gauging stations, have been provided by the Hydrological Offices of the Autonomous Provinces of Trento [www.floods.it] and Bolzano [www.provincia.bz.it/hydro]. Some of them provide daily

historical data for the last two decades, while others (e.g., the gauging station in Trento which has a drainage area of about $9,700 \text{ km}^2$) have been continuously operated since 1920.

High-resolution data are also available with the time step of 10 minutes. For this study, sub-daily time series were aggregated to daily scale in order to extend and to fill the gaps of the daily time series.

In the attribution exercise of hydrological changes, specifically applied to the Adige catchment, we considered in particular four gauging stations (i.e., Adige at Trento and Bronzolo, Avisio at Soraga and Gadera at Mantana; see Figure 2.2). The rationale in this selection was to include the longest time series of station located in representative sub-basins, characterized by peculiar climatic and water uses conditions.

Ebro River Basin In the Ebro River Basin, mean daily streamflow was obtained from the Confederaciòn Hidrogràfica del Ebro (CHE). A total of 296 streamflow gauges with data until September 2012 are listed in the CHE database, but the amount of years with streamflow measurements greatly varies between stations. We pre-selected stations with streamflow data from 1971 on and water quality data of more than 10 years.

Sava River Basin In the Sava River Basin, daily streamflow data can be obtained from the Global Runoff Data Centre (GRDC; provided by the Bundesanstalt für Gewässerkunde, BfG), the TransNational Monitoring Network (TNMN; initiated by the International Commission for the Protection of the Danube River, ICPDR) and national water agencies of the countries within the Sava River Basin. The temporal and spatial resolution and length of these time series greatly differ. Apart from Slovenia, daily streamflow data from national water agencies are barely available for more than a few years.

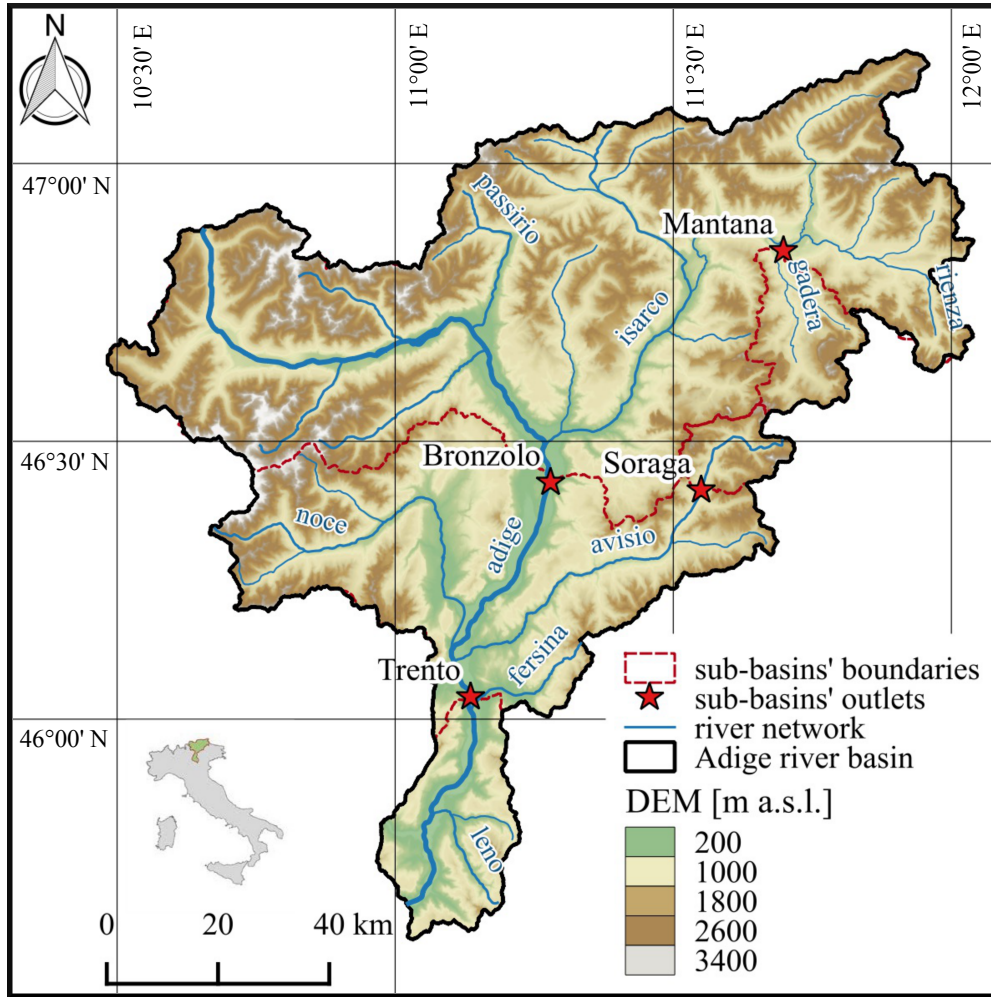


Figure 2.2: Location of the four selected sub-catchments within the Adige River Basin. The inset in the lower-left panel shows the location of the Adige River in the Italian territory.

Gap filling For the Ebro River Basin and Sava River Basin datasets, gaps of one day in daily streamflow were set to the average of discharge one day before and after the day with missing data. Gaps of more than one day were filled based on discharge data from donor stations (i.e., "similar" stations in the dataset) according to Hughes and Smakhtin [82]. First, all stations with a Pearson's correlation above 0.8 in daily streamflow were chosen as potential donor stations for each site [106]. Second, monthly flow duration curves (i.e., empirical distribution functions of discharge values separated per month)

were calculated for all stations. Third, gaps were filled with the discharge value of the flow duration curve at the target station evaluated at the flow percentile value of the donor station on the respective day with missing data. As donor stations might have a gap on the same day as the respective target station, this procedure had to be repeated for all potential donor stations in descending order of the correlation coefficients until the gap was filled or all donor stations were checked. The remaining data gaps were not filled. Gap filling was not necessary for the Adige River Basin, as time series of daily streamflow were complete in the considered time frame.

2.3 Methods

The techniques illustrated in the following are applied to reach two different goals: the former is the detection and attribution of trends in streamflow, precipitation and air temperature time series in the Adige River Basin (Section 2.3.1) and the comparison of these trends with those of other European river basins (Section 2.3.3); the latter is the evaluation of the hydrological coherence of different climate datasets, widely used in literature for climate change impact studies, in order to discourage the use of those that are not appropriate for simulating streamflow (Section 2.3.4).

2.3.1 Attribution of hydrological changes in the Adige River Basin

Interpolation of meteorological data The first step in performing a hydrological budget is to determine the spatial distribution of precipitation and temperature within the catchment of interest from available measurements at meteorological stations and then average over the catchment

itself. The average was estimated as the arithmetic mean of the values interpolated over a regular 1 km -size grid. Preliminary evaluations showed that using a finer grid resolution would not improve the accuracy of the estimates. The quantities that are first interpolated and then spatially averaged are the daily precipitation as well as daily minimum, maximum and mean temperatures. All these time series were interpolated by using both Ordinary Kriging (OK) and Kriging with the External drift (KED) (Goovaerts [66]). We used a geostatistical interpolation scheme because it provides both the conditional mean and standard deviation of the estimate at each grid note, which has been used to obtain the most probable mean and its interval of confidence in all the sub-catchments where the trends are performed.

Kriging accounts for the proximity of data x_i to the location x (being estimated through the covariance terms $C_R(x_i, x)$) and it informs the system on data redundancy. In fact, weights decrease as the data location are far from the estimation location and they can also be negative when clustered data screen one to each other, leading, in some cases, to nonphysical estimates. In order to deal with negative weights we applied the simple and robust correction suggested by Deutsch (Deutsch [50]) but only when the interpolation resulted in negative precipitations. According to this scheme, negative weights, which absolute value was larger than a selected threshold, are set to zero and the remaining rescaled such as they sum to 1, as required by the first condition of unbiased estimation. Notice that since our dataset is composed by a rather homogeneous distribution of the meteorological stations only rarely the solution of the kriging system produced negative weights. All these cases were recorded and carefully analyzed before accepting the interpolated value.

Interpolation was conducted with both OK and KED by using measurements at the closest 8, 16 and 32 meteorological stations, thereby obtaining 6 independent estimates at each grid node. Leave-one-out cross-validation was then used to select the most suitable interpolation scheme and the optimal number of neighboring stations (Goovaerts [66]). This procedure indicated KED with 16 stations as the most suitable interpolations scheme for all the four interpolated variables (precipitation, mean, maximum and minimum temperature). The obtained mean of the absolute error was 1.3 mm for daily precipitation and 0.02 °C for the daily average temperature. In the Kriging With External Drift (KED) the estimate, $Z(x)^*$, of the variable Z at the location x is expressed as a linear combination of $n(x)$ measurements $z(x_i)$, located at x_i , $i = 1, \dots, n(x)$:

$$Z^*(x) = \sum_{i=1}^{n(x)} \lambda_i(x) Z(x_i) \quad (2.1)$$

where $\lambda_i(x)$ is the weight assigned to the measurement $z(x_i)$. The standard deviation of the estimation error is given by $SD[Z(x)] = \sqrt{\sigma_Z^2(x)}$, where $\sigma_Z^2(x)$ is the conditional variance at the location x provided by Eq. (2.3). The system of $n(x) + 2$ linear equations providing the $n(x)$ weights $\lambda_i(x)$, $i = 1, \dots, n(x)$ to be used into Eq. (2.1) assumes the following form:

$$\begin{cases} \sum_{j=1}^{n(x)} \lambda_j(x) C_R(x_i, x_j) + \mu_0(x) + \mu_1(x) y(x_i) = C_R(x_i, x), & i=1, \dots, n(x) \\ \sum_{j=1}^{n(x)} \lambda_j(x) = 1 \\ \sum_{j=1}^{n(x)} \lambda_j(x) y(x_j) = y(x) \end{cases} \quad (2.2)$$

where $\mu_0(x)$ and $\mu_1(x)$ are the Lagrangian multipliers, which are introduced such as to transform the minimum of the error variance $\sigma_Z^2(x)$ under the unbiased condition that the ensemble mean of the estimate $Z^*(x)$ is equal to the theoretical (unknown) mean $\langle Z(x) \rangle$ into the unconditional

(absolute) minimum. In addition, $C_R(x_i, x_j)$ is the covariance function, which for a stationary random function depends only on the distance between the pair of nodes respect to which it is evaluated, i.e. $C_R(x_i, x_j) = C_R(x_i - x_j)$.

The minimized error variance (i.e. the variance of the random variable Z conditional to the $n(x)$ measurements) is given by:

$$\sigma_Z^2(x) = C_R(0) - \sum_{i=1}^{n(x)} \lambda_i(x) C_R(x_i, x) - \mu_0(x) - \mu_1(x) y(x) \quad (2.3)$$

Potential Evapotranspiration Model Reference crop potential evapotranspiration (ET_0) has been estimated by using the Hargreaves - Samani model [e.g., 72, 149, 157] (2.4), which we preferred to Pennman-Montieth model due to the very limited availability of meteorological data other than temperature and precipitation. According to the Hargreaves - Samani model the Potential Evapotranspiration ET_0 [$mm d^{-1}$] of a reference crop (grass) under standard conditions is given by:

$$ET_0 = 0.408[0.0023 \times RA \times TD^{0.50} \times (T_{mean} + 17.8)] \quad (2.4)$$

where RA is the theoretical solar radiation [$MJ m^{-2} d^{-1}$], which depends only on the location (i.e., the effect of topographic shadow and cloud cover is not included), $TD = \bar{T}_{max} - \bar{T}_{min}$ is the difference between the daily maximum \bar{T}_{max} and minimum \bar{T}_{min} temperature [$^{\circ}C$] and T_{mean} is the daily mean temperature [$^{\circ}C$].

Potential evapotranspiration, is then obtained by multiplying ET_0 by crop coefficients K_c (Allen et al. [5]): $ET_p = K_c ET_0$, with K_c depending on the site-specific vegetation and of the growth stage. In addition, following Hargreaves [71], Allen et al. [5] and PAT [130], a 30% reduction factor was applied, in order to counterbalance the tendency of the Hargreaves-Samani model (Eq. 2.4) to overestimate ET_p under non-standard conditions.

ET_p represents the upper limit of actual evapotranspiration, since saturation conditions at the land's surface and atmospheric conditions may reduce the maximum amount of water that crops and vegetation may absorb in the absence of water stress (McMahon et al. [115]). Therefore, climate-driven actual evapotranspiration AET_{clim} has been computed as follows: $AET_{clim} = \alpha ET_p$, where $\alpha < 1$ is a stress factor reducing the potential evapotranspiration. The method used to infer α is described in the following paragraph.

Water budget At the (sub-)catchment scale the annual water budget assumes the following form:

$$P - Q - AET - \Delta V = 0 \quad (2.5)$$

where P [mm] is the precipitation total, Q [mm] is the annual streamflow volume, AET [mm] is the actual evapotranspiration and ΔV [mm] denotes annual change in water storage.

The last two terms of equation 2.5 are typically unknown since they cannot be measured directly. Since no other equations can be written involving only these terms, a closure hypothesis should be introduced. As customary, and following Destouni et al. [49] and Levi et al. [104], we introduce the assumption that the inter-annual storage ΔV is negligible. With this hypothesis Eq. (2.5) applied at the annual scale leads to:

$$P - Q - AET_{wb} = 0 \quad (2.6)$$

with AET_{wb} usually termed as "water balance constrained Actual Evapotranspiration" [49] and accounting for both climate-driven and water uses changes. Eq. (2.6) can thus be generalized to include explicitly water uses W :

$$P - Q - \alpha ET_p - W = 0 \quad (2.7)$$

where, $\alpha = (\bar{P} - \bar{Q}) / \bar{ET}_p$, and \bar{P} , \bar{Q} and \bar{ET}_p are the long term averages of annual hydrological fluxes present in Eq. (2.7) evaluated during the period 1920 -1950, when water uses can be considered marginal in the Adige catchment such that $\bar{W} \simeq 0$ (Zolezzi et al. [181]). The resulting value of the stress coefficient, evaluated for the Adige basin closed at the gauging station of Ponte S. Lorenzo at Trento (Italy) is of $\alpha = 0.6986$. Other methods for estimating α are discussed by Lyra et al. [109]. With this approach it is thus possible to disentangle the pure climate-driven evapotranspiration ($AET_{clim} = \alpha ET_p$) from water uses (W). In fact, Eq. (2.7) can be used to obtain the effect of water uses W on the water budget of the sub-catchments described in Section 2.1 (see also Figure 2.2).

Mann Kendall Trend Analysis Time series of the aforementioned hydrological variables (P , αET_p) have been calculated at each cell of the grid following the procedure described in Section 2.3.1 and then aggregated over the drainage area of the 4 selected sub-catchments. Successively, trends of P , αET_p and Q were calculated by applying the nonparametric Man Kendall test (Mann [114], Kendall [88], Hirsch et al. [78]). The MK-test is applied for detection of monotonic increasing or decreasing trends independent of the underlying parameter distribution. It has been widely used for trend analysis of hydroclimatic time series. we used the R-statistics package "Kendall". Field significance of streamflow trends was assessed by the bootstrap method described in Yue et al. [177]. The sign and magnitude of trends was determined by Sen's slope estimator [153], whereas the statistical significance of trends was defined using a significance level of 5% by considering both annual and seasonal aggregations and a moving time window of 30 years. The width of the moving window was selected in order

to mitigate the effects of small (temporal) scale fluctuations (see e.g., Szolgayova et al. [159] and Zolezzi et al. [181]).

Change point detection Disentangling trends in hydrological fluxes due to anthropogenic and climatic causes is a daunting task, particularly when data on water uses are highly uncertain or not available. Promising methodologies are based on the observation that changes in water uses are typically sharp, and therefore they may be detected by means of change point detection methods, though their effect on streamflow is often masked by natural variations of hydrological fluxes. In the present study we used the Pettitt's test [134] to identify sharp changes in streamflow time series. The Pettitt's test, which is used in hydrology [see e.g., 148], verifies the null-hypothesis of no change in the hydrological time series against the alternative hypothesis of change, with the initial distribution unknown. The test uses a non-parametric statistic K_T , defined as follows:

$$K_T = \max |U_{t,T}|, \quad (2.8)$$

where

$$U_{t,T} = \sum_{i=1}^t \sum_{j=1+1}^T \text{sgn}(X_i - X_j) \quad (2.9)$$

X_i and X_j are the two samples (i.e., two subsets of a time series) that are tested to come from the same population. The statistic $U_{t,T}$ is considered for values of t with $1 \leq t < T$. The symbol sgn is the sign function, providing 1, 0 or -1 if its argument is positive, null or negative respectively. If the statistic K_T is statistically significant (i.e., $p \simeq 2 \exp \left(\frac{-6 K_T^2}{T^3 + T^2} \right) \leq 0.05$) the change point is defined by its position in the time series. The analysis was performed by means of the R statistical software package "trend" by Pohlert [139].

2.3.2 Auxiliary statistical methods

The Spearman rank correlation [156] was calculated to estimate the level of correlation between hydrological alterations and the analyzed drivers. Spearman's R is a particular case of the Pearson coefficient in which the data are converted to ranks before calculating the correlation coefficient. Notice that Spearman rank correlation was calculated separately for each of the investigated drivers, in order to identify correlations as general descriptors of the interplay between hydrological alteration and drivers. As a quantitative measure of the influence and relative importance of the processes controlling the hydrological alterations we employed the one-way multivariate analysis of variance [MANOVA; see e.g., 126]. In this way, we could assess the relative weights of the potential concurrent drivers by estimating the share of variance of the hydrological alteration of interest attributable to each one of these factors [see e.g., 6]. The analysis is performed using the R statistical software package "stats" [34] and the assessment of the significance of the MANOVA was based on F-tests.

2.3.3 Comparison of hydrological trends in Europe

MK-trends were also computed in the European river basins considered in this thesis (i.e., Adige, Ebro and Sava) for the annual mean of daily average temperature, annual sum of daily precipitation, annual means of daily mean streamflow, the 10- and 90-percentiles of the annual flow duration curve (i.e., Q10 and Q90, respectively) and annual minimum streamflow on seven consecutive days (i.e., MAM7). Streamflow trends were also analysed in view of sub-basin specific climate trends. To this end, annual averages of daily mean temperature and annual precipitation totals were averaged over the drainage

areas of selected sub-basins and MK-trends were computed for the resulting time series. Overlaying the resulting trend maps with those of the streamflow trends allows highlighting potential relationships and spatial correlations between climate and streamflow. To ensure comparability between the three river basins, the time frames for the trend analyses were set to the longest period possible providing sufficient data in all basins. Trends in climate and streamflow in the Adige River Basin and Sava River Basin were computed for the period 1971 to 2010. In the Ebro River Basin, streamflow trends were also examined for the period between 1971 and 2010, but climate trends were analysed until 2007 only as meteorological data from the Ebro River Basin were not available after 2007.

2.3.4 Hydrological Coherence Test (HyCoT)

Before using them as input in hydrological simulations, all climate datasets were resampled to the same computational grid with 5-km spacing, covering the Adige river basin. This has been done in a conservative way, that is, by first disaggregating each dataset to the highest resolution grid (i.e., the ADIGE grid), by interpolation with the nearest neighbor interpolation method, and then by aggregating the results onto the common 5-km computational grid by areal averaging. Afterwards, five hydrological model inversions were performed using as input precipitation and temperature as combined in the same dataset. Where not available (i.e., for APGD and MSWEP), temperature data have been inherited from the ADIGE dataset. Hydrological simulations were performed with the HYPERstream routing scheme (recently proposed by Piccolroaz et al. [137]), coupled with a continuous SCS-CN module for surface flow generation [120, see Figure 2.3]. HYPERstream routing scheme is specifically designed for being easily

coupled with climate models and, in general, with gridded climate datasets. In fact, HYPERstream can share the same computational grid as that of any overlaying product providing the meteorological forcing, still preserving geomorphological dispersion of the river network [143] irrespectively of the grid resolution. This "perfect upscaling" [see 137]) can be achieved by application of suitable transfer functions derived from a high-resolution Digital Elevation Model of the study area. The continuous soil-moisture accounting model for surface flow generation, based on the SCS-CN methodology, is here coupled with a non-linear bucket model for soil moisture depletion [111].

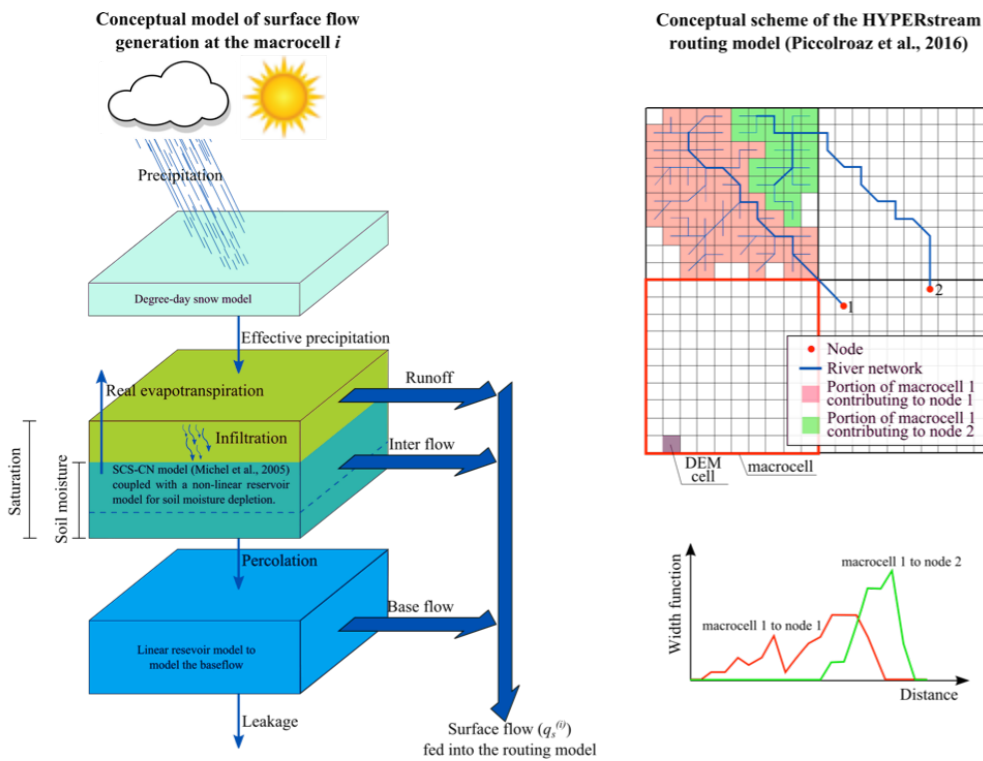


Figure 2.3: On the left it is schematized the surface flow generation module, on the right it is represented the HYPERstream routing scheme applied at each 5-km cell of the computational grid. The conceptual scheme of the hydrological modeling framework is provided by the coupling of the two modules.

As anticipated, the hydrological model was calibrated against

streamflow observations with the meteorological forcing provided by the above mentioned five climate datasets. A genetic Particle Swarming Optimization algorithm (i.e., PSO) [89] was used with the Nash-Sutcliffe efficiency index as objective function to maximize (NSE; [122]). In doing this, Bronzolo and Trento gauging stations were used in a multi-site calibration framework (i.e., NSE is defined as the average of individual efficiencies obtained at the two stations), whereas the remaining six stations were used only for validation purposes. The first two years of the time series, 1989 and 1990, were used as spin up of the simulations and therefore were excluded from the computation of the NSE. The accuracy of performances was also evaluated at all gauging stations using the PBIAS (i.e. Percent BIAS) metric [69]. Positive values of PBIAS are associated to a general underestimation of streamflow, while negative ones denote overestimation.

Application of the methods explained in the previous chapter are presented in the following. In Section 3.1.1 are reported the uncertainty analysis of precipitation estimation, the representation of spatial distribution of hydro-meteorological data and their trends and the comparison of these trends among three European river basins. Finally, Section 3.2 presents the first application of the Hydrological Coherence Test (HyCoT) to the Adige River Basin.

3.1 Hydrological changes: detection and attribution

3.1.1 Detection and attribution of hydrological changes in a large Alpine river basin

Uncertainty of precipitation estimation In the present work we neglected measurement errors at the meteorological stations because of the high reliability of the temperature measurements and the lack of information concerning the

errors associated to precipitation measurements. Instead, we evaluated the uncertainty introduced by the spatialization of point measurements assumed as free of errors [136]. To account for this type of uncertainty, we performed 5,000 Monte Carlo simulations of the precipitation time series associated to each grid cell of the study domain, which were proven to be enough to obtain convergence of the ensemble mean. We also assumed that the precipitation at each grid point follows a Gamma distribution with mean and variance at each time step given by the conditional mean and variance provided by KED, after verifications that the measurements at the meteorological stations follow this distribution [see e.g., 174]. Finally, based on the results of the 5,000 simulations we aggregated the estimates over the four selected sub-catchments in order to derive the average annual precipitation time series and the associated uncertainty. The investigation revealed that the uncertainty bounds in the annual estimates of precipitation (here defined as the average distances between the upper and lower limits of the 95% confidence interval of the annual estimates) were narrow for all the investigated sub-catchments and in the range from 2.2 mm year^{-1} (Adige at Trento) to $15.4 \text{ mm year}^{-1}$ (Avisio at Soraga). The highest uncertainties were found at the headwater catchments of the Gadera and upper Avisio Rivers, due to a limited number of neighboring gauging stations, but it was however lower than the 1.5% of the average annual rainfall total. In view of these results we concluded that the uncertainty linked to the spatialization of precipitation was negligible for this particular case study and thus can be neglected in the ensuing analyses.

Analysis of spatial distribution of hydro-meteorological data

The long term (1956-2013) averages of total annual

precipitation, annual mean temperature and climatic evapotranspiration were evaluated at the center of the cells obtained by dividing the river basin into a regular grid with spacing of 1 km and are shown in Figure 3.1. The annual average precipitation (panel a) ranges from the relatively low 500 mm in the North-West (i.e. Val Venosta) to $1,600\text{ mm}$ in the southern portion of the basin. Typical climatic characteristics of the region, as well as the orographic effect present in the North-East, were clearly captured. As expected, the orographic effect is much more evident for the temperature (panel b) with the long term annual mean that reduces from about $15\text{ }^{\circ}\text{C}$ in the deep valleys to $0\text{ }^{\circ}\text{C}$ at the top of the mountains. Finally, the climatic evapotranspiration AET_{clim} (panel c) was obtained at each point of the grid by aggregating at the annual scale the daily values of the ET_p multiplied by α (see Section 2.3.1). As expected, a strong orographic effect is also observed for this variable, accompanied by a clear reduction from South to North.

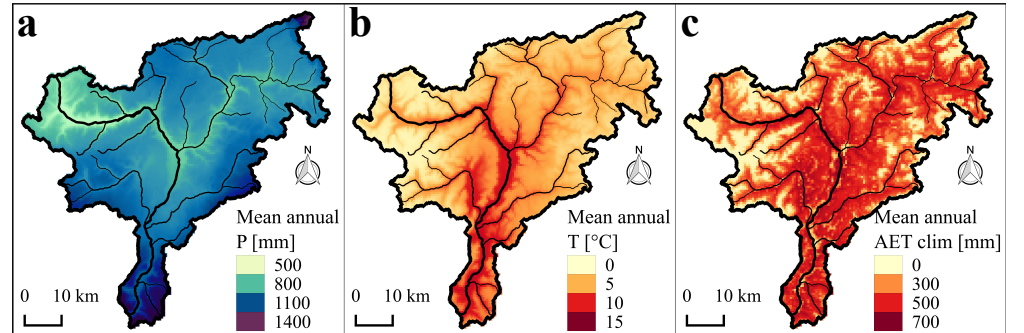


Figure 3.1: Maps of average annual precipitation (a), mean temperature (b) and climatic evapotranspiration AET_{clim} (c) over the Adige River Basin. Averages refer to the period 1956-2013.

The annual streamflow volume Q , expressed in mm , at the four gauging stations of Trento, Bronzolo, Mantana and Soraga is shown in the Figure 3.2a. As customary the volume is normalized with respect to the catchment area. Despite the

large difference in the drainage areas and in the locations within the river basin, the time series of annual streamflow volume are similar in all the gauging stations and they range, in the observational period, between a minimum of about 400 *mm* to a maximum of about 1,200 *mm*. Differences in precipitation between the four sub-catchments are of the same order of magnitude, with the average annual rainfall ranging between a minimum of 600 *mm* to a maximum of 1,400 *mm*, though the total annual precipitation in the upper Avisio catchment (Soraga gauging station) is consistently higher than in the other sub-catchments (Figure 3.2b).

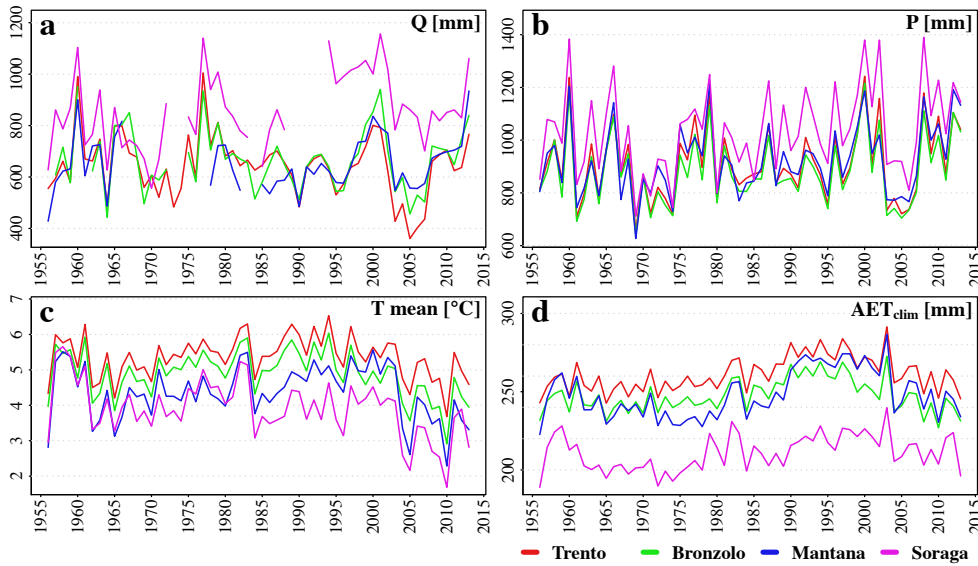


Figure 3.2: Time series of total annual streamflow volume (a), annual precipitation (b), annual mean temperature (c) and annual climatic evapotranspiration AET_{clim} (d) referred to the four selected sub-catchments. All the annual cumulate fluxes are expressed in *mm*.

The mean annual temperature (Figure 3.2c) is always larger than 0 °C in all the sub-catchments and, as expected, influenced by the mean elevation, with the highest values associated to the entire catchment contributing to the gauging station of Trento, being this in line with its lower average elevation compared to the nested sub-catchments. The

influence of elevation on the mean temperature is more evident in the recent years. The annual climatic evapotranspiration ranges from about 200 to 300 *mm* (Figure 3.2d), and in average it reflects the behavior of the mean temperature. It is worth noting that in the upper part of the Avisio catchment, closed at the gauging station of Soraga, evapotranspiration is much smaller than in the other catchments, smaller than one would expect by looking at the mean temperature, only.

Trend analysis Trend analysis was conducted at seasonal and annual time scales by using the Mann Kendall test (see Section 2.3.1) with significance level set to 0.05. Since trends change with time, overlapping moving time windows of 30 years, with origin from 1956 to 1984, were used and the trend was computed moving the window of one year at a time. The results are shown in Figure 3.3 for each sub-catchment at both annual and seasonal time scales with the time axis indicating the initial year of the time window. A filled symbol indicates that the trend is significant, with 5% level of confidence, while empty symbols indicate that the trend is not significant. Analyses are shown for the main water fluxes entering into the hydrological budget (precipitation P , streamflow volume Q and climate-driven evapotranspiration (AET_{clim})).

Annual aggregation of the data (first row of Figure 3.3) evidences relatively large trends, though not always statistically significant, for precipitation (P) and streamflow volume (Q), while climate-driven evapotranspiration shows a small positive trend (at most 2 mm year^{-1}) with statistical significance extending over longer periods. Precipitation trends are similar in all sub-catchments, except for the catchment contributing to the gauging station of Soraga in the upper part of the Avisio tributary (see Figure 2.2), where large positive trends of about

7 mm year^{-1} are observed in the period 1967-2003.

Statistically not significant trends, either positive or negative, are observed in all the other sub-catchments with significant positive trends observed locally, as for example between 1971 and 2001 in the upper portion of the Adige basin (identified by the gauging station of Bronzolo). A slight general upward trend in precipitation for the Adige basin was also detected by Lutz et al. [108] during the period 1971-2010 and also by Beniston et al. [18] and Scherrer et al. [152] with reference to Swiss Alpine catchments during the past century. Streamflow volume follows the observed trends in precipitation only partially. Adige at Trento experienced a significant reduction of the streamflow in the period 1975-2009 (about -9 mm year^{-1}), whereas at Bronzolo streamflow does not evidence any particular trend. However, in the nested small sub-catchment of Gadera at Mantana (close to the confluence with the Isarco tributary) and Avisio at Soraga, streamflow shows positive trends in the range $4 \div 6\text{ mm year}^{-1}$ from 1971 inward, in the former, and up to 10 mm year^{-1} from 1970 to 2005 in the latter.

When aggregated at the seasonal scale (see the rows from the second to the fifth of Figure 3.3) the variables show different behaviors. Climate-driven evapotranspiration shows negligible trends in all seasons, except in summer when the trend is slightly positive, thereby showing that changes in evapotranspiration are small and limited to the summer season. Precipitation denotes similar patterns in all the nested sub-catchments, but with contrasting values between the different seasons. In fact, significant negative trends are observed in winter during the period 1970-2010, with maximum decrease of about -4 mm year^{-1} . Springs show positive significant trends in the first part of the study period, whereas from the '70s negative trends prevail. Summer

precipitation is nearly constant (no significant trends) in the whole study period. At all locations autumn precipitation trends are first negative, but becomes positive in the period 1970-2000. This is more evident in the upper Avisio catchment (closed at Soraga), where positive trends of about 7 mm year^{-1}) are observed. Similarly to what observed at the annual scale, streamflow volume vary in space. In the last 30 years, winter trends are nearly absent at Trento gauging station and slightly positive at Bronzolo. Conversely, significant positive trends characterize streamflow in the other, smaller, nested sub-catchments since the '70s. Notice that streamflow trends are often opposite to trends of precipitation, indicating a complex response of the river basin to changes of the climatic forcing, which will be discussed in the ensuing Section 4.1.1. In spring, trends of precipitation and streamflow are more consistent. Significant negative trends are observed for summer streamflow starting from the '70s, especially at Trento gauging station in which negative trends reach almost -6 mm year^{-1} in the period 1977-2007. As in winter, this patterns are not reflecting changes in precipitation. Finally, autumn trends in streamflow are higher in the small nested sub-catchments of Gadera at Mantana and Avisio at Soraga than in the Adige at Trento and Bronzolo located along the main stem of the Adige River and with a much larger contribution area. In this season, maximum increasing trends in the Avisio at Soraga amount to $+5 \text{ mm year}^{-1}$. Patterns at all the investigate locations are similar to that of precipitation in the same season.

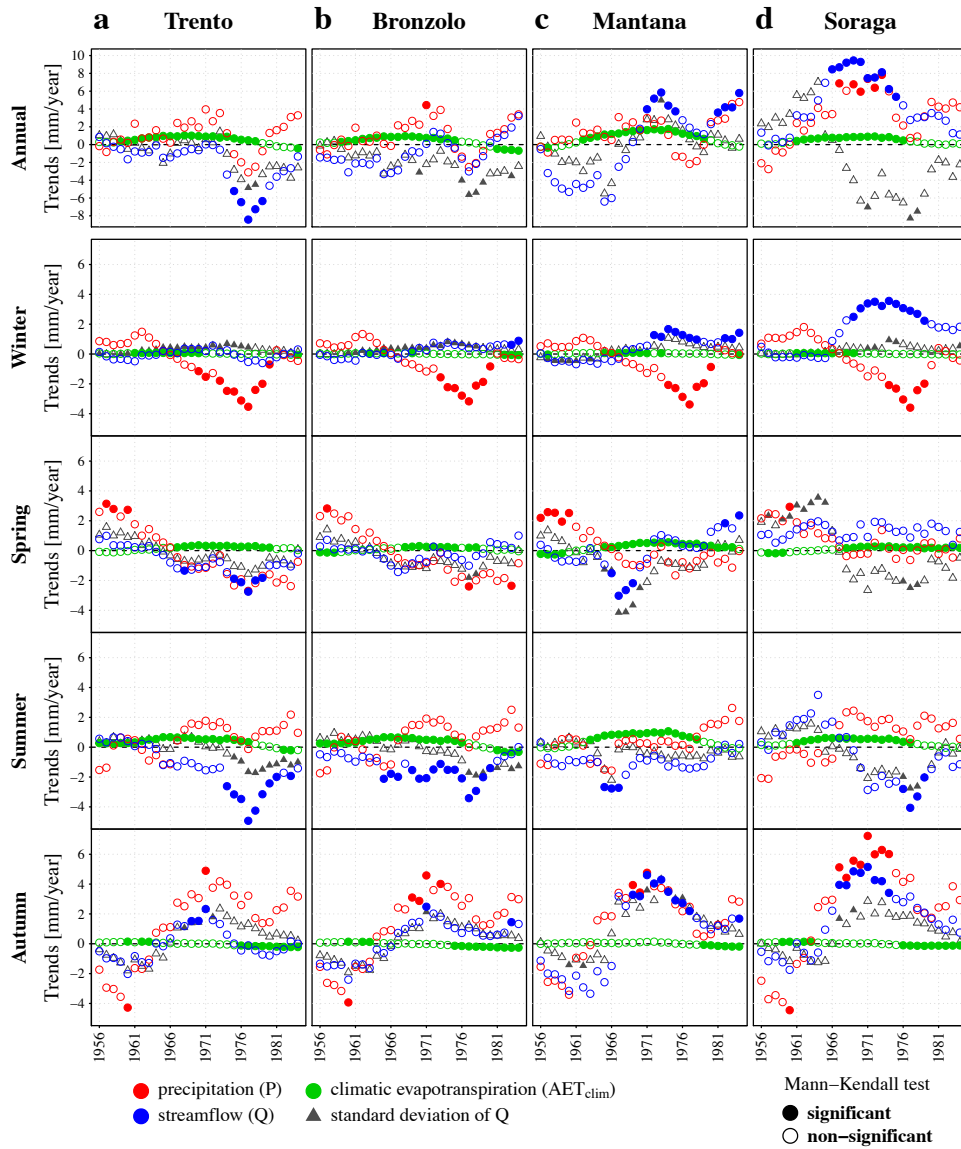


Figure 3.3: Trend analysis of the selected hydro-climatic variables in the Adige river basin at Trento (a), Bronzolo (b), Mantana, on the Gadera tributary, (c) and Soraga, on the Avisio tributary (d). Trends in annual precipitation (P), annual streamflow volume (Q) and climate-driven evapotranspiration (AET_{clim}) are calculated, in addition to trends in standard deviation of Q, with Mann-Kendall test on 30 years moving time windows for the 4 analyzed basins at annual and seasonal scales. The values of trend is associated to the starting year of the respective time windows.

Additional analyses for the attribution of these observed trends to selected possible concurrent drivers are presented and discussed in the following Section 4.1.1.

3.1.2 Hydroclimatic and water quality trends across three European river basins

Mann-Kendall trend analysis indicates that annual temperature averages in the Adige River Basin have slightly increased between 1971 and 2010 (Figure 3.4a). The annual mean of daily temperatures shows significant increasing trends in more than half of the basin, yielding an average increase of $+0.004\text{ }^{\circ}\text{C year}^{-1}$ (standard deviation of $0.03\text{ }^{\circ}\text{C year}^{-1}$). The highest increase (maximum positive value of $+0.091\text{ }^{\circ}\text{C year}^{-1}$) has occurred in the Southern part of the catchment and in the lower areas. In addition, positive significant trends have been detected in the North-East (Isarco valley). Some areas of the Adige River Basin show significant decreasing trends in mean temperature (maximum negative value of $-0.089\text{ }^{\circ}\text{C year}^{-1}$), especially in headwater catchments in the North-West (upper Noce and upper Adige) and in the East (upper Avisio). Annual precipitation in the Adige River Basin does not show a general trend between 1971 and 2010 since local divergent trends are present (Figure 3.4b). This means that some parts of the basin show increasing trends (i.e., mainly in the upper Passirio and Isarco valleys in the North and in the upper Noce and Avisio valleys in the centre), whereas other areas show decreasing trends (i.e., mainly in the lower lands of Noce, Isarco and Avisio valleys in the North and centre of the Adige River Basin). Mean annual precipitation has changed by $+1.48\text{ mm year}^{-1}$ on average (standard deviation of 1.15 mm year^{-1}), with a maximum positive value of $+7.76\text{ mm year}^{-1}$ and a maximum negative trend of $-1.70\text{ mm year}^{-1}$. While temperature trends are statistically significant in most of the basin, precipitation trends are significant in a small part of the basin only and exclusively in areas with upwards trends (mainly in the upper Passirio and Isarco valleys).

Mann-Kendall trend analysis indicates a temperature increase in the Ebro River Basin between 1971 and 2007 (Figure 3.4c). More specifically, the annual mean of daily temperatures shows significant increasing trends in nearly the entire basin, yielding an average increase of $0.05\text{ }^{\circ}\text{C year}^{-1}$ across the basin (standard deviation of $0.03\text{ }^{\circ}\text{C year}^{-1}$; range of -0.02 to $0.18\text{ }^{\circ}\text{C year}^{-1}$). The largest increase has occurred in headwater catchments in the centre of the Central-Eastern Pyrenees. A temperature decrease has been detected for a few cells in the Central Pyrenees and a small patch in the South-Eastern tip of the basin only. Annual precipitation in the Ebro River Basin has decreased between 1971 and 2007, with the exception of the Northern fringe of the Eastern-Central Pyrenees (Figure 3.4d). The average trend across the basin is -3.0 mm year^{-1} (standard deviation of 2.77 mm year^{-1} ; range of -11.43 to 8.84 mm year^{-1}). The decreasing trend in precipitation is significant in a wide strip from the Western Pyrenees to the Northern Mediterranean fringe of the Ebro River Basin. Significant increasing trends in annual precipitation have not been detected in the Ebro River Basin. In view of the significant downward trends in most of the Northern half of the basin, this area can be considered most prone to changes in the hydrological regime due to changing precipitation patterns and quantities. As runoff in the Ebro River Basin will increasingly rely on the Pyrenees region [106], this highlights the risk of increasing water scarcity for the entire basin. Annual mean temperature in the Sava River Basin shows a significant upwards trend in the entire basin (Figure 3.4e), yielding an average trend of $0.04\text{ }^{\circ}\text{C per year}$ across the basin (standard deviation of $0.004\text{ }^{\circ}\text{C year}^{-1}$; range of 0.033 to $0.058\text{ }^{\circ}\text{C year}^{-1}$). Temperature has increased to a larger extent in the upstream part and East of the Sava River Basin compared to

the centre of the basin. Spatial differences in the magnitude of temperature changes appear to be minor, which might, however, partly result from smearing of the spatial temperature distribution due to the relatively coarse grid resolution. Annual precipitation shows an overall increase in the Sava River Basin (Figure 3.4f), with an average of $1.57 \text{ mm year}^{-1}$ (standard deviation of $1.48 \text{ mm year}^{-1}$; range of -3.00 to $12.27 \text{ mm year}^{-1}$). However, alternating clusters of non-significant upwards and downwards trends yield a spatially diverse pattern of annual precipitation trends. The headwater catchments in the West show the largest downward (albeit non-significant) trends in annual precipitation. However, one grid cell in the most Western tip of the basin shows an opposite trend with a large precipitation increase of $12.27 \text{ mm year}^{-1}$. Significant trends are restricted to small patches in the West (downward) and East of the Sava River Basin (upward), where annual precipitation has moderately decreased and increased, respectively.

For the streamflow analysis, stations were excluded from the analysis if information was missing for more than the 60% of the study period 1971-2010. This threshold was set in order to obtain a good spatial coverage with streamflow gauges in all basins. This procedure provided a subset of 24 stations for the Adige, 41 stations for the Ebro, and 20 stations for the Sava. Analysis of streamflow data at 24 stations in the Adige River Basin does not reveal a clear overall trend in annual mean streamflow between 1971 and 2010. Annual mean streamflow (QMean) has decreased at twelve stations (50%); the other half shows an increasing trend. The change in QMean with respect to the long-term mean over the study period is -0.4% on average, ranging from -75% to 86%. The change in specific discharge (Sen's slope per year divided by sub-basin area) is,

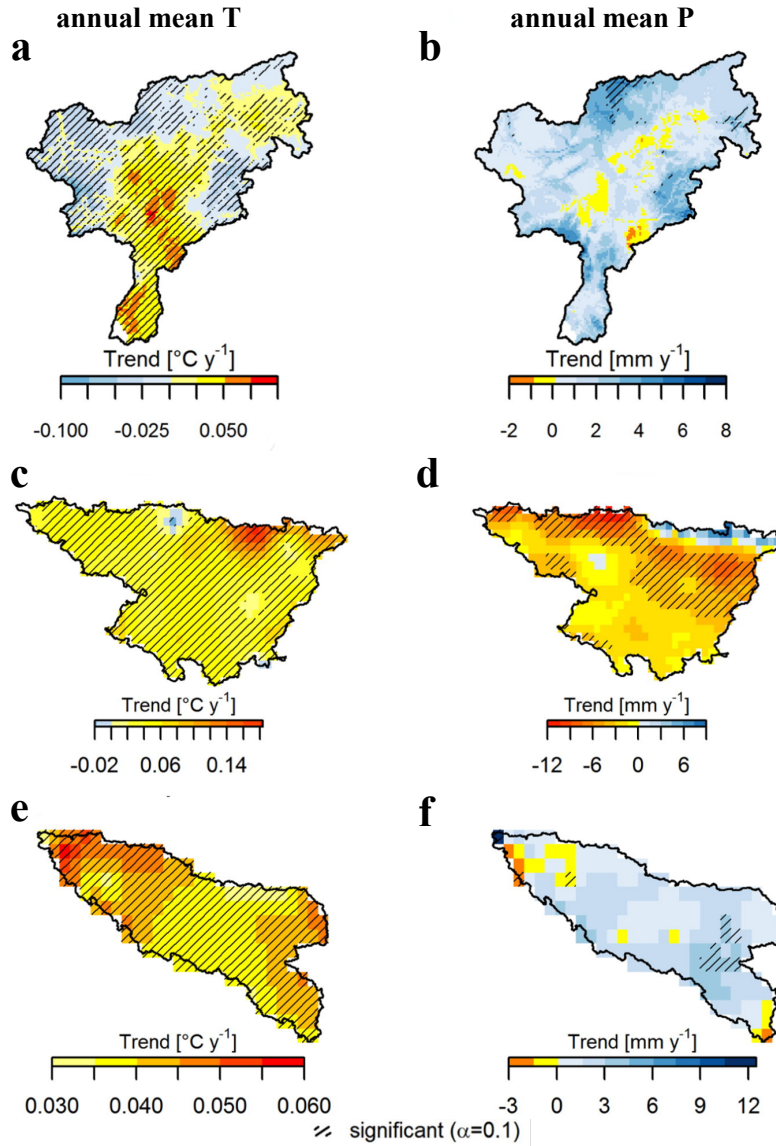


Figure 3.4: Mann-Kendall trend analysis of annual mean temperature (left-panels) and total precipitation (right-panels) in the Adige (a, b), Ebro (c, d) and Sava (e, f) river basins (1971-2010). Colours show Sen's slope estimator ($^{\circ}\text{C year}^{-1}$ for temperature and mm year^{-1} for precipitation, respectively) for each grid cell. Significant trends ($\alpha = 0.1$) are shown as hatched areas.

on average, $-0.01 \text{ L s}^{-1} \text{ km}^{-2} \text{ year}^{-1}$ (with the largest decrease of $-0.50 \text{ L s}^{-1} \text{ km}^{-2} \text{ year}^{-1}$ found at the gauge of river Noce at Mezzolombardo, IDRTN08, while the highest increase is equal to $0.33 \text{ L s}^{-1} \text{ km}^{-2} \text{ year}^{-1}$, found at the gauge Rio Fleres at Colle Isarco, 31950PG). If the MK-significance is considered,

only one gauge shows a significant increasing trend (Torrente Leno at Stedileri, IDRTN21) with a slope equal to $0.18 \text{ L s}^{-1} \text{ km}^{-2} \text{ year}^{-1}$), and no gauge exhibits a significant decreasing trend. Moreover, no overall trend in MAM7 becomes apparent, with 13 gauges showing a positive trend (4 significant) and 11 gauges showing a negative trend (3 significant). The figures are similar for the second low flow index (i.e., Q90). The only index exceeding the minimum number for field significance of the trend is Q10, which shows a significant downward trend at 5 stations (21%; field significance for two or more stations).

Analysis of streamflow data at 41 stations in the Ebro River Basin indicates a clear overall decreasing trend in annual mean streamflow (QMean) between 1971 and 2010. The change in streamflow relative to the long-term mean over the study period is, on average, more than 50% (range of between -134% and 2%). QMean has decreased at all stations but one, among which 19 show a significant decreasing trend (46% of all stations). The change in specific discharge (Sen's slope per year divided by sub-basin area) is, on average, $-0.16 \text{ L s}^{-1} \text{ km}^{-2} \text{ year}^{-1}$, with the largest decrease ($-2.1 \text{ L s}^{-1} \text{ km}^{-2} \text{ year}^{-1}$) at station Riezu in the Western Central Pyrenees and the only upward trend ($0.9\text{e-}2 \text{ L s}^{-1} \text{ km}^{-2} \text{ year}^{-1}$) occurring at station Anzánigo in the Central Pyrenees. The additionally analysed indices emphasize this trend towards decreasing streamflow: Q10 and MAM7 have both significantly decreased at 16 stations (39%), and Q90 shows a significant decline at more than half of the stations (51%). This corroborates the presence of an overall trend towards diminishing streamflow in the Ebro River Basin. Annual mean streamflow in the Sava River Basin has increased at 2 stations (10%) and declined at 18 stations (90%) between 1971 and 2010. Twelve (60%) of the decreasing trends are

significant, whereas none of the increasing trends is significant. In terms of change in specific discharge, this corresponds to a mean change of $-0.08 \text{ L s}^{-1} \text{ km}^{-2} \text{ year}^{-1}$, ranging from $-0.19 \text{ L s}^{-1} \text{ km}^{-2} \text{ year}^{-1}$ (station Radece in Slovenia) to $0.15 \text{ L s}^{-1} \text{ km}^{-2} \text{ year}^{-1}$ (station Hrstnik; downstream of Radece after the confluence of river Savinja). The change in QMean with respect to the long-term average over the study period is -11% on average, ranging from -31% to 19%. This indicates an overall trend toward diminishing streamflow in the Sava River Basin, which is also suggested by trend analysis of low and high flow indices. The decrease appears to be more severe during low flow compared to high flow periods, as 30% of all trends are significant negative for Q90, while only 15% are significant negative for Q10. This is also reflected in a similar percentage of significant decreases in the low-flow index MAM7 (i.e., 25% of all stations). The amount of significant decreasing trends is field-significant for all indices, which confirms the tendency towards declining streamflow in the Sava River Basin.

The joint analysis of streamflow, temperature and precipitation trends (Figure 3.5a) highlights that negative streamflow trends are mainly found in the Central-Southern part of the Adige River Basin along the main stream. This cannot be explained by decreasing precipitation since sub-basin precipitation has increased in most sub-basins (Figure 3.5b). In contrast, the spatial pattern in sub-basin temperature trends suggests a correlation between discharge and temperature trends (Fig. 4a): aggregated temperature averages have especially risen in the Eastern and Southern sub-basins, with the latter being an area of mostly decreasing QMean. The basin of the Leno tributary in the South is the only sub-basin where temperatures have, on average, increased and precipitation decreased. Considering land use in 1990 to 2012 (Corine Land

Cover, //www.eea.europa.eu/publications/COR0-landcover), no significant changes in land use cover of the Adige River Basin have occurred. It is thus likely that land use change is not a major driver of change and does not significantly affect the observed trends of the hydro-meteorological variables. Spatial analysis of sub-basin temperature trends in the Ebro River Basin shows that all sub-basins apart from one in the Western Central Pyrenees have undergone significant temperature increases (Figure 3.5c). As seen in the grid-based analysis (Figure 3.4c), the most pronounced increase has occurred in the Eastern Pyrenees, with mean sub-basin trends from 0.1 to 0.15 °C year⁻¹. In the only sub-basin where a downward (non-significant) trend in mean temperature has occurred (i.e., station Anzánigo at river Gallego), streamflow still shows a significant decrease, presumably due to a significant precipitation decrease during the same period (Figure 3.5d). In 36 out of the 41 sub-basins (88%), temperature trends are upward and precipitation trends downward. This indicates the risk of increasing water scarcity in the Ebro River Basin, which is also reflected in the decreasing streamflow trends. Sub-basins in the Western part of the Ebro River Basin appear to have undergone a more pronounced change in climate compared to sub-basins in the East, as both increasing temperature and decreasing precipitation trends are significant in this region. In the Eastern part of the Ebro River Basin, in contrast, precipitation decreases are non-significant, and precipitation has even increased in three headwaters in the Eastern Pyrenees. Nonetheless, streamflow has significantly decreased in these headwaters. This indicates that the precipitation increase has been counterbalanced by a substantial temperature increase and, consequently, emphasizes the role of evapotranspiration for streamflow changes in this area.

Temperature and precipitation trends are upward in all investigated sub-basins of the Sava River Basin (Figure 3.5). The combined plot of discharge and temperature trends in each sub-basin (Figure 3.5e) shows that temperature trends are mostly accompanied by downward streamflow trends. In particular in the upstream part of the Sava River Basin, the cluster of significant downward trends in streamflow coincides with large temperature increases. In contrast, precipitation and streamflow trends are of opposite sign for all but two sub-basins (Figure 3.5f). This suggests that the significant upward trends in temperature have enhanced evapotranspiration such that the non-significant upward trends in precipitation have not led to increased streamflow. An exception of this might be reflected in the switch from a significant downward to an upward trend in streamflow between the middle part and the most downstream station in the Sava (i.e., stations Slavonski Brod and Sremska Mitrovica, respectively). The area between these two stations exhibits a relatively small temperature increase ($0.04\text{ }^{\circ}\text{C year}^{-1}$) and a relatively large precipitation increase (1.35 mm year^{-1}). Hence, in this area, the surplus in precipitation results in increased runoff instead of being counterbalanced by larger evapotranspiration, as seems to be the case for most parts of the Sava River Basin.

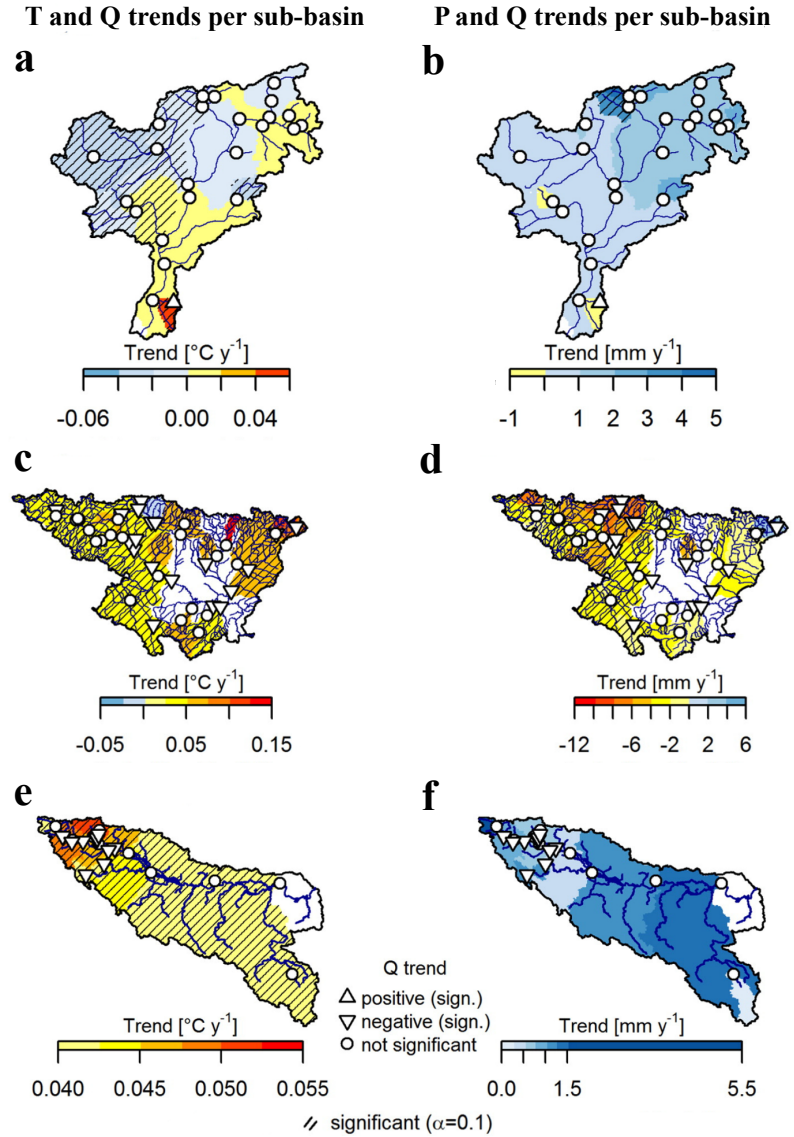


Figure 3.5: Trends in annual mean streamflow (dots and triangles in both panels) and trends in (left-side panels) annual mean sub-basin temperature and (right-side panels) annual sub-basin precipitation totals in the Adige (a, b), Ebro (c, d) and Sava (e, f) river basins according to Mann-Kendall trend analysis (between 1971 and 2010; significance level of $\alpha = 0.1$). Significant trends in streamflow are presented as triangles (upward-pointing for upward trend and downward-pointing for downward trend) and non-significant streamflow as dots, respectively. Significant trends in sub-basin climate are shown as hatched areas.

3.2 On the use of hydrological modeling for testing the spatio-temporal coherence of high-resolution gridded precipitation and temperature datasets in the Alpine region

3.2.1 Uncertainty of climate datasets

In this section uncertainty associated to the climate datasets is evaluated for multi-annual averages of precipitation and temperature. Uncertainty is here defined as the range of variation of the estimates provided by the datasets (i.e., the difference between the upper and the lower estimate, as in Prein and Gobiet [140]) normalized according to the associated mid-range value.

Precipitation Spatial patterns of annual mean precipitation from the five datasets are rather different from each other, except for APGD and ADIGE, which use similar observational datasets within the study area, with the latter showing smaller annual mean precipitations than the former (Figures 3.6 and 3.7). According to APGD the mean annual rainfall within the Adige catchment ranges from 500 to 2300 mm. The largest annual totals are observed over the pre-Alpine reliefs (i.e., southernmost river basin), due to orographic lifting of moist air masses flowing from south [60], and over the mountains close to the main Alpine divide in the northernmost basin, where summer convective activity is most intense [172]. Instead, the driest areas are the interior of the catchment and, especially, in the major valley floors in the upper basin. Despite its high nominal spatial resolution (about 5 km), MESAN reveals rather coarse precipitation field structures. Also, differently from APGD and ADIGE, its annual pattern does not resemble much the underlying topography (Figure 3.6). On one hand, this is

possibly related to the limited number of ground stations used for assimilation in MESAN; on the other, it reveals that using reanalyses from climate models as first guess for assimilation does not improve much the effective resolution of the final results with respect to the interpolation of station data (see E-OBS performances). Notice that the effective resolution of numerical weather model outputs can be estimated about seven times as large as their grid spacing, and that calculations are performed with a smoothed topography for numerical stability reasons [see 141]. According to the above considerations, it is no surprising that MESAN effective resolution is much lower than its nominal resolution. The large precipitation totals (above 2500 mm) in the pre-Alpine area may also be explained by the well-known tendency of climate models to overestimate precipitation in mountain areas [see 97]. In general, both 0.25° resolution maps (E-OBS and MSWEP) are much smoother than the others. However, despite its coarse grid, MSWEP shows spatial patterns closer to APGD and ADIGE than E-OBS. Catchment-averaged monthly precipitations, illustrated in Figure 3.7, exhibit a clear bimodal distribution in all datasets, with a primary peak in summer (mainly associated with intense convection over mountain tops; [172]) and a secondary peak in autumn. The largest discrepancies among the datasets are generally observed in the wetter months (i.e., May to November), when the uncertainty (i.e., the range of variation of monthly estimates) is of 17-35 mm (corresponding to 20-36% when normalized with the corresponding mid-range values), while in drier and colder months it typically ranges between 10 and 17 mm (16 to 48%). As expected, monthly estimates from APGD and ADIGE agree very well, since they are obtained with a similar density of observations. MESAN estimates are also rather close, except for a pronounced

underestimation (by about 20 mm) in October and November. A similar underestimation is also found in E-OBS. On the other hand, E-OBS shows systematic overestimates (about 10 mm) during winter (i.e., January, February, March and December). As for MSWEP, its annual cycle is similar to that of APGD and ADIGE with monthly totals being systematically higher. The annual precipitation totals averaged over the Adige basin for the five datasets range between 883 and 1052 mm, corresponding to an annual uncertainty of 169 mm, i.e. 17% (see right y-axis in Figure 3.7). In particular, MSWEP cumulates the highest totals, APGD ranks second and ADIGE third, with MESAN and E-OBS returning the lowest rainfall totals.

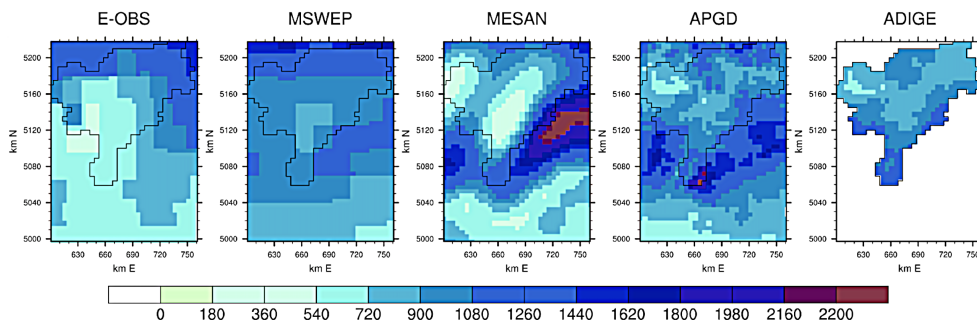


Figure 3.6: *Maps of mean annual precipitation totals (1989-2008 average) according to the five different climate datasets.*

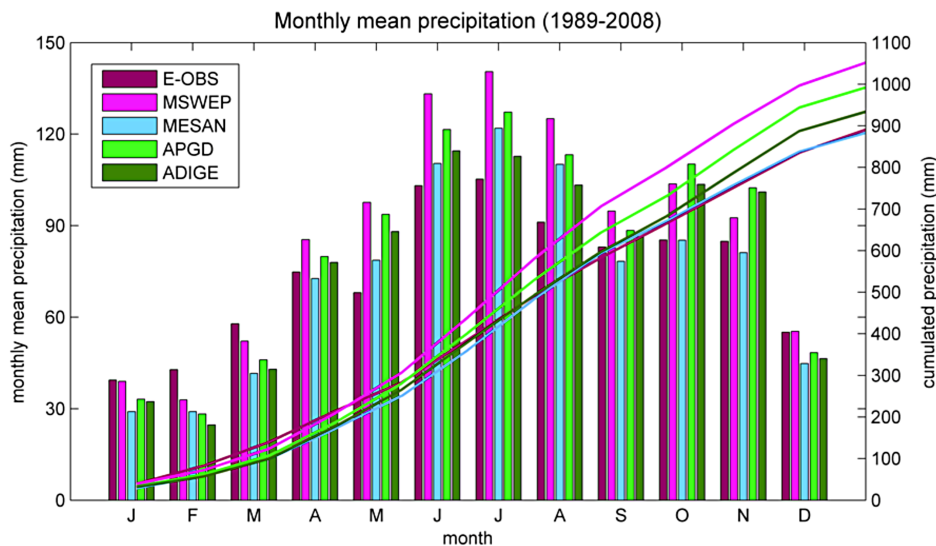


Figure 3.7: *Annual cycle of monthly mean precipitation totals (1989-2008 average), averaged over the entire study area, according to the five different climate datasets (color bars). The associated evolution of cumulated precipitation totals is also shown (color lines).*

Air Temperature The added value of using grids of increasing resolution is more evident for mean annual air temperature than for annual precipitation, with the spatial distribution of the former following closely the terrain topography (see Figure 3.8). This is an expected result for ADIGE dataset, since the interpolation scheme considers explicitly the elevation-temperature relationship (i.e., the vertical gradient of temperature) and thus the major morphological features of the domain, such as the network of valleys and mountain crests, are visible in the resulting field. This topographic effect is also accounted for, although to a lesser extent, in MESAN, while is almost absent in E-OBS, due to the smoothing effect of grid-scale aggregation. In the north-western part of the basin ADIGE shows systematically warmer temperatures at high elevation (see Figure 3.8), which are evident despite small-scale discrepancies between the three temperature maps, i.e., both positive and negative local differences up to 5 °C, partially due to the different grid resolutions and/or to the different topographic data used in the interpolation scheme adopted in the datasets. These differences can be attributed not only to the nominal resolution of the datasets, but also to different densities of gauging stations used, as well as to the different interpolation schemes adopted. Annual cycles of catchment-averaged monthly mean temperatures are illustrated in Figure 3.9: the uncertainty (i.e., range of variation) of these estimates span the range from 1.5 to 2.3 °C, typically larger in warmer months. Notice that ADIGE is the warmest dataset, except in late spring and summer (May, June

and July), when MESAN shows slightly higher temperatures.

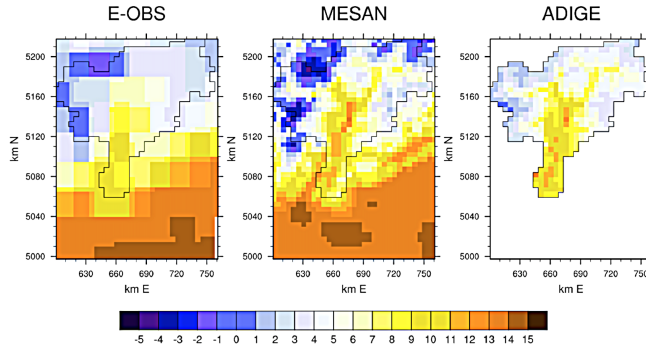


Figure 3.8: Maps of mean annual temperature (1989-2008 average) according to the three climate datasets providing temperature data.

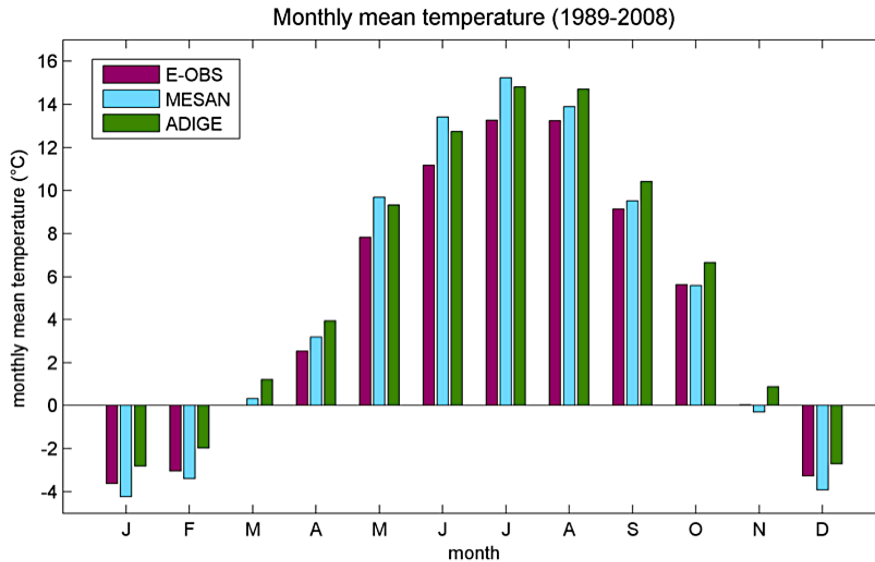


Figure 3.9: Monthly mean temperature (1989-2008 average), averaged over the entire study area, according to the three climate datasets providing temperature data.

3.2.2 Testing the hydrological coherence of the datasets

In this section the coherence of the gridded climate datasets is evaluated according to their ability to reproduce the observed streamflow time series in the Adige catchment, evaluated in the period 1991-2008 by computing the NSE and PBIAS

indexes (see Section 2.3.4) at all gauging stations, as shown in Figure 3.10. In addition to the NSE metric, which is customarily used to assess the performance in reproducing the observed streamflow, the PBIAS metric was used, which indicates how closely the model reproduces the streamflow volume. Following Moriasi et al. [121], values of NSE and PBIAS can be considered satisfactorily good when they are respectively larger than 0.5 and smaller (in absolute value) than 15. As specified in Section 2.3.4, the parameters of the hydrological model are set for each dataset by maximizing the average NSE of Trento and Bronzolo gauging stations. At these two gauging stations the highest NSE are obtained with the dataset ADIGE and APGD, followed by MSWEP, with E-OBS providing the lowest NSE at both gauging stations. On the other hand, PBIAS values at Trento suggest that all the datasets provide satisfactorily simulations, with E-OBS and MESAN showing negligible bias, and the remaining datasets slightly overestimating (i.e., with a negative PBIAS) the observed streamflows (by only 6-10%; see Figure 3.10B). We remind here that the optimisation is performed on NSE efficiency and that PBIAS is computed on the basis of the simulated streamflow time series that maximizes NSE. Small negative PBIAS values, obtained at Trento with ADIGE, APGD and especially MSWEP, are in agreement with the fact that, on an annual basis, these datasets cumulate larger rainfall totals with respect to E-OBS and MESAN (by 7-19%). However, results at Bronzolo provide a somewhat contrasting picture (except for MSWEP): MESAN, APGD and ADIGE slightly underestimates observed water volumes (by 6-8%), while E-OBS slightly overestimates the observed streamflow (by 7%). At the validation stations, APGD and ADIGE provide in general the best performances in terms of NSE, with APGD slightly better than ADIGE, while the other

datasets produces significantly smaller values in almost all the validation sub-catchments (Figure 3.10A). In particular, MESAN and E-OBS produce worst results in small sub-catchments (i.e., lower than 2000 km^2), with low and even negative NSE found in the northeastern part of the simulation domain. Conversely, MSWEP shows a single negative value at a gauging station in the northwestern part of the basin (i.e., Tel), where also APGD and ADIGE are not satisfactory (i.e., $\text{NSE} < 0.5$). Investigation of PBIAS at validation stations confirms the better performances of ADIGE and APGD in reproducing observed data (PBIAS everywhere within the 15% threshold). None of the remaining datasets are better in this respect, especially at the gauging stations of Vandoies, Mantana and Soraga (corresponding to the eastern tributaries of the Adige river; see Figure 3.10B). At most locations we found an agreement between PBIAS and NSE indexes, i.e. small under/overestimation of water volumes generally associated to a satisfactory NSE efficiency. Nevertheless, at some gauging stations low NSE indexes are associated with satisfactory PBIAS values (see e.g., Malé for MESAN and Tel for four out of five investigated datasets). The latter result suggests that a non-satisfactory reproduction of observed streamflow, as indicated by a low NSE, is not necessarily associated to a bias in the simulated total water volumes, and thus to a bias of the rainfall totals as provided by the different datasets, and that other factors may play a major role, like, for example, the spatio-temporal patterns of input meteorological forcing. This latter aspect will be further investigated in the ensuing section.

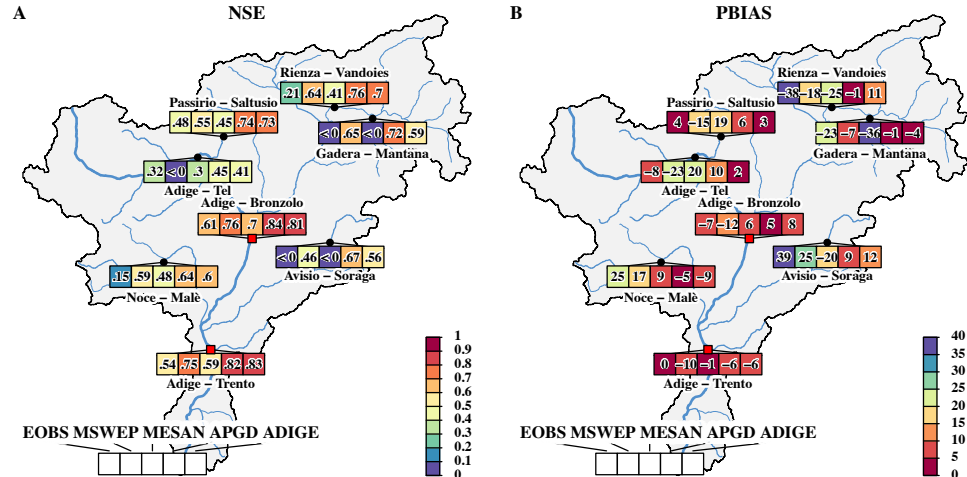


Figure 3.10: (A) Map of the NSE values calculated at the gauging stations of the Adige river basin. (B): as in (A) but for PBIAS values. Positive PBIAS values indicate underestimates of observations by the model, while negative values indicate overestimates. Simulated streamflow are obtained through HYPERstream with model's parameters selected such as to maximize the average NS at the gauging stations of Trento and Bronzolo, separately for each dataset.

3.2.3 Analysis of a simple correction scheme applied to precipitation forcing

In this section, we assess the role of spatio-temporal patterns and their difference across the datasets in shaping the hydrological response. In particular, we test whether and to what extent the application of simple rescaling improves hydrological simulations associated with biased meteorological forcing. The main scope being to check whether a simple rainfall correction procedure can improve the performance of biased datasets. Linear Scaling (LS) [102] is a simple multiplicative correction method, generally applied to correct biases in meteorological forcing as derived from Regional Climate Models (RCMs) simulations. Despite its simplicity, this method is among those used on regular basis in hydrological climate change impact assessments studies (see e.g. the reviews by Teutschbein and Seibert [160] and Chen et al. [35]).

Here LS was applied to the precipitation input retrieved from MESAN dataset (here selected as representative of less performing datasets), using APGD as observational benchmark due to its higher accuracy in reproducing the observed streamflow. The datasets were chosen because characterized by the same nominal resolution, thereby avoiding possible gridding effects. In particular, the LS method consists in rescaling MESAN precipitation by a constant multiplicative factor given by the ratio between the precipitations of APGD and MESAN both cumulated over a given period, which can be the entire year or single months. This correction is applied to the entire time series subdivided in intervals, such that the two time series aggregated at the level of the selected time interval (i.e., year or month) are the same. Corrections were applied directly over the common computational 5-km grid, and the modified precipitation input was then fed into HYPERstream (coupled with the unmodified MESAN temperature input) in order to carry out new optimization runs. This correction was applied considering annual and monthly totals of the mean precipitation computed over the entire river basin (identified with scenario 1 and scenario 2, respectively) and cell by cell (identified with scenario 3 and scenario 4 for the annual and monthly rescaling factors, respectively), thereby resulting in a total of 4 possible rescaling scenarios. The comparison of NSE indexes at all the calibration and validation nodes is illustrated in Figure 3.11 in the four LS scenarios described above. For the sake of clarity we also show again the NSE indexes obtained using APGD and MESAN as input meteorological forcing. The most striking result is that none of the LS scenarios is able to match or even get close to the performance of APGD. We emphasize here that HYPERstream has been calibrated on each one of the four scenarios, such that the resulting model

parameters are optimal for each of them. This conclusion is valid for all the investigated locations. A general and moderate improvement of NSE index with respect to the original MESAN simulation is however achieved, although not for all the LS scenarios. In particular, scenarios 1 and 2 (i.e., those based on catchment-averaged totals) often lead to a small deterioration of the NSE index with respect to the original MESAN dataset (e.g. at Tel, Vandoies and Malé). On the other hand, scenarios 3 and 4, i.e. cell-by-cell corrections, lead to a general improvement of the accuracy, which is a reasonable result, given the pronounced spatial variability of the precipitation field in the study area which is an important determinant of the differences in the specific streamflow (i.e., the water discharge divided by the area of the catchment) at the stream gauges. At some locations such improvement is extremely relevant: for instance, at Mantana and Soraga NSE indexes shift from negative (i.e., complete model failure) to small positive values (0.20-0.35 range), while at Vandoies NSE increases significantly from 0.3 to 0.65. As a general result, corrections applied at the monthly scale (scenarios 2 and 4) perform slightly better than the annual basis counterparts (scenarios 1 and 3), as they allow a better reproduction of the seasonal rainfall pattern of the benchmark dataset. As expected, scenario 4 shows the largest improvement in performance, with the exceptions of Malé, Bronzolo and Trento stations, where NSE efficiency does not show any appreciable improvement with respect to the original MESAN performance. We attribute this fact to the balancing and smoothing effects entailed by both the hydrological model calibration process (independently carried out for each dataset) and the spatio-temporal averaging effect of the catchment, which increases in importance as the size of the catchment increases.

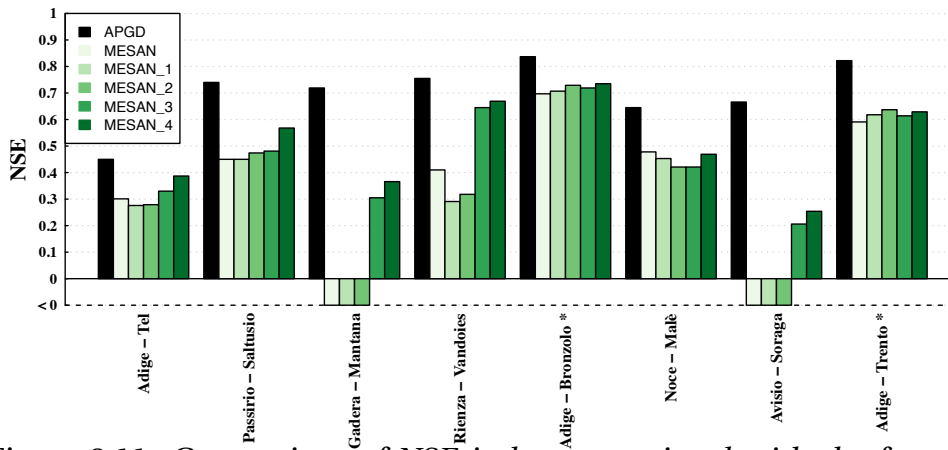


Figure 3.11: Comparison of NSE indexes associated with the four LS scenarios (MESAN₁ to MESAN₄), together with the values obtained during the optimization of the hydrological model using APGD (black) and MESAN (in green scale) as input meteorological forcing.

DISCUSSION

Our analyses revealed interesting results, partly in agreement with the existing literature and partly showing original findings, sometimes diverging from the common scientific opinions. A detailed discussion is presented in the following.

4.1 Hydrological changes: detection and attribution

4.1.1 Detection and attribution of hydrological changes in a large Alpine river basin

The trend analysis applied to the Adige River Basin, illustrated in the previous section, shows several statistically significant trends in the seasonal and annual hydro-meteorological fluxes of the Adige river basins. These results highlight non-stationary features of the hydrological dynamics in this large Alpine area. In this work, we focused on two main outcomes: i) the decrease of summer streamflow of the Adige at Trento and ii) the increase of winter streamflow at the headwaters of Gadera and

Avisio rivers. Herein, we attempt to attribute these changes to their controlling factors by using a multiple-method framework. In particular, we test the following hypotheses:

1. The decreasing summer streamflow at Trento is due to the intensified water withdrawals for irrigated agriculture in the drainage area of the Noce river, a tributary of the Adige.
2. The increasing winter streamflow at the headwaters is caused by a larger groundwater contribution triggered by a proportional increase of groundwater recharge in Autumn due to larger precipitations.

In the following paragraphs, various techniques (i.e., Mann Kendall trend test, standard deviation analysis, Pettitt's test, computation of freezing days, Spearman's rank correlation and analysis of variance) are applied in order to provide proofs of consistency of the tested hypotheses and proofs of inconsistency of the possible alternatives.

Attribution of decreasing summer streamflow at the outlet Since the '70s the annual streamflow volume experienced a reduction at the gauging station of Trento ($9,852 \text{ km}^2$), chiefly due to a large reduction of both spring and summer streamflows, but not at the upstream gauging station of Bronzolo ($6,891 \text{ km}^2$). We test the hypothesis that this reduction is due to an increase of water uses for agriculture in the lower portion of the river basin, downstream Bronzolo. Other possible alternative causes that might be associated with the observed alterations are considered. In the following we outline the most likely:

A1) summer precipitation reduction;

A2) raised summer evapotranspiration, as a consequence of air warming;

A3) reduction of winter snow.

Unfortunately, the lack of reliable data on changes of water uses, hinders a direct attribution, and therefore we proceed by elimination of causes that may be proved to be inconsistent with the observed changes [see e.g., 117]. In Figure 4.1 it is shown that the downward streamflow trends are statistically significant in most of the 30-years time windows since 1974 (filled blue dots).

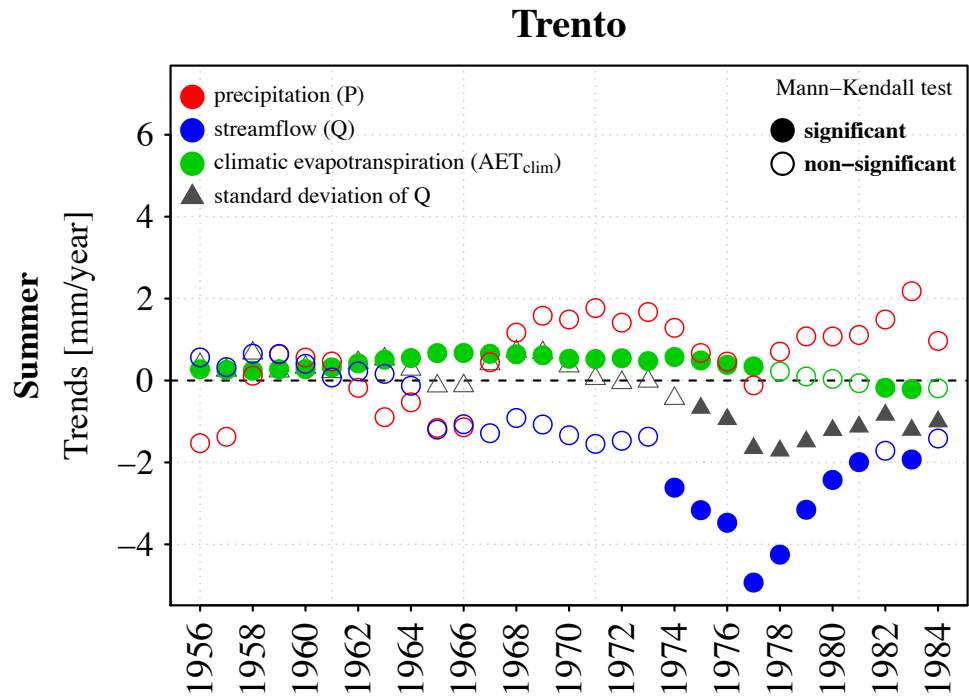


Figure 4.1: Trend analysis of the selected hydro-climatic variables in the Adige River Basin at Trento in the summer season. Trends in precipitation (P), streamflow volume (Q) and climatic evapotranspiration (AET_{clim}) are showed, in addition to trends in standard deviation of Q , computed by the Mann Kendall test with a 30 years moving time windows. The resulting trends are plotted versus the starting year of the time windows. Filled symbols indicate statistically significant trends with 5% level of confidence, while open symbols indicate statistically non-significant trends.

By simply analyzing Figure 4.1 we can exclude **A1** because summer precipitation is rather increasing in the same period (red dots), even if non-significantly.

Moreover, also climate-driven evapotranspiration (i.e., **A2**) is not the cause of this water depletion, indeed, the magnitude of trends of AET_{clim} is negligible with respect to that of streamflow.

Analysis of land use changes over time revealed little variations in the river basin since 1990, with most of variations associated to a reduction of about 20% in glacier surfaces in the period 1990-2012, whereas the observed variation of agricultural land use is of about -0.2% . In this respect, the governing drivers of the observed reduction in streamflow are likely occurred before 1990. This hypothesis was supported by the data of apple production in the middle and lower valley of the Noce, a tributary of the Adige contributing with a total area of $1,385\text{ km}^2$, where starting from the '70s, apple production almost doubled from 69 to about 130 *tons* in about 10 years [179, in Italian]. In addition, trends in standard deviation (Figure 4.1) of streamflow vary in proportion to trends in streamflow up to the '70s, as expected when changes in streamflow are triggered by changes in the climatic forcing [116]. Later, trends of the standard deviation are lower than those of streamflow indicating that the change of the latter, observed in this period, cannot be attributed to changes in the climatic forcing, but rather to a component that varies slowly in time, and causing streamflow reduction. A similar behavior, though much weaker, was observed also at the upstream section of Bronzolo. This is in agreement with the intensification of apple production in the Noce catchment, and in the upper Adige catchment as well, which was accompanied by an increased water use during summer, corresponding to the apple growing season. In other words, the increased water use during summer can be seen as a slowly in time component that is subtracted to the streamflow

signal, which entails a reduction of the trend in the standard deviation of streamflow with respect to streamflow itself. Another proof of consistency of our statement is provided by the change point detection through the Pettitt's test (see Section 2.3.1) applied to the time series of the difference of the Adige summer streamflow between Trento and Bronzolo. In Figure 4.2 we compare the observed streamflow time series (black line) with the corresponding simulated fluxes (red line) obtained by applying the hydrological model described in Section 2.3.4 calibrated in the period 1920-1950, when climatic trends and hydropower activities were negligible, in order to simulate a natural scenario. In case of lack of change in the hydrological characteristics of the lowlands of the Adige river, the streamflow of the inter-basin between Bronzolo and Trento should be free of break points, according to the Pettitt's test. Indeed, a change point is detected (black dashed line) corresponding to the early '90s in the observed time series, whereas the natural scenario does not reveal any break point. The presence of the change point only in the measured streamflow time series confirms the hypothesis that the change point in the observed time series cannot be due to climate change, which effects are already included into the meteorological forcing used for the hydrological simulation. The climate origin of the changes in the mean annual streamflow observed at Trento should therefore be excluded.

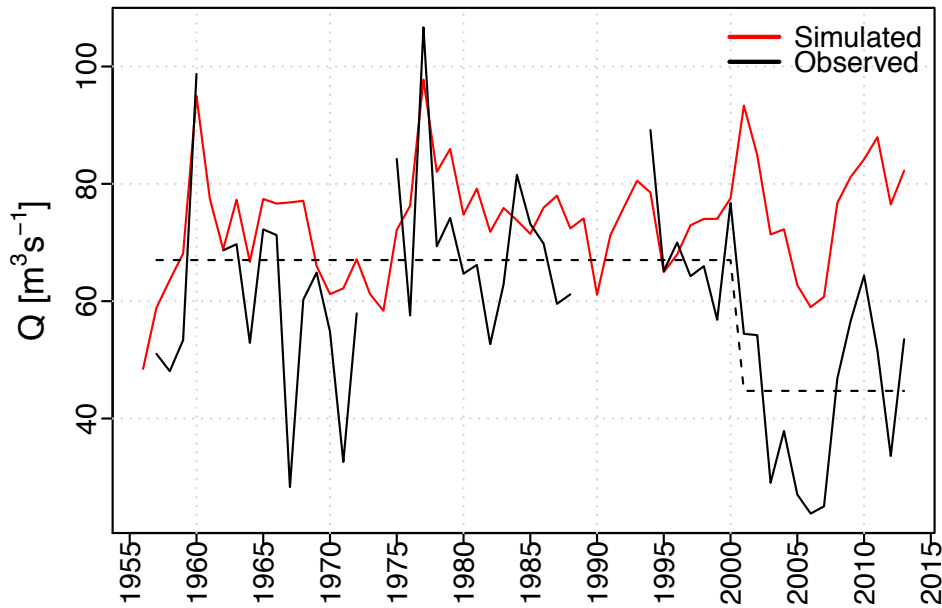


Figure 4.2: *Difference of Adige streamflow between Trento and Bronzolo in the period 1956 - 2013, aggregated at annual scale. Observed aggregated time series are shown as black lines, whereas the simulated values are reported as red lines. A significant break point is detected in the year 1990, only in the observed streamflows, by means of Pettitt's test (the black dashed line traces the local means in the two periods before and after 1990).*

The remaining hypothesized driver (**A3**) is the reduction in winter snow accumulation, which entails diminished streamflow contribution from snow-melting in the following warm season. The time series of accumulated snow water equivalent was estimated by subtracting, for each estimation point, the precipitation of days with mean daily temperature above 0 °C from the total winter precipitation, under the hypothesis that precipitations occurring when the air temperature was higher than 0 °C were liquid and thereby did not accumulate. In particular, we observed that the trends in winter snow are coherent with those of streamflow. Hence, besides the water uses for irrigation in summer, also the reduction of winter snow (**A3**) exerts a strong control on the

summer streamflow alterations. In addition, a strong significant correlation was found between summer streamflow at Trento and the trends in winter snow ($R = 0.85$).

Attribution of increasing winter streamflow at the headwaters

Another relevant finding concerns the changes of the hydrological fluxes observed in the headwater sub-catchments of Gadera at Mantana and Avisio at Soraga (Figures 4.3a and b, respectively). Here, land and water uses differ with respect to the Adige Basin at Bronzolo and Trento. For instance, the Gadera catchment is free of reservoirs and the upper Avisio includes only the Fedaia Dam, at the top of the catchment, retaining water of glacier melting. In addition, the agricultural land in the latter is very limited, providing much less evapotranspiration than in the Adige valley, at the same temperature (see 3.2). In Figure 4.3 it is shown that while winter streamflow increased, the same does not hold for winter precipitation which showed the opposite trend; in addition, trends of evapotranspiration are negligible.

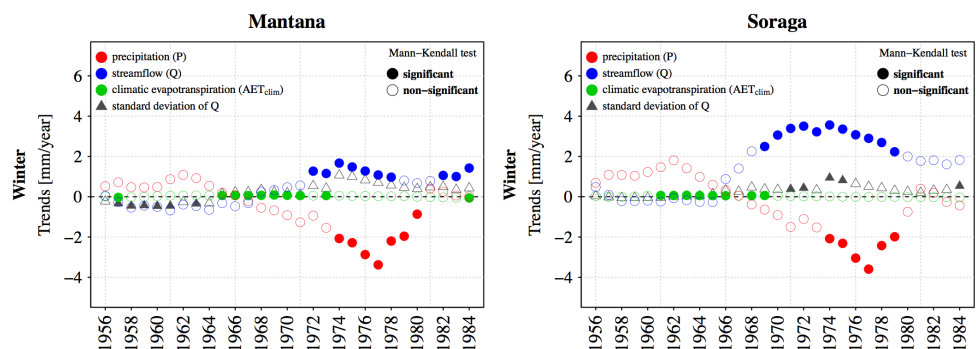


Figure 4.3: *Trend analysis of the selected hydro-climatic variables in the Gadera at Mantana and Avisio at Soraga in the winter season. Trends in precipitation (P), streamflow volume (Q) and climatic evapotranspiration (AET_{clim}) are showed, in addition to trends in standard deviation of Q, computed by the Mann Kendall test with a 30 years moving time windows. The resulting trends are plotted versus the starting year of the time windows. Filled symbols indicate statistically significant trends with 5% level of confidence, while open symbols indicate statistically non-significant trends.*

We test the hypothesis that the upward trends of winter streamflow are due to a change in groundwater dynamics, reflecting shifts in the seasonal distribution of precipitation. Other possible alternative might be the following:

- B1)** raised snow and glacier melting, as a consequence of air warming;
- B2)** increasing winter liquid precipitation (rainfall), induced by warmer temperatures.

Glacier melting (**B1**) is not likely to provide the excess of water in the global budget. In fact, although Marmolada Glacier (i.e. the natural spring of the Avisio River) shrunk in the last century [44], the resulting larger streamflow volume was diverted by the Fedaia Dam to the conterminous Cordevole catchment for hydropower production [131].

A partial shift of winter precipitations from solid to liquid (**B2**) is the hypothesis suggested by Birsan et al. [20] and Bocchiola [22] in studies concerning Swiss and Italian Alpine catchments, respectively. Projected increases in winter streamflow for high altitude first order streams in Switzerland, with glaciers in their catchment, are discussed also by Bavay et al. [12], and explained by an increasing number of melt events in the winter and by precipitation falling as rain instead of snow, due to the higher air temperatures scenarios provided until 2095.

Analogous results are reported in Majone et al. [112] for the Noce catchment with reference to the time window 2040-2070. Nevertheless, this was hardly the cause of the observed increase of winter streamflow volume because, assuming a direct relationship between air temperature and this phenomenon, temperature was rather slightly decreasing in the headwater catchments of the Adige River Basin (see Figures 3.2 and 4.4). Given that data about variations in time of the snow cover was not available over the whole study period, we analyzed the changes in the surface area above the freezing point (i.e. altitude at which average daily temperature is equal to 0 °C), assuming that it represents an approximation of the land surface potentially covered by snow. The rationale behind this is the hypothesis that an increase in temperature would reduce the freezing days enlarging the area of the catchment in which winter precipitation falls as rainfall, thereby increasing streamflow. In particular, we analyzed the changes in the occurrence of freezing days as a function of the percentage area of the basin with mean daily temperature below freezing (see Figure 4.4). Starting from the '90s the curves become steeper showing an increase in the number of freezing days at high elevations (upper left side of the graph) and a parallel reduction of the number of freezing days at low elevations. This suggests that the number of freezing days reduced at elevations below 1,500 m a.s.l., corresponding to about 40% of the river basin, as confirmed by several studies at large scale principally based on the analysis of time series of stations at middle-low elevations [see e.g., 26], but increased at higher elevations. Consequently, the rise in winter streamflow volume could not be attributed to a shift of winter precipitation from solid to liquid, given that the number of days (mainly in the winter season) with temperature below freezing increased in

about 60% of the catchment area, which includes the typical elevations of both Gadera and upper Avisio catchments. Differently, in Swiss watersheds (where more than half of the land surface is above 1,000 m a.s.l.), Birsan et al. [20] observed in the period 1961-2000 substantial decrease in the number of days with minimum daily air temperature below 0 °C.

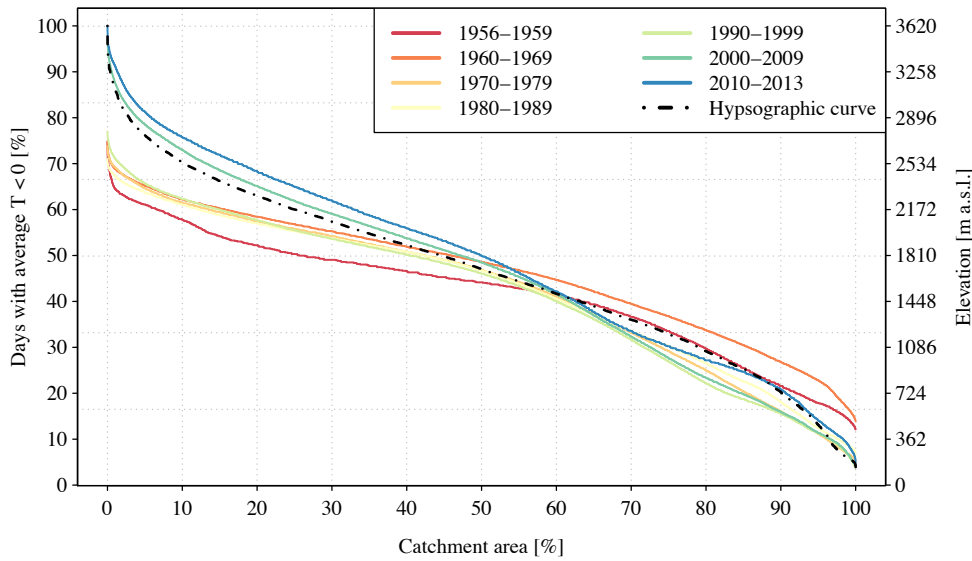


Figure 4.4: Average annual number of freezing days as a function of the percentage area of the basin with mean daily temperature below 0 °C in the Adige river basin closed at Trento. Colored continuous lines indicate different decades. The hypsographic curve of the basin, that provides the percentages of catchment area above a given elevations, is also shows with a black dashed line (elevations are provided on the secondary ordinate axis on the right).

To further reject the alternatives **B1** and **B2** and to support our hypothesis we performed a correlation analysis among the trends of the variables of interest: i) trend of autumn aquifer recharge (testing hypothesis); ii) intensification of snow and glacier melting (**B1**); iii) shift from solid to liquid precipitation in winter (**B2**). The first is represented by the residuals of the autumn water budget. The second is represented by the number of winter days in which the mean temperature of the

catchment is above 3 °C (value in line with the findings of Laiti et al. [98] for the Adige catchment). Finally, the third is embodied by the rainfall time series obtained from the precipitation data by discarding, for each estimation point, the values corresponding to freezing days, when precipitation is supposed to fall as snow.

Correlation analysis highlights that winter streamflow trends in the Gadera at Mantana and Avisio at Soraga are not correlated neither with the change in snow and glacier melting (**B1**) nor with the dynamics of changing phase of precipitation (**B2**). Also the analysis of trends in standard deviation confirms that winter precipitation pattern is not the main driver of streamflow trends, since the signal of streamflow variations are not consistent with that of precipitation.

These considerations lead to the conclusion that the rise of winter streamflow in these two headwater catchments was caused by other factors than the changes in the winter precipitation characteristics and the direct consequences of changing temperature.

In a recent study Zampieri et al. [178] observed that the change of seasonality of total precipitation plays a major role in timing seasonal streamflows, especially regarding the earlier spring streamflow over most of the Alps. In our case, the surplus of precipitation in autumn entered groundwater, where it resides longer than in the other hydrological compartments (i.e. surficial waters), to finally contribute to winter streamflow, more than when autumn precipitations were lower. This hypothesis is confirmed by the analysis of the standard deviation of winter streamflow (Figure 4.3). In fact, if the increase of winter streamflow was due to the increase of winter rainfall the standard deviation of streamflow would rise in proportion [116], however, this was not the case since the

standard deviation did not change, remaining smaller than in all the other seasons, thereby corroborating the hypothesis of increasing baseflow as the main cause of raising streamflow. Furthermore, Spearman's rank correlation is found to be close to 1 (strong positive correlation) between the trends in autumn aquifer recharge and the increase of winter streamflow.

A quantitative measure of the influence and relative importance of possible controlling processes is provided by means of inferential statistical tools. In particular it is performed the one-way multivariate analysis of variance (MANOVA) between the increase of winter streamflow and the three possible drivers assumed as independent variables. In this way, after verifying that the errors are independent and normally distributed, we can quantitatively assess the relative strengths of these drivers by estimating the share of variance of increasing winter streamflow attributable to each one of these factors [see e.g., 6, 126]. In particular, in the headwater catchments the $\Pr(>F) < 0.05$ (i.e., the significance level) only for the variable "autumn trends in aquifer recharge" (i.e., $\Pr(>F) \approx 10^{-8}$). On the contrary, the "shift from solid to liquid precipitation in winter" and the "intensification of snow and glacier melting" play a negligible role, being characterized by $\Pr(>F) > 0.05$. Hence, our testing hypothesis is the remaining plausible reasoning for the increasing winter streamflow.

4.1.2 Hydroclimatic and water quality trends across three European river basins

Climate In general, the comparison among the three basins at European scale (i.e., Adige, Ebro and Sava) exhibits a trend towards increasing temperatures from 1971 on. However, the magnitude of the average increase is much lower in the Adige River Basin ($+0.004\text{ }^{\circ}\text{C year}^{-1}$) compared to the Ebro River

Basin ($0.05\text{ }^{\circ}\text{C year}^{-1}$) and Sava River Basin ($0.04\text{ }^{\circ}\text{C year}^{-1}$), respectively. Moreover, large areas with significant temperature decreases can be found in the Adige River Basin (Figure 3.4a), which is not the case for the other two basins (Figures 3.4c and e, respectively). Local climate trends can become masked with increasingly coarse grid resolution, which might explain the small spatial variability of trends in the Sava River Basin (standard deviation of $0.004^{\circ}\text{C year}^{-1}$) compared to the other two basins (standard deviation of $0.03\text{ }^{\circ}\text{C year}^{-1}$ in both). Nonetheless, it becomes apparent from this analysis that the Ebro and Sava river basins are at much higher risk of rising temperatures in the coming years than the Adige River Basin. This agrees with climate projections for the Alpine region, which generally predict moderate temperature increases for the first half of this century followed by more pronounced increases during the second half [65]. The only region in the Adige River Basin prone to significant temperature increases in the near future might be the Southern part, where droughts (especially in summer) have become more frequent in recent years [37]. As opposed to temperature trends, precipitation trends appear to be more consistent for the Adige and Sava river basins compared to the Ebro River Basin. Both Adige and Sava catchments show net increases in precipitation (1.48 mm year^{-1} and 1.1 mm year^{-1} , respectively), whereas the Ebro River Basin shows a net decrease (-3.0 mm year^{-1}). With the Eastern fringe of the Pyrenees being an area of upward trends as opposed to the rest of the basin, the Ebro River Basin shows the largest standard deviation in total precipitation changes (standard deviation of 2.77 mm year^{-1} versus 1.15 mm year^{-1} in the Adige River Basin and 1.48 mm year^{-1} in the Sava River Basin, respectively). The opposing precipitation trends among the study basins might be related to their

geographical location, as the transition zone between increasing precipitation in Northern Europe and decreasing precipitation in Southern Europe crosses the Alpine region [65]. Correspondingly, the most severe precipitation decrease by the end of this century is predicted for the Western and Eastern Part of the Mediterranean, whereas the Alps are expected to mitigate the precipitation decline to some extent [64]. This would also be consistent with projections for the period 2071 to 2100 that suggest secondary changes in total annual precipitation for both Northern Italy and the Northern Balkan region [135]. We suggest that a more detailed analysis including descriptors such as seasonal or drought characteristics can reveal additional differences in climate trends among the three basins. By analysing the most general descriptors (i.e., mean annual temperature and precipitation), it was, nonetheless, possible to describe in this study the overall climate trend in each basin. Concluding from this analysis, the Ebro River Basin has to be considered most vulnerable to changing climate among the river basin: precipitation decrease has been accompanied by rising temperatures, which results in enhanced evapotranspiration and thus decreasing water resources. In contrast, and in line with the local-scale survey discussed in Section 4.1.1, the Adige River Basin seems the least affected by changing climate, as mean temperatures show a minor increase and precipitation has mostly increased rather than decreased across the basin.

Streamflow Streamflow between 1971 and 2010 has, on average, decreased by 0.4% in the Adige River Basin, more than 50% in the Ebro River Basin, and 11% in the Sava River Basin, respectively. The mean trend in specific discharge at the analysed stations is $-0.01 \text{ L s}^{-1} \text{ km}^{-2} \text{ year}^{-1}$ for the Adige River

Basin, $-0.16 \text{ L s}^{-1} \text{ km}^{-2} \text{ year}^{-1}$ for the Ebro, and $-0.08 \text{ L s}^{-1} \text{ km}^{-2} \text{ year}^{-1}$ for the Sava river basins, respectively. This confirms that the Ebro River Basin is at highest risk of water scarcity among the analysed river basins. An overall trend towards decreasing streamflow becomes also apparent in the Sava River Basin, despite less severe than in the Ebro River Basin. In contrast, the Adige River Basin has not been subject to a strong general reduction of streamflow in the period 1971-2010 but, as observed in Section 4.1.1 and in the work of Chiogna et al. [37], water scarcity may affect the southern part of the catchment in the near future, especially in summer. In our analysis, Q10 is the only parameter showing a general trend across the Adige River Basin (i.e., no significant increasing trend, but significant decreasing trends at 21% of the stations). This might be associated with flood control by major reservoirs that are used for both hydropower generation and flood protection [68]. In contrast to the Adige River Basin, the number of stations with significant downward trends in the Ebro River Basin is similar for the low-flow and high flow indices. This suggests that streamflow trends in the Ebro River Basin are mainly climate-driven and are, therefore, reflected in a decline of all analysed streamflow indices, whereas streamflow trends in the Adige River Basin are to a large extent governed by anthropogenic flow alteration (i.e., withdrawal for irrigation, reservoirs and dams). Based on the streamflow analysis, streamflow changes in the Sava River Basin are more consistent with the trend pattern in the Ebro compared to the Adige River Basin, although the Sava River Basin is geographically closer to the Adige River Basin. However, with the Adige River Basin being mainly an Alpine catchment, it appears to be less affected by changing climate and increasing water scarcity than other basins in the Mediterranean. This

would also agree with the fact that, apart from one exception, no sub-basin in the Adige River Basin has been subject to both increasing temperatures and decreasing precipitation.

Nonetheless, even minor changes in climate variables might aggravate streamflow alteration by agriculture and hydropower plants, which have already led to substantial changes in flow regime in the Adige River from the 1960s on Zolezzi et al. [181]. The largest changes in specific streamflow are observed in headwaters of the Pyrenees in the Ebro and in the upstream reaches of the Sava River in Slovenia. Such a correlation between elevation and magnitude of streamflow trends does not apply to the Adige, where streamflow trends are generally positive, especially in winter (see Section 4.1.1). Hence, considering links between altitude, temperature, rainfall, snowfall, glacier melt and snowmelt, mountainous headwater catchments can have low resilience to changing climatic conditions. Correspondingly, climate projections for Eastern Switzerland indicate that high-elevation catchments dominated by glacier and snow melt will be most affected of increasing temperatures, particularly in the second half of the 21st century [12]. In view of increasing temperatures, the three basins might thus be subject to streamflow changes associated with earlier snowmelt or increasing rainfall relative to snowfall [106]. Such shifts in snowmelt timing or the rainfall to snowfall ratio due to increasing temperatures have been observed for mountainous catchments in Western Austria between 1980 and 2010 [96]. However, in the headwaters of the Adige catchment we observed a general reduction of winter temperature, hence we claim that a shift from snowfall to rainfall has not occurred here in the past decades. These hydrological alterations affect hydropower production, which is likely to decrease throughout the 21st century and has to be adapted to changing hydrologic

regimes in Alpine regions [57]. Changes in snowmelt regimes might, therefore, become a major driver of future change in streamflow in the alpine Adige catchment and the mountainous parts of the Sava River Basin, as well as in headwater catchments in the Pyrenees and, due to their importance for runoff generation in the river basin, in the entire Ebro River Basin. Nonetheless, future trends in seasonal streamflow might greatly differ among mountainous catchments depending on their flow regime [9]. Hence, while the Adige River Basin might be able to buffer the impact of climate change on streamflow (at least at a scale larger than that of the headwaters), changes in the Pyrenees or the upstream part of the Sava River Basin might be much more dramatic, as also suggested by the discharge trends analysed in this study. Apart from the evident influence of changing climate, streamflow decreases in the Ebro River Basin might have been intensified by other anthropogenic impacts such as flow alteration by reservoirs [11], water consumption for irrigation [146] and increasing forest cover due to abandonment of agricultural land [62]. Indeed, land abandonment in the Ebro River Basin associated with increasing forest cover has started in the late 1980s [29] and might thus have contributed to the decreasing streamflow trend between 1971 and 2010. Land use change with feedback on, particularly, streamwater quality has also occurred in the Sava due to political and economic changes after 1990 [168]. In the Adige, on the contrary, there is no evidence for major land use changes and ensuing streamflow alteration but, in the southern part of the catchment, intensification of the irrigation demand for agriculture may have caused a reduction of streamflow in the summer season (see Section 4.1.1). The impact of those anthropogenic influences on streamwater quantity and quality can only be assessed in a more detailed

analysis of, among others, land use and land use change, hydrological alteration by damming, and seasonal streamflow indices. An example of this kind of rigorous analysis was presented here for the Adige River Basin. However, even at the spatial and temporal scale of this comparative analysis among three European river basins, the role of changing climate as major driver of change has become apparent, particularly as streamflow trends proved to be more significant in the basins with distinct climate trends (i.e., Ebro and Sava river basins).

4.2 On the use of hydrological modeling for testing the spatio-temporal coherence of high-resolution gridded precipitation and temperature datasets in the Alpine region

The five widely available datasets examined in the present work provide very different spatial distributions of precipitation and temperature over the study domain. In particular, while APGD and ADIGE agree very well with each other (due to their similar network of weather stations used to generate the gridded datasets), MSWEP, E-OBS and MESAN show substantially different precipitation patterns (despite the fact they are obtained from the same set of data). Notice that for the Adige basin Duan et al. [53] also found extremely different annual precipitation maps from eight satellite products and a station-based dataset. Expectedly, the largest uncertainty (i.e., the largest deviations between datasets) generally occurs in the most elevated mountain areas, where precipitation is most abundant and ground-based observations are generally scarce. In addition, the different interpolation schemes used in the datasets introduce significant differences in the estimates. When aggregated at the river basin scale, this variability

amounts to 17% for annual precipitation totals, but increases to about 35-50% at the monthly time scale (see Section 3.2). For temperature only three datasets are available, characterized by different station densities (i.e., effective resolution), different interpolation methods and also different grid spacing (i.e., nominal resolution). Indeed, while the topographic features of the domain can be recognized easily in ADIGE (1-km grid) and also in MESAN (about 5-km grid), they are almost completely lost in E-OBS due to the smoothing effect of aggregation at a rather coarse grid scale (about 22 km). Accordingly, local differences in mean annual temperature maps reach a maximum of about 5°C (especially over the most elevated areas in the northern part of the catchment). When aggregated at the river basin scale differences in the annual cycle of monthly mean temperature ranges between 1.5 and 2.3°C (see Section 3.2). A detailed comparison of such spatio-temporal differences in the meteorological forcing is however a major challenge, and a point-scale verification procedure may not be able to reveal potential deficits associated to individual datasets. These deficits may be due to the complex interactions of several factors, such as the spatially-varying weather station density in the case of both interpolated products and satellite-based estimates (which are routinely calibrated against ground observations), the accuracy of the retrieval algorithms applied to satellite products, limitations in the representation of sub-grid processes (convection and associated precipitation) for re-analysis products, or a combination of the above factors in case of a multi-source product (e.g., MSWEP and also MESAN). To this purpose, we proposed here a benchmarking process of observational datasets by employing the HyCoT framework, in which simulated, after a process of optimization, and observed streamflow time series are compared at several

gauging station within the case study area. In particular, we argue that the river-basin is the correct scale of assessment of climate forcing datasets to be used in hydrological simulations and that the benchmarking through hydrological modeling of streamflow allows to integrate in a natural manner all the above sources of errors. The results of HYPERstream optimizations, fed by the five datasets, identified APGD and ADIGE as the most accurate gridded products for hydrological modeling applications in the study area. Indeed, they provided the most accurate performances at both calibration and validation gauging stations. On the other hand, MSWEP, MESAN and especially E-OBS resulted less accurate, and unable to correctly reproduce the observed streamflow at the validation sites, particularly when the drainage area is small. Nevertheless, we found that applying the hydrological model at several streamflow gauging locations within the study area (in particular those not included in the definition of the efficiency metrics) allowed to verify how the suitability of the different datasets varies in space. This is particularly evident for stations with small drainage areas (see e.g., NSE efficiencies at Tel, Mantana, and Soraga in Figure 3.10A) where the limited averaging effect of the catchment highlight the importance of an accurate and spatially well resolved dataset of the climatic forcing [77]. This entails that the accuracy in the reproduction of the spatio-temporal patterns of precipitation and temperature inputs, which is especially hard to achieve in the domain of analysis and in the broader Alpine region, is crucial for obtaining accurate estimates of local-scale hydrological processes (see also [162]). Results of this analysis are also relevant for climate change impact assessments in the Alpine region where available gridded products are in general characterized by low observational density (i.e., low effective

spatial resolution and accuracy; see also [53, 162]). In particular, we highlight the deficiencies of hydrological simulations driven by inaccurate input meteorological forcing, i.e. datasets which did not pass hydrological validation at relevant spatial scales. Following the concept introduced by Knutti [93], we argue that the selection of observational gridded datasets should not be "democratic", since not all the datasets are equally performing. In this sense, we agree with the recommendations of Prein and Gobiet [140] to not neglect this source of uncertainty by selecting a priori a single dataset as observational reference. However we disagree when it is suggested to consider the full ensemble of precipitation datasets in both RCM evaluation process and climate-hydrology modeling chain. Inaccurate datasets, once tested through hydrological modeling, should be discarded, or weighted in order to avoid inflating the interval of confidence of the simulations or, even worst, causing the emergence of fictitious spatial and temporal patterns. This measure of agreement between model predictions and observation, generally termed as "likelihood", can for example be used in a Bayesian Model Averaging (BMA) framework [80, 145] aimed at providing a probabilistic weighted average prediction of projected streamflows. However, the negative impact of a wrong dataset, i.e., a dataset not able to provide an acceptable reproduction of streamflow when coupled with a hydrological model, is only reduced, yet not eliminated, by any kind of Bayesian weighting, being preferable its elimination from the collections of datasets. From a Bayesian point of view this elimination can be considered as part of prior information to be included in the updating process. Results obtained with the Linear Scaling (LS) approach discussed in Section 3.2 confirm that the correct reproduction of the spatio-temporal distribution of the precipitation field, more than a

correspondence of rainfall totals, is fundamental for an accurate reproduction of hydrological processes in climate change impact studies. Such finding is particularly relevant when assessments are performed at small spatial scales and in areas characterized by complex topography, where the spatio-temporal variability of the precipitation field is increased by topographic uplift [112]. Despite its simplicity, the Linear Scaling exercise revealed how downscaling methods used in climate change impact assessment studies may not be able to counterbalance the inadequate representation of spatial patterns in meteorological forcing that are crucial for hydrological application. In this sense, we show that, besides the selection/ranking of the most accurate observational datasets, also the selection of the most appropriate bias correction approach can be achieved through hydrological benchmarking. It is acknowledged that more sophisticated methods than LS [160] might have been tested, but this would be beyond the scope of the present work. Besides the results illustrated above, a couple of minor remarks about specific datasets can be also drawn. The first is that embedding high-resolution model reanalyses in MESAN, in order to achieve accurate precipitation and temperature fields, does not bring much improvement in the region of interest. In fact, hydrological simulations driven by MESAN show performances similar to those of the hydrological model driven by E-OBS, which shares the same observational database but has a five times coarser grid. Observational stations' density is thus confirmed to be a crucial factor in determining the effective resolution (i.e., the accuracy) of a gridded dataset. The second consideration concerns the newly developed MSWEP dataset. According to the present study, which represents one of the first hydrological applications of such dataset in the Alpine

region, MSWEP is sub-optimal with respect to products obtained exclusively with interpolation of ground observations (i.e., APGD and ADIGE). This may be due to the low resolution of its grid, which makes error prone its use in hydrological modeling in the Alps. On the other hand, MSWEP performs better than E-OBS and MESAN, despite the higher nominal resolution of the latter. This indicates that the merging of multiple data sources might be a convenient approach for improving the accuracy of gridded climate products. Notice however that, differently from the other datasets, MSWEP already includes a correction for precipitation under-catch based on streamflow observations (see Section 2.2.1).

CONCLUSIONS

The present PhD thesis explores the effects of changes in hydro-climatic variables and the anthropogenic impact on the hydrological cycle, over a range of temporal and spatial scales. Specifically, two different fields are investigated: 1) trend detection and attribution of changes in climatic and hydrological variables in the Adige River Basin (i.e., Northeastern Italy) and comparison to the trends detected in other large European river basins (i.e., Ebro and Sava); 2) introduction and development of a framework for evaluating the hydrological coherence of available gridded meteorological datasets, including one developed in the first part of the thesis. In the former, we analyzed long term time series of daily streamflow, precipitation and temperature, recorded in three European river basins (i.e., the Adige, Ebro and Sava river basins) with the goal of (i) determining the most significant trends; (ii) comparing the study basins with respect to their resilience to the observed hydro-climatic alterations and (iii) identifying the potential drivers of change, with particular

attention to the Adige River Basin.

In the latter, we compared high-resolution gridded daily datasets of precipitation and temperature available over the Alpine catchment of the Adige river, for the 1989-2008 period. Their uncertainty was investigated by comparing spatial and temporal distributions of both variables, while their accuracy was indirectly evaluated with an integrated approach through the numerical simulation of hydrological processes in the basin. This was done by applying a distributed hydrological model with climate inputs extracted from each dataset and by validating the results against streamflow observations. The proposed method, coined in the paper of Laiti et al. [98] as Hydrological Coherence Test (HyCoT), consists in the use of a physically-based hydrological model as a tool for testing the hydrological coherence of the rainfall and temperature datasets, i.e. their compatibility with the physical processes ruling the rainfall-runoff transformation and the observed streamflow. The method allows ranking the datasets according to their accuracy in modeling observed streamflows, providing useful indications on the coherence of each dataset with the observed streamflow.

5.1 Hydrological changes: detection and attribution

Trends of climatic forcing variables, hydrological fluxes and storage term in the water budget were computed and compared in 4 nested sub-catchments of the river basin closed at the gauging station of Trento. The analyses evidenced temporal patterns differentiated within the river basin depending on the reciprocal strength of water uses (and their changes in time) and climate change. In particular two main

changes were detected in the available time series: i) a reduction of summer streamflow of the Adige at Trento and ii) an increase of winter streamflow in the Gadera and upper Avisio catchments. The attribution of the observed alterations to their main causes was made as rigorously as data availability allowed. The attribution of the observed alterations to their main causes was performed by providing evidences of consistency or inconsistency of different plausible hypotheses following the approach proposed by Merz et al. [117]. A summary of the attribution exercise is shown in Table 5.1.

Table 5.1: *Summary of the attribution exercise.*

Hydrological alterations	Possible causes	Yes/No Reasons	
Decreasing summer streamflow at the outlet	- precipitation reduction	<i>No</i>	inconsistent with trends of P
	- raised evapotranspiration	<i>No</i>	inconsistent with trends of ET
	- agriculture	<i>Yes</i>	change point detection data of apple production standard deviation analysis
	- decreasing winter snow	<i>Yes</i>	trend analysis standard deviation analysis
Increased winter streamflow at the headwaters	- snow and glacier melting	<i>No</i>	glacier waters diverted outside basin absence of correlation analysis of variance
	- shift from solid to liquid precipitation	<i>No</i>	increasing freezing days absence of correlation analysis of variance
	- autumn aquifer recharge	<i>Yes</i>	consistent with trends of autumn P high correlation analysis of variance

At the headwaters positive trends in the winter streamflow are detected at the gauging stations of Gadera at Mantana and Avisio at Soraga, which are observed also at the annual scale, despite an evident reduction of winter precipitation. Accurate analyses of both trends and water budgets revealed that this change cannot be attributed to a shift of winter precipitation from solid to liquid, rather to a larger groundwater contribution triggered by a proportional increase of

groundwater recharge in Autumn due to larger precipitations. This is the stigma of climate change, given that headwaters are only marginally impacted by agricultural activities and seasonal storage for hydropower is very limited. This effect vanishes as the drainage area increases moving downstream, with only a marginal increase of winter streamflow observed at the Bronzolo and Trento gauging stations. On the contrary, starting from the middle '70s a strong decrease of summer streamflow is observed at Trento gauging station, due to the overwhelming effect of withdrawals for irrigation. In fact, an intense development of irrigated agriculture in the drainage area of the Noce river, a tributary of the Adige, is recorded in the same period. In the southern part of the river basin, therefore, agricultural uses offset the impact of climate change. To summarize, climate change is the main driver of recent changes only in headwater basins, while water uses overwhelm its effects in the southern part of the catchment. This variability occurs at a spatial scale that is smaller than the resolution of today's climate models (see Section 2.2.1) and at a temporal scale imposed by the seasonal dynamics, thereby assessment of impacts of climate change in the Alpine area should be performed with caution, particularly at the local scale. The comparative analysis of these trends to those of other European catchments indicate substantial differences (by reference to the common time window 1971-2010). In particular, changes in climate and streamflow are detected especially in the semi-arid Ebro River Basin, suggesting that this river basin is at highest risk of severe water scarcity due to changing climate. In contrast, the annual trends in water resources in the most of the Alpine Adige River Basin are less evident in this period, with the exception of the most southern part. The Sava River Basin shows characteristics of both the Adige and

the Ebro river basins (i.e., alpine flow regime in upstream parts and continental flow regime more downstream). This is also reflected in its intermediate resilience to hydroclimatic changes. Overall, this analysis suggests that European catchments are generally prone to drier climate and declining water resources, but local conditions can increase the resilience of river basins to climate change. However, this comparative analysis focused on annual trend patterns, whereas some stressors on aquatic ecosystems might become apparent at sub-annual scale only. For instance, Alpine catchments (as for the Adige River Basin) are mostly subject to seasonal and small-scale dynamics (e.g., snow and glacier melting, orographic precipitations) and need to be studied deeper (as, for example, in Section 4.1.1), with particular attention to the accuracy and resolution of data and by using appropriate techniques to provide real detection and attribution of hydrological changes. On the other hand, this comparative analysis of the recent hydroclimatic trends in Europe represents an important reference for the river management at large scale, emphasizing the most crucial factors, that are the agricultural sector and damming of rivers for water supply and hydropower generation. Measures of adapted river management could include the abandonment of certain crop types with a high water demand or the shutdown of reservoirs inducing the largest impact on natural flow regimes and aquatic ecosystems.

5.2 On the use of hydrological modeling for testing the spatio-temporal coherence of high-resolution gridded precipitation and temperature datasets in the Alpine region

The main results provided by the Hydrological Coherence Test (HyCoT), applied to the Adige River Basin, can be listed as follows:

- The analysis of gridded precipitation and temperature datasets revealed large variability of both climate variables provided by the datasets. Large differences are observed in spatial patterns as well as in the seasonal variability of precipitation and temperature. In particular, the largest discrepancies were detected in high elevation areas, poorly covered by meteorological stations, and in general can be ascribed to the effective resolution (i.e., accuracy) of the datasets, which is controlled by the density of the observations included in each product. Indeed, the two precipitation datasets characterized by the highest station densities, i.e. APGD and ADIGE, provided similar precipitation patterns, while MSWEP, MESAN and E-OBS showed rather diverse spatio-temporal distributions. The uncertainty, defined as the maximum difference among the datasets, of the mean annual precipitation aggregated over the entire catchment was estimated in approximately 17%, while the uncertainty of the annual cycle of monthly mean temperature was found to be around 2 °C.
- The proposed screening method, based on HYPERstream hydrological simulations, allowed to rank the five gridded climate datasets (see Section 2.2.1) according to their accuracy in the simulation of the hydrological processes

in the study area. The results identified APGD and ADIGE as the best candidates for hydrological applications in the Adige catchment. On the contrary, despite acceptable results at the larger scale, E-OBS, MESAN and MSWEP were found unable to correctly reproduce the observed streamflow at small Alpine catchments.

- The fundamental role of observational density in determining the effective accuracy of gridded climate products was thus clearly confirmed, emphasizing the key importance of an accurate representation of spatio-temporal patterns of precipitation and temperature (see also [81, 84]). This is especially true in complex-topography areas, where the spatio-temporal variability of meteorological fields is exacerbated and the availability of a sufficiently large amount of ground-based data (or, possibly, high-resolution satellite data) is crucial.
- It was found that simple correction methods based on linear scaling of rainfall data, which are formally similar (although not identical) to simple bias-correction approaches, may not be able to alleviate the aforementioned problems plaguing the coarser datasets. More sophisticated bias correction approaches may perform differently; still we surmise that the proposed HyCoT benchmarking procedure can be effectively employed also for assessing the performances of such approaches.

Summarizing, the proposed HyCoT methodology is a useful tool to sort available gridded meteorological datasets to be used as climatic forcing in hydrological applications and, in case, to eliminate those that are not coherent with streamflow observations. HyCoT may find useful application in the

identification of biases and inaccuracies of climate data in regional climate studies, e.g., to consistently reduce the uncertainty of projections that employ multiple datasets. We acknowledge that epistemic model errors, biases in the observed streamflow time series and even the model calibration procedure itself may affect the method; nevertheless, we believe that the physically-based nature of the modeling approach provides a rational and consistent framework which helps in discriminating gridded datasets of meteorological forcing with different origin. In fact, the procedure falsifies the hypothesis that a gridded dataset is hydrologically coherent if, after calibration, the reproduction of hydrological observational data are not satisfying according to a selected metric, compensation effects of hydrological models, notwithstanding. In other words, we are not trying to identify here the best dataset, rather exclude those that after calibration are still not able to reproduce observational data, while other datasets do. Hydrological modeling has been performed with HYPERstream routing scheme coupled with a continuous SCS-CN module for surface flow generation, but any other hydrological model can be used.

BIBLIOGRAPHY

- [1] Abera, W., Formetta, G., Borga, M., and Rigon, R. (2017).
Estimating the water budget components and their
variability in a pre-alpine basin with jgrass-newage.
Advances in Water Resources, 104:37–54.
- [2] Acero, F., García, J. A., Gallego, M. C., Parey, S., and
Dacunha-Castelle, D. (2014).
Trends in summer extreme temperatures over the iberian
peninsula using nonurban station data.
Journal of Geophysical Research: Atmospheres, 119(1):39–53.
- [3] Aguilera, R., Marcé, R., and Sabater, S. (2015).
Detection and attribution of global change effects on river
nutrient dynamics in a large mediterranean basin.
Biogeosciences, 12(13):4085–4098.
- [4] Allen, M. and Stott, P. (2003).
Estimating signal amplitudes in optimal fingerprinting, part
i: Theory.
Climate Dynamics, 21(5-6):477–491.
- [5] Allen, R. G., Pereira, L. S., Raes, D., Smith, M., et al. (1998).
Crop evapotranspiration-guidelines for computing crop
water requirements-fao irrigation and drainage paper 56.
FAO, Rome, 300(9):D05109.
- [6] Anderson, M. J. (2001).

A new method for non-parametric multivariate analysis of variance.

Austral ecology, 26(1):32–46.

[7] Autorità di Bacino del Fiume Adige (2008).

Quaderno sul bilancio idrico superficiale di primo livello.

Bacino idrografico del fiume Adige, Trento.

[8] Barceló, D. and Sabater, S. (2010).

Water quality and assessment under scarcity: prospects and challenges in mediterranean watersheds.

[9] Bard, A., Renard, B., Lang, M., Giuntoli, I., Korck, J.,

Koboltschnig, G., Janža, M., d'Amico, M., and Volken, D. (2015).

Trends in the hydrologic regime of alpine rivers.

Journal of Hydrology, 529:1823–1837.

[10] Barnett, T. P., Adam, J. C., and Lettenmaier, D. P. (2005).

Potential impacts of a warming climate on water availability in snow-dominated regions.

Nature, 438(7066):303–309.

[11] Batalla, R. J., Gomez, C. M., and Kondolf, G. M. (2004).

Reservoir-induced hydrological changes in the ebro river basin (ne spain).

Journal of Hydrology, 290(1):117–136.

[12] Bavay, M., Grünewald, T., and Lehning, M. (2013).

Response of snow cover and runoff to climate change in high alpine catchments of eastern switzerland.

Advances in water resources, 55:4–16.

[13] Beck, H. E., van Dijk, A. I., Levizzani, V., Schellekens, J.,

Miralles, D. G., Martens, B., and de Roo, A. (2017).

- Mswep: 3-hourly 0.25 global gridded precipitation
(1979-2015) by merging gauge, satellite, and reanalysis
data.
Hydrology and Earth System Sciences, 21(1):589.
- [14] Bénichou, P. and Le Breton, O. (1987).
Aurelhy: une méthode d'analyse utilisant le relief pour les
besoins de l'hydrométéorologie.
- [15] Beniston, M. (2003).
Climatic change in mountain regions: a review of possible
impacts.
In *Climate variability and change in high elevation regions:
Past, present & future*, pages 5–31. Springer.
- [16] Beniston, M. (2012a).
Impacts of climatic change on water and associated
economic activities in the swiss alps.
Journal of Hydrology, 412:291–296.
- [17] Beniston, M. (2012b).
Is snow in the alps receding or disappearing?
Wiley Interdisciplinary Reviews: Climate Change,
3(4):349–358.
- [18] Beniston, M., Rebetez, M., Giorgi, F., and Marinucci, M.
(1994).
An analysis of regional climate change in switzerland.
Theoretical and applied climatology, 49(3):135–159.
- [19] Beven, K. (2002).
Towards an alternative blueprint for a physically based
digitally simulated hydrologic response modelling system.
Hydrological processes, 16(2):189–206.

- [20] Birsan, M.-V., Molnar, P., Burlando, P., and Pfaundler, M. (2005).
Streamflow trends in switzerland.
Journal of Hydrology, 314(1):312–329.
- [21] Bjelajac, D., Leščešen, I., Micić, T., and Pantelić, M. (2013).
Estimation of water quality of sava river (vojvodina, serbia)
in the period 2004-2011 using serbian water quality
index (swqi).
Geographica Pannonica, 17(4):91–97.
- [22] Bocchiola, D. (2014).
Long term (1921–2011) hydrological regime of alpine
catchments in northern italy.
Advances in Water Resources, 70:51–64.
- [23] Bogdal, C., Nikolic, D., LuÅàthi, M. P., Schenker, U.,
Scheringer, M., and HungerbuÅàhler, K. (2010).
Release of legacy pollutants from melting glaciers: model
evidence and conceptual understanding.
Environmental science & technology, 44(11):4063–4069.
- [24] Botter, G., Basso, S., Rodriguez-Iturbe, I., and Rinaldo, A. (2013).
Resilience of river flow regimes.
Proceedings of the National Academy of Sciences,
110(32):12925–12930.
- [25] Bouza-Deaño, R., Ternero-Rodríguez, M., and
Fernández-Espinosa, A. (2008).
Trend study and assessment of surface water quality in the
ebro river (spain).
Journal of Hydrology, 361(3):227–239.
- [26] Brunetti, M., Maugeri, M., Monti, F., and Nanni, T. (2006a).

- Temperature and precipitation variability in Italy in the last two centuries from homogenised instrumental time series. *International journal of climatology*, 26(3):345–381.
- [27] Brunetti, M., Maugeri, M., Nanni, T., Auer, I., Böhm, R., and Schöner, W. (2006b).
Precipitation variability and changes in the greater alpine region over the 1800–2003 period.
Journal of Geophysical Research: Atmospheres, 111(D11).
- [28] Bruno, M. C., Siviglia, A., Carolli, M., and Maiolini, B. (2013).
Multiple drift responses of benthic invertebrates to interacting hydropeaking and thermopeaking waves.
Ecohydrology, 6(4):511–522.
- [29] Buendia, C., Batalla, R. J., Sabater, S., Palau, A., and Marcé, R. (2016).
Runoff trends driven by climate and afforestation in a pyrenean basin.
Land Degradation & Development, 27(3):823–838.
- [30] Burn, D. H. and Elnur, M. A. H. (2002).
Detection of hydrologic trends and variability.
Journal of hydrology, 255(1):107–122.
- [31] Cargnelutti, M., Quaranta, N., Refsgard, A., and Basberg, L. (1999).
Application of Mike SHE to the alluvial aquifer of river Adige, Adige valley.
In *Proceedings of the 3rd DHI Software Conference, Helsingor, Denmark*, pages 7–11.
- [32] Carturan, L., Baroni, C., Becker, M., Bellin, A., Cainelli, O., Carton, A., Casarotto, C., Dalla Fontana, G., Godio, A., Martinelli, T., et al. (2013).

Decay of a long-term monitored glacier: Careser glacier
(ortles-cevedale, european alps).

The Cryosphere, 7(6):1819.

- [33] Castagna, M., Bellin, A., and Chiogna, G. (2015).

Uncertainty estimation and evaluation of shallow
aquifers,Â exploitability: the case study of the adige
valley aquifer (italy).

Water, 7(7):3367–3395.

- [34] Chambers, J. and Hastie, T. (1992).

Statistical models in s. pacific grove, ca: Wadsworth.

ChambersStatistical Models in, page S1992.

- [35] Chen, J., Brissette, F. P., Chaumont, D., and Braun, M.
(2013).

Finding appropriate bias correction methods in downscaling
precipitation for hydrologic impact studies over north
america.

Water Resources Research, 49(7):4187–4205.

- [36] Chiew, F. and McMahon, T. (1996).

Trends in historical streamflow records.

In *Regional Hydrological Response to Climate Change*, pages
63–68. Springer.

- [37] Chiogna, G., Majone, B., Paoli, K. C., Diamantini, E., Stella,
E., Mallucci, S., Lencioni, V., Zandonai, F., and Bellin, A.
(2016).

A review of hydrological and chemical stressors in the adige
catchment and its ecological status.

Science of The Total Environment, 540:429–443.

- [38] Chiogna, G., Santoni, E., Camin, F., Tonon, A., Majone, B.,
Trenti, A., and Bellin, A. (2014).

- Stable isotope characterization of the vermigliana catchment.
Journal of hydrology, 509:295–305.
- [39] Ciabatta, L., Marra, A. C., Panegrossi, G., Casella, D., Sanò, P., Dietrich, S., Massari, C., and Brocca, L. (2017).
Daily precipitation estimation through different microwave sensors: Verification study over italy.
Journal of Hydrology, 545:436–450.
- [40] Clark, M. P., Wilby, R. L., Gutmann, E. D., Vano, J. A., Gangopadhyay, S., Wood, A. W., Fowler, H. J., Prudhomme, C., Arnold, J. R., and Brekke, L. D. (2016).
Characterizing uncertainty of the hydrologic impacts of climate change.
Current Climate Change Reports, 2(2):55–64.
- [41] Contractor, S., Alexander, L. V., Donat, M. G., and Herold, N. (2015).
How well do gridded datasets of observed daily precipitation compare over australia?
Advances in Meteorology, 2015.
- [42] Coppola, E. and Giorgi, F. (2010).
An assessment of temperature and precipitation change projections over italy from recent global and regional climate model simulations.
International Journal of Climatology, 30(1):11–32.
- [43] Cover, C. L. (2006).
Seamless vector data,Â€european environment agency.
- [44] Crepaz, A., Cagnati, A., and De Luca, G. (2009).
Evoluzione dei ghiacciai delle dolomiti negli ultimi cento anni.
ARPAV.

- [45] Dahlgren, P., Landelius, T., Kållberg, P., and Gollvik, S. (2016).
A high-resolution regional reanalysis for europe. part 1:
Three-dimensional reanalysis with the regional
high-resolution limited-area model (hirlam).
Quarterly Journal of the Royal Meteorological Society,
142(698):2119–2131.
- [46] Daly, C., Neilson, R. P., and Phillips, D. L. (1994).
A statistical-topographic model for mapping climatological
precipitation over mountainous terrain.
Journal of applied meteorology, 33(2):140–158.
- [47] Dee, D. P., Uppala, S., Simmons, A., Berrisford, P., Poli, P.,
Kobayashi, S., Andrae, U., Balmaseda, M., Balsamo, G.,
Bauer, P., et al. (2011).
The era-interim reanalysis: Configuration and performance
of the data assimilation system.
Quarterly Journal of the royal meteorological society,
137(656):553–597.
- [48] Della Chiesa, S., Bertoldi, G., Niedrist, G., Obojes, N.,
Endrizzi, S., Albertson, J., Wohlfahrt, G., Hörtnagl, L., and
Tappeiner, U. (2014).
Modelling changes in grassland hydrological cycling along
an elevational gradient in the alps.
Ecohydrology, 7(6):1453–1473.
- [49] Destouni, G., Jaramillo, F., and Prieto, C. (2013).
Hydroclimatic shifts driven by human water use for food
and energy production.
Nature Climate Change, 3(3):213–217.
- [50] Deutsch, C. V. (1996).
Correcting for negative weights in ordinary kriging.

Computers & Geosciences, 22(7):765–773.

- [51] Diamantini, E., Lutz, S. R., Mallucci, S., Majone, B., Merz, R., and Bellin, A. (2017).

Driver detection of water quality trends in three large european river basins.

Science of The Total Environment, —:—.

- [52] Douglas, E., Niyogi, D., Froking, S., Yeluripati, J., Pielke Sr., R., Niyogi, N., Vörösmarty, C., and Mohanty, U. (2006).

Changes in moisture and energy fluxes due to agricultural land use and irrigation in the indian monsoon belt.

Geophysical Research Letters, 33(14).

- [53] Duan, Z., Liu, J., Tuo, Y., Chiogna, G., and Disse, M. (2016).

Evaluation of eight high spatial resolution gridded precipitation products in adige basin (italy) at multiple temporal and spatial scales.

Science of The Total Environment, 573:1536–1553.

- [54] El Kenawy, A., López-Moreno, J., and Vicente-Serrano, S. (2011).

Recent trends in daily temperature extremes over northeastern spain (1960-2006).

Natural Hazards and Earth System Sciences, 11(9):2583.

- [55] Farinotti, D., Usselman, S., Huss, M., Bauder, A., and Funk, M. (2012).

Runoff evolution in the swiss alps: projections for selected high-alpine catchments based on ensembles scenarios.

Hydrological Processes, 26(13):1909–1924.

- [56] Fekete, B. M., Vörösmarty, C. J., Roads, J. O., and Willmott, C. J. (2004).

Uncertainties in precipitation and their impacts on runoff estimates.

Journal of Climate, 17(2):294–304.

- [57] Finger, D., Heinrich, G., Gobiet, A., and Bauder, A. (2012).
Projections of future water resources and their uncertainty
in a glacierized catchment in the swiss alps and the
subsequent effects on hydropower production during the
21st century.

Water Resources Research, 48(2).

- [58] Fiori, A., Cvetkovic, V., Dagan, G., Attinger, S., Bellin, A.,
Dietrich, P., Zech, A., and Teutsch, G. (2016).

Debates,Ästochastic subsurface hydrology from theory to
practice: The relevance of stochastic subsurface
hydrology to practical problems of contaminant
transport and remediation. what is characterization and
stochastic theory good for?

Water Resources Research, 52(12):9228–9234.

- [59] François, B., Borga, M., Anquetin, S., Creutin, J., Engeland,
K., Favre, A., Hingray, B., Ramos, M., Raynaud, D.,
Renard, B., et al. (2014).

Integrating hydropower and intermittent climate-related
renewable energies: a call for hydrology.

Hydrol. Process, 28(21):5465–5468.

- [60] Frei, C. and Schär, C. (1998).

A precipitation climatology of the alps from high-resolution
rain-gauge observations.

International Journal of climatology, 18(8):873–900.

- [61] Füssel, H.-M., Jol, A., et al. (2012).

Climate change, impacts and vulnerability in europe 2012
an indicator-based report.

- [62] Gallart, F. and Llorens, P. (2004).

- Observations on land cover changes and water resources in the headwaters of the ebro catchment, iberian peninsula. *Physics and Chemistry of the Earth, Parts A/B/C*, 29(11):769–773.
- [63] Gampe, D., Nikulin, G., and Ludwig, R. (2016).
Using an ensemble of regional climate models to assess climate change impacts on water scarcity in european river basins.
Science of The Total Environment, 573:1503–1518.
- [64] Giorgi, F. and Lionello, P. (2008).
Climate change projections for the mediterranean region.
Global and planetary change, 63(2):90–104.
- [65] Gobiet, A., Kotlarski, S., Beniston, M., Heinrich, G., Rajczak, J., and Stoffel, M. (2014).
21st century climate change in the european alps,Äa review.
Science of the Total Environment, 493:1138–1151.
- [66] Goovaerts, P. (1997).
Geostatistics for natural resources evaluation.
Oxford University Press on Demand.
- [67] Gosling, S. N. and Arnell, N. W. (2011).
Simulating current global river runoff with a global hydrological model: model revisions, validation, and sensitivity analysis.
Hydrological Processes, 25(7):1129–1145.
- [68] Gumiero, B., Maiolini, B., Rinaldi, M., Surian, N., Boz, B., and Moroni, F. (2009).
The italian rivers.
Rivers of Europe. Academic Press, Amsterdam, pages 467–495.
- [69] Gupta, H. V., Sorooshian, S., and Yapo, P. O. (1999).

Status of automatic calibration for hydrologic models:

Comparison with multilevel expert calibration.

Journal of Hydrologic Engineering, 4(2):135–143.

[70] Guthke, A. (2017).

Defensible model complexity: A call for data-based and
goal-oriented model choice.

Groundwater, 55(5):646–650.

[71] Hargreaves, G. H. (1994).

Defining and using reference evapotranspiration.

Journal of Irrigation and Drainage Engineering,
120(6):1132–1139.

[72] Hargreaves, G. H. and Samani, Z. A. (1985).

Reference crop evapotranspiration from temperature.

Appl. Eng. Agric, 1(2):96–99.

[73] Harrigan, S., Murphy, C., Hall, J., Wilby, R., and Sweeney, J.
(2014).

Attribution of detected changes in streamflow using
multiple working hypotheses.

Hydrol. Earth Syst. Sci, 18:1935–1952.

[74] Harris, I., Jones, P., Osborn, T., and Lister, D. (2014).

Updated high-resolution grids of monthly climatic
observations—the cru ts3. 10 dataset.

International Journal of Climatology, 34(3):623–642.

[75] Hasselmann, K. (1997).

Multi-pattern fingerprint method for detection and
attribution of climate change.

Climate Dynamics, 13(9):601–611.

[76] Haylocka, M., Hofstrab, N., Tankc, A. K., Klok, E., Jonesa,
P., Newb, M., and Haylock, M. (2008).

- A european daily high-resolution gridded dataset of surface temperature and precipitation.
- [77] Heistermann, M. and Kneis, D. (2011).
Benchmarking quantitative precipitation estimation by conceptual rainfall-runoff modeling.
Water Resources Research, 47(6).
- [78] Hirsch, R. M., Slack, J. R., and Smith, R. A. (1982).
Techniques of trend analysis for monthly water quality data.
Water resources research, 18(1):107–121.
- [79] Hodgkins, G. A., Whitfield, P. H., Burn, D. H., Hannaford, J., Renard, B., Stahl, K., Fleig, A. K., Madsen, H., Mediero, L., Korhonen, J., et al. (2017).
Climate-driven variability in the occurrence of major floods across north america and europe.
Journal of Hydrology, 552:704–717.
- [80] Hoeting, J. A., Madigan, D., Raftery, A. E., and Volinsky, C. T. (1999).
Bayesian model averaging: a tutorial.
Statistical science, pages 382–401.
- [81] Hofstra, N., New, M., and McSweeney, C. (2010).
The influence of interpolation and station network density on the distributions and trends of climate variables in gridded daily data.
Climate Dynamics, 35(5):841–858.
- [82] Hughes, D. and Smakhtin, V. (1996).
Daily flow time series patching or extension: a spatial interpolation approach based on flow duration curves.
Hydrological Sciences Journal, 41(6):851–871.
- [83] Huo, Z., Feng, S., Kang, S., Li, W., and Chen, S. (2008).

Effect of climate changes and water-related human activities
on annual stream flows of the shiyang river basin in arid
north-west china.

Hydrological processes, 22(16):3155–3167.

[84] Isotta, F. A., Vogel, R., and Frei, C. (2015).

Evaluation of european regional reanalyses and
downscalings for precipitation in the alpine region.

Meteorologische Zeitschrift, 24:15–37.

[85] ISRBC, I. S. R. B. C. (2013).

Significant pressures identified in the sava river basin.
international sava river basin commission.

Sava River Basin management plan. Background paper no. 3.

[86] Jaramillo, F., Prieto, C., Lyon, S. W., and Destouni, G. (2013).

Multimethod assessment of evapotranspiration shifts due to
non-irrigated agricultural development in sweden.

Journal of Hydrology, 484:55–62.

[87] Kelley, C., Ting, M., Seager, R., and Kushnir, Y. (2012).

Mediterranean precipitation climatology, seasonal cycle, and
trend as simulated by cmip5.

Geophysical Research Letters, 39(21).

[88] Kendall, M. (1975).

Rank correlation methods (4th edn.) charles griffin.

San Francisco, CA, page 8.

[89] Kennedy, R. (1995).

J. and eberhart, particle swarm optimization.

In *Proceedings of IEEE International Conference on Neural
Networks IV*, pages, volume 1000.

[90] Kidd, C., Bauer, P., Turk, J., Huffman, G., Joyce, R., Hsu,

K.-L., and Braithwaite, D. (2012).

- Intercomparison of high-resolution precipitation products over northwest europe.
Journal of Hydrometeorology, 13(1):67–83.
- [91] Kidd, C., Dawkins, E., and Huffman, G. (2013).
Comparison of precipitation derived from the ecmwf operational forecast model and satellite precipitation datasets.
Journal of Hydrometeorology, 14(5):1463–1482.
- [92] Klok, E. and Klein Tank, A. (2009).
Updated and extended european dataset of daily climate observations.
International Journal of Climatology, 29(8):1182–1191.
- [93] Knutti, R. (2010).
The end of model democracy?
- [94] Kolditz, O., Rügner, H., Grathwohl, P., Dietrich, P., and Streck, T. (2013).
Wess: an interdisciplinary approach to catchment research.
- [95] Komatina, D. and Grošelj, S. (2015).
Transboundary water cooperation for sustainable development of the sava river basin.
In *The Sava River*, pages 1–25. Springer.
- [96] Kormann, C., Francke, T., Renner, M., and Bronstert, A. (2015).
Attribution of high resolution streamflow trends in western austria—an approach based on climate and discharge station data.
Hydrology and Earth System Sciences, 19(3):1225–1245.

- [97] Kotlarski, S., Keuler, K., Christensen, O. B., Colette, A., Déqué, M., Gobiet, A., Goergen, K., Jacob, D., Lüthi, D., van Meijgaard, E., et al. (2014).
Regional climate modeling on european scales: a joint
standard evaluation of the euro-cordex rcm ensemble.
Geoscientific Model Development, 7(4):1297–1333.
- [98] Laiti, L., Mallucci, S., Piccolroaz, S., Bellin, A., Zardi, D., Fiori, A., Nikulin, G., and Majone, B. (2017).
Accuracy of high-resolution gridded precipitation and
temperature datasets in the alps: evaluation by
hydrological modelling in the adige catchment.
Water Resources Research, —(—):—.
- [99] Landelius, T., Dahlgren, P., Gollvik, S., Jansson, A., and Olsson, E. (2016).
A high-resolution regional reanalysis for europe. part 2: 2d
analysis of surface temperature, precipitation and wind.
Quarterly Journal of the Royal Meteorological Society,
142(698):2132–2142.
- [100] Lassaletta, L., García-Gómez, H., Gimeno, B. S., and Rovira, J. V. (2009).
Agriculture-induced increase in nitrate concentrations in
stream waters of a large mediterranean catchment over
25years (1981–2005).
Science of the Total Environment, 407(23):6034–6043.
- [101] Leibundgut, C., Maloszewski, P., and Külls, C. (2009).
Artificial tracers.
Tracers in Hydrology, pages 57–122.
- [102] Lenderink, G., Buishand, A., and Deursen, W. v. (2007).
Estimates of future discharges of the river rhine using two
scenario methodologies: direct versus delta approach.

- Hydrology and Earth System Sciences*, 11(3):1145–1159.
- [103] Lespinas, F., Ludwig, W., and Heussner, S. (2010).
Impact of recent climate change on the hydrology of coastal
mediterranean rivers in southern france.
Climatic Change, 99(3-4):425–456.
- [104] Levi, L., Jaramillo, F., Andričević, R., and Destouni, G.
(2015).
Hydroclimatic changes and drivers in the sava river
catchment and comparison with swedish catchments.
Ambio, 44(7):624–634.
- [105] Loarie, S., Lobell, D., Asner, G., Mu, Q., and Field, C.
(2011).
Direct impacts on local climate of sugar-cane expansion in
brazil.
Nature Climate Change, 1(2):105–109.
- [106] López-Moreno, J., Vicente-Serrano, S., Moran-Tejeda, E.,
Zabalza, J., Lorenzo-Lacruz, J., and García-Ruiz, J. (2011).
Impact of climate evolution and land use changes on water
yield in the ebro basin.
Hydrology and Earth System Sciences, 15(1):311.
- [107] Ludwig, R., Roson, R., Zografos, C., and Kallis, G. (2011).
Towards an inter-disciplinary research agenda on climate
change, water and security in southern europe and
neighboring countries.
Environmental Science & Policy, 14(7):794–803.
- [108] Lutz, S. R., Mallucci, S., Diamantini, E., Majone, B.,
Bellin, A., and Merz, R. (2016).
Hydroclimatic and water quality trends across three
mediterranean river basins.
Science of The Total Environment, 571:1392–1406.

- [109] Lyra, G. B., de Souza, J. L., da Silva, E. C., Lyra, G. B., Teodoro, I., Ferreira-Júnior, R. A., and de Souza, R. C. (2016).
Soil water stress co-efficient for estimating actual evapotranspiration of maize in northeastern brazil.
Meteorological Applications, 23(1):26–34.
- [110] Majone, B., Bellin, A., and Borsato, A. (2004).
Runoff generation in karst catchments: multifractal analysis.
Journal of hydrology, 294(1):176–195.
- [111] Majone, B., Bertagnoli, A., and Bellin, A. (2010).
A non-linear runoff generation model in small alpine catchments.
Journal of hydrology, 385(1):300–312.
- [112] Majone, B., Villa, F., Deidda, R., and Bellin, A. (2016).
Impact of climate change and water use policies on hydropower potential in the south-eastern alpine region.
Science of the Total Environment, 543:965–980.
- [113] Mallucci, S., Majone, B., and Bellin, A. (2018).
Detection and attribution of hydrological changes in a large alpine river basin.
submitted to Water Resources Research, -:-.
- [114] Mann, H. (1945).
Non-parametric tests against trend. *econometrica*, 13, 245-259.
- [115] McMahon, T., Peel, M., Lowe, L., Srikanthan, R., and McVicar, T. (2013).
Estimating actual, potential, reference crop and pan evaporation using standard meteorological data: a pragmatic synthesis.
Hydrology and Earth System Sciences, 17(4):1331.

- [116] McMahon, T. A., Vogel, R. M., Peel, M. C., and Pegram, G. G. (2007).
Global streamflows—part 1: Characteristics of annual streamflows.
Journal of Hydrology, 347(3):243–259.
- [117] Merz, B., Vorogushyn, S., Uhlemann, S., Delgado, J., and Hundsdoerfer, Y. (2012).
Hess opinions" more efforts and scientific rigour are needed to attribute trends in flood time series".
Hydrology and Earth System Sciences, 16(5):1379–1387.
- [118] Meteotrentino (2011).
Evoluzione e monitoraggi recenti dei ghiacciai trentini.
- [119] Michaelides, S., Levizzani, V., Anagnostou, E., Bauer, P., Kasparis, T., and Lane, J. (2009).
Precipitation: Measurement, remote sensing, climatology and modeling.
Atmospheric Research, 94(4):512–533.
- [120] Michel, C., Andréassian, V., and Perrin, C. (2005).
Soil conservation service curve number method: How to mend a wrong soil moisture accounting procedure?
Water Resources Research, 41(2).
- [121] Moriasi, D. N., Arnold, J. G., Van Liew, M. W., Bingner, R. L., Harmel, R. D., and Veith, T. L. (2007).
Model evaluation guidelines for systematic quantification of accuracy in watershed simulations.
Transactions of the ASABE, 50(3):885–900.
- [122] Nash, J. E. and Sutcliffe, J. V. (1970).
River flow forecasting through conceptual models part i, A discussion of principles.
Journal of hydrology, 10(3):282–290.

- [123] Nasonova, O., Gusev, Y. M., and Kovalev, Y. E. (2011).
Impact of uncertainties in meteorological forcing data and
land surface parameters on global estimates of terrestrial
water balance components.
Hydrological Processes, 25(7):1074–1090.
- [124] Navarro-Ortega, A., Acuña, V., Bellin, A., Burek, P.,
Cassiani, G., Choukr-Allah, R., Dolédec, S., Elozegi, A.,
Ferrari, F., Ginebreda, A., et al. (2015).
Managing the effects of multiple stressors on aquatic
ecosystems under water scarcity. the globaqua project.
Science of the Total Environment, 503:3–9.
- [125] Norbiato, D., Borga, M., Merz, R., Blöschl, G., and Carton,
A. (2009).
Controls on event runoff coefficients in the eastern italian
alps.
Journal of Hydrology, 375(3):312–325.
- [126] O'brien, R. G. and Kaiser, M. K. (1985).
Manova method for analyzing repeated measures designs:
an extensive primer.
Psychological bulletin, 97(2):316.
- [127] PAB, P. A. d. B. (2010).
Pguap piano generale di utilizzazione delle acque pubbliche.
Delibera della giunta provinciale n. 704 del 26.04.2010.
- [128] Pagán, B. R., Ashfaq, M., Rastogi, D., Kendall, D. R., Kao,
S.-C., Naz, B. S., Mei, R., and Pal, J. S. (2016).
Extreme hydrological changes in the southwestern us drive
reductions in water supply to southern california by mid
century.
Environmental Research Letters, 11(9):094026.

- [129] Pandžić, K., Trninić, D., Likso, T., and Bošnjak, T. (2009).
Long-term variations in water balance components for
croatia.
Theoretical and applied climatology, 95(1):39–51.
- [130] PAT, P. A. d. T. (2006).
Pguap piano generale di utilizzazione delle acque pubbliche.
Trento. URL: <http://pguap.provincia.tn.it/>.
- [131] PAT, P. A. d. T. (2012).
Bilanci idrici - relazione tecnica - il bacino dell'avisio.
Trento. URL: <http://pguap.provincia.tn.it/>.
- [132] Penna, D., Engel, M., Mao, L., Dell'Agnese, A., Bertoldi,
G., and Comiti, F. (2014).
Tracer-based analysis of spatial and temporal variations of
water sources in a glacierized catchment.
Hydrology and Earth System Sciences, 18(12):5271–5288.
- [133] Penna, D., Mao, L., Comiti, F., Engel, M., Dell'Agnesse,
A., and Bertoldi, G. (2013).
Hydrological effects of glacier melt and snowmelt in a
high-elevation catchment.
Bodenkultur, 64:93–98.
- [134] Pettitt, A. (1979).
A non-parametric approach to the change-point problem.
Applied statistics, pages 126–135.
- [135] Philandras, C., Nastos, P., Kapsomenakis, J., Douvis, K.,
Tselioudis, G., and Zerefos, C. (2011).
Long term precipitation trends and variability within the
mediterranean region.
Natural Hazards and Earth System Sciences, 11(12):3235.
- [136] Phillips, D. L. and Marks, D. G. (1996).

Spatial uncertainty analysis: propagation of interpolation errors in spatially distributed models.

Ecological Modelling, 91(1-3):213–229.

- [137] Piccolroaz, S., Di Lazzaro, M., Zarlenga, A., Majone, B., Bellin, A., and Fiori, A. (2016).

Hyperstream: a multi-scale framework for streamflow routing in large-scale hydrological model.

Hydrology and Earth System Sciences, 20(5):2047–2061.

- [138] Piovan, S. (2008).

Evoluzione paleoidrografica della pianura veneta meridionale e rapporto uomo-ambiente nell’olocene.

Dipartimento di Geografia, -(–):–.

- [139] Pohlert, T. (2016).

trend: Non-Parametric Trend Tests and Change-Point Detection.

R package version 0.2.0.

- [140] Prein, A. F. and Gobiet, A. (2017).

Impacts of uncertainties in european gridded precipitation observations on regional climate analysis.

International Journal of Climatology, 37(1):305–327.

- [141] Prein, A. F., Langhans, W., Fosser, G., Ferrone, A., Ban, N., Goergen, K., Keller, M., Tölle, M., Gutjahr, O., Feser, F., et al. (2015).

A review on regional convection-permitting climate modeling: Demonstrations, prospects, and challenges.

Reviews of geophysics, 53(2):323–361.

- [142] Renner, M., Brust, K., Schwärzel, K., Volk, M., and Bernhofer, C. (2014).

- Separating the effects of changes in land cover and climate:
a hydro-meteorological analysis of the past 60 yr in
saxony, germany.
Hydrology and Earth System Sciences, 18:389–405.
- [143] Rinaldo, A., Marani, A., and Rigon, R. (1991).
Geomorphological dispersion.
Water Resources Research, 27(4):513–525.
- [144] Río, S. d., Herrero, L., Fraile, R., and Penas, A. (2011).
Spatial distribution of recent rainfall trends in spain
(1961–2006).
International Journal of Climatology, 31(5):656–667.
- [145] Roy, T., Serrat-Capdevila, A., Gupta, H., and Valdes, J.
(2017).
A platform for probabilistic multimodel and multiproduct
streamflow forecasting.
Water Resources Research, 53(1):376–399.
- [146] Sabater, S., Feio, M. J., Graça, M. A., Muñoz, I., and
Romaní, A. (2009).
The iberian rivers.
Rivers of Europe, pages 113–149.
- [147] Sadegh, M. and Vrugt, J. A. (2014).
Approximate bayesian computation using markov chain
monte carlo simulation: Dream (abc).
Water Resources Research, 50(8):6767–6787.
- [148] Sagarika, S., Kalra, A., and Ahmad, S. (2014).
Evaluating the effect of persistence on long-term trends and
analyzing step changes in streamflows of the continental
united states.
Journal of Hydrology, 517:36–53.

- [149] Samani, Z. (2000).
Estimating solar radiation and evapotranspiration using
minimum climatological data.
Journal of Irrigation and Drainage Engineering,
126(4):265–267.
- [150] Schadler, B. (1987).
Long water balance time series in the upper basins of four
important rivers in europe-indicators for climatic changes.
In *Proceedings of the Vancouver Symposium, on the Influence
of Climatic Change and Climatic Variability on the
Hydrologic Regime and Water Resources*.
- [151] Scherrer, S. C., Appenzeller, C., and Laternser, M. (2004).
Trends in swiss alpine snow days: The role of local-and
large-scale climate variability.
Geophysical Research Letters, 31(13).
- [152] Scherrer, S. C., Begert, M., Croci-Maspoli, M., and
Appenzeller, C. (2015).
Long series of swiss seasonal precipitation: regionalization,
trends and influence of large-scale flow.
International Journal of Climatology.
- [153] Sen, P. K. (1968).
Estimates of the regression coefficient based on kendall's tau.
Journal of the American Statistical Association,
63(324):1379–1389.
- [154] Smiatek, G., Kunstmann, H., and Senatore, A. (2016).
Euro-cordex regional climate model analysis for the greater
alpine region: Performance and expected future change.
Journal of Geophysical Research: Atmospheres,
121(13):7710–7728.

- [155] Sousa, P., Trigo, R., Aizpurua, P., Nieto, R., Gimeno, L., and Garcia-Herrera, R. (2011).
Trends and extremes of drought indices throughout the 20th century in the mediterranean.
Natural Hazards and Earth System Sciences, 11(1):33–51.
- [156] Spearman, C. (1904).
The proof and measurement of association between two things.
The American journal of psychology, 15(1):72–101.
- [157] Subedi, A. and Chávez, J. L. (2015).
Crop evapotranspiration (et) estimation models: a review and discussion of the applicability and limitations of et methods.
Journal of Agricultural Science, 7(6):50.
- [158] Sunyer, M., Sørup, H. J. D., Christensen, O. B., Madsen, H., Rosbjerg, D., Mikkelsen, P. S., and Arnbjerg-Nielsen, K. (2013).
On the importance of observational data properties when assessing regional climate model performance of extreme precipitation.
Hydrology and Earth System Sciences, 17(11):4323.
- [159] Szolgayova, E., Parajka, J., Blöschl, G., and Bucher, C. (2014).
Long term variability of the danube river flow and its relation to precipitation and air temperature.
Journal of Hydrology, 519:871–880.
- [160] Teutschbein, C. and Seibert, J. (2012).
Bias correction of regional climate model simulations for hydrological climate-change impact studies: Review and evaluation of different methods.

Journal of Hydrology, 456:12–29.

- [161] Tomer, M. D. and Schilling, K. E. (2009).
A simple approach to distinguish land-use and
climate-change effects on watershed hydrology.
Journal of hydrology, 376(1):24–33.
- [162] Tuo, Y., Duan, Z., Disse, M., and Chiogna, G. (2016).
Evaluation of precipitation input for swat modeling in alpine
catchment: A case study in the adige river basin (italy).
Science of the Total Environment, 573:66–82.
- [163] Van de Griend, A., Seyhan, E., Engelen, G., and Geirnaert,
W. (1986).
Hydrological characteristics of an alpine glacial valley in the
north italian dolomites.
Journal of Hydrology, 88(3-4):275–299.
- [164] Vicente-Serrano, S. M. and Cuadrat-Prats, J. (2007).
Trends in drought intensity and variability in the middle
ebro valley (ne of the iberian peninsula) during the
second half of the twentieth century.
Theoretical and Applied Climatology, 88(3):247–258.
- [165] Villa, S., Negrelli, C., Finizio, A., Flora, O., and Vighi, M.
(2006).
Organochlorine compounds in ice melt water from italian
alpine rivers.
Ecotoxicology and environmental safety, 63(1):84–90.
- [166] Viviroli, D., Archer, D. R., Buytaert, W., Fowler, H. J.,
Greenwood, G., Hamlet, A. F., Huang, Y., Koboltschnig, G.,
Litaor, I., López-Moreno, J. I., et al. (2011).
Climate change and mountain water resources: overview and
recommendations for research, management and policy.
Hydrology and Earth System Sciences, 15(2):471–504.

- [167] Vörösmarty, C. J., McIntyre, P. B., Gessner, M. O., Dudgeon, D., Prusevich, A., Green, P., Glidden, S., Bunn, S. E., Sullivan, C. A., Liermann, C. R., et al. (2010). Global threats to human water security and river biodiversity. *Nature*, 467(7315):555–561.
- [168] Vrzel, J. and Ogrinc, N. (2015). Nutrient variations in the sava river basin. *Journal of Soils and Sediments*, 15(12):2380–2386.
- [169] Weber, R. O., Talkner, P., Auer, I., Böhm, R., Gajić-Čapka, M., Zaninović, K., Brazdil, R., and Faško, P. (1997). 20th-century changes of temperature in the mountain regions of central europe. In *Climatic Change at High Elevation Sites*, pages 95–112. Springer.
- [170] Weiland, F. C. S., Vrugt, J. A., Weerts, A. H., Bierkens, M. F., et al. (2015). Significant uncertainty in global scale hydrological modeling from precipitation data errors. *Journal of Hydrology*, 529:1095–1115.
- [171] Weingartner, R., Viviroli, D., and Schadler, B. (2007). Water resources in mountain regions: a methodological approach to assess the water balance in a highland-lowland-system. *Hydrological processes*, 21(5):578–585.
- [172] Weissmann, M., Braun, F. J., Gantner, L., Mayr, G. J., Rahm, S., and Reitebuch, O. (2005). The alpine mountain–plain circulation: Airborne doppler lidar measurements and numerical simulations. *Monthly weather review*, 133(11):3095–3109.

- [173] Wilby, R. L. and Dessai, S. (2010).
Robust adaptation to climate change.
Weather, 65(7):180–185.
- [174] Wilks, D. S. (1990).
Maximum likelihood estimation for the gamma distribution
using data containing zeros.
Journal of Climate, 3(12):1495–1501.
- [175] Xoplaki, E., Gonzalez-Rouco, J., Luterbacher, J., and
Wanner, H. (2003).
Mediterranean summer air temperature variability and its
connection to the large-scale atmospheric circulation
and ssts.
Climate Dynamics, 20(7-8):723–739.
- [176] Yang, Y., Wang, G., Wang, L., Yu, J., and Xu, Z. (2014).
Evaluation of gridded precipitation data for driving swat
model in area upstream of three gorges reservoir.
PloS one, 9(11):e112725.
- [177] Yue, S., Pilon, P., Phinney, B., and Cavadias, G. (2002).
The influence of autocorrelation on the ability to detect
trend in hydrological series.
Hydrological processes, 16(9):1807–1829.
- [178] Zampieri, M., Scoccimarro, E., Gualdi, S., and Navarra, A.
(2015).
Observed shift towards earlier spring discharge in the main
alpine rivers.
Science of the total environment, 503:222–232.
- [179] Zanon, V. (1978).
Cenni storici sulla evoluzione della frutticoltura trentina.
Frutta del Trentino.

- [180] Zhang, L., Potter, N., Hickel, K., Zhang, Y., and Shao, Q. (2008).
Water balance modeling over variable time scales based on the budyko framework–model development and testing. *Journal of Hydrology*, 360(1):117–131.
- [181] Zolezzi, G., Bellin, A., Bruno, M., Maiolini, B., and Siviglia, A. (2009).
Assessing hydrological alterations at multiple temporal scales: Adige river, Italy. *Water resources research*, 45(12).
- [182] Zolezzi, G., Siviglia, A., Toffolon, M., and Maiolini, B. (2011).
Thermopeaking in alpine streams: event characterization and time scales. *Ecohydrology*, 4(4):564–576.

In the present thesis, the effect of changes in hydro-climatic variables on the hydrological cycle is investigated over a range of temporal and spatial scales. In the first part, spatial and temporal patterns of change in the hydrological cycle of the Adige River Basin (i.e., Northeastern Italy) have been identified by applying statistical methods (i.e., Mann-Kendall trend tests, Sen's slope estimates, multivariate data analyses and Kriging algorithms) to annual and seasonal water budget components performed in representative sub-basins characterized by different climatic and water uses conditions. The results suggest that climate change is the main driver in headwater basins, while water uses overcome its effect along the main stream and the lower end of the tributaries. In addition, a comparative analysis of recent trends in hydro-climatic parameters in three climatologically different European watersheds (i.e., the Adige, Ebro and Sava River Basins) has been performed highlighting that the highest risk of increasing water scarcity refers to the Ebro, whereas the Adige shows better resilience to a changing climate.

In the second part, this thesis deals with the uncertainty associated with climate datasets, that typically represents the largest part of the total uncertainty in climate change impact studies. In particular, a new framework for assessing the coherence of gridded meteorological datasets with streamflow observations (i.e., HyCoT - Hydrological Coherence Test) has been introduced and tested. Application to the Adige catchment reveals that using inverse hydrological modeling allows testing the accuracy of gridded temperature and precipitation datasets and it may represent a tool for excluding those that are inconsistent with the hydrological response.

Stefano Mallucci graduated with a bachelor's degree in Civil and Environmental Engineering at the Marche Polytechnic University and then he received a master's degree in Civil Engineering - Hydraulics at the Polytechnic of Turin. After a period at the Vienna University of Technology, he became a Ph.D. student at the University of Trento. His research interests are linked to climate change and to anthropogenic stressors altering the hydrological cycle and the eco-system functioning of river basins. He is author of several publications on international scientific journals and he attended conferences and courses in Europe.